UNCLASSIFIED

AD NUMBER
AD860689
LIMITATION CHANGES
TO: **Approved for public release; distribution is unlimited.**
FROM: **Distribution authorized to U.S. Gov't. agencies and their contractors; Administrative/Operational Use; JUL 1969. Other requests shall be referred to Army Aviation Materiel Labs., Fort Eustis, VA.**
AUTHORITY
USAAMRDL ltr 18 Jun 1971

THIS PAGE IS UNCLASSIFIED

Best

Available

Copy

AD

AD 860689

USAAVLABS TECHNICAL REPORT 69-50

EXPLORATORY STUDY OF THE NATURE OF HELICOPTER ROTOR BLADE BOUNDARY LAYERS

DDC
RECEIVED
OCT 30 1969
B

By

H. R. Velkoff
D. A. Blaser
G. C. Shumaker
K. M. Jones

STATEMENT #2 UNCLASSIFIED

This document is subject to special export controls and each transmittal to foreign governments or foreign nationals may be made only with prior approval of

July 1969

U. S. ARMY AVIATION MATERIEL LABORATORIES
FORT EUSTIS, VIRGINIA

CONTRACT DAAJ02-67-C-0001
THE OHIO STATE UNIVERSITY
RESEARCH FOUNDATION
COLUMBUS, OHIO

Each transmittal of this document outside the Department of Defense must have prior approval of U.S. Army Aviation Materiel Laboratories, Fort Eustis, Virginia 23604

U. S. ARMY MATERIEL COMMAND

Reproduced by the
CLEARINGHOUSE
for Federal Scientific & Technical
Information Springfield Va. 22151

103

Disclaimers

The findings in this report are not to be construed as an official Department of the Army position unless so designated by other authorized documents.

When Government drawings, specifications, or other data are used for any purpose other than in connection with a definitely related Government procurement operation, the United States Government thereby incurs no responsibility nor any obligation whatsoever; and the fact that the Government may have formulated, furnished, or in any way supplied the said drawings, specifications, or other data is not to be regarded by implication or otherwise as in any manner licensing the holder or any other person or corporation, or conveying any rights or permission, to manufacture, use, or sell any patented invention that may in any way be related thereto.

Trade names cited in this report do not constitute an official endorsement or approval of the use of such commercial hardware or software.

Disposition Instructions

Destroy this report when no longer needed. Do not return it to the originator.

ACCESSION for
CFSTI WHITE SECTION ☐
DDC BUFF SECTION ☑
UNANNOUNCED ☐
JUSTIFICATION per letter attached
BY
DISTRIBUTION/AVAILABILITY CODES
DIST. AVAIL. and/or SPECIAL
2

DEPARTMENT OF THE ARMY
U. S. ARMY AVIATION MATERIEL LABORATORIES
Fort Eustis, Virginia 23604

ERRATUM

USAAVLABS Technical Report 69-50
TITLE: Exploratory Study of the Nature of Helicopter Rotor Blade Boundary Layers

Delete the statement on cover, title page, and block 10 of DD Form 1473 which reads

> "Each transmittal of this document outside the Department of Defense must have prior approval of US Army Aviation Materiel Laboratories, Fort Eustis, Virginia 23604."

and replace with the following statement:

> "This document is subject to special export controls, and each transmittal to foreign governments or foreign nationals may be made only with prior approval of US Army Aviation Materiel Laboratories, Fort Eustis, Virginia 23604."

DEPARTMENT OF THE ARMY
U. S. ARMY AVIATION MATERIEL LABORATORIES
FORT EUSTIS, VIRGINIA 23604

The report described a unique flow visualization technique for analyzing the three-dimensional boundary layer characteristics of a rotor blade in hover and forward flight.

The results are distributed to increase knowledge in the area of rotor boundary layer influence on blade circulation.

Task 1F162204A14234
Contract DAAJ02-67-C-0001
USAAVLABS Technical Report 69-50
July 1969

EXPLORATORY STUDY OF THE NATURE OF HELICOPTER ROTOR BLADE BOUNDARY LAYERS

Final Report

By

H. R. Velkoff
D. A. Blaser
G. C. Shumaker
K. M. Jones

Prepared By

The Ohio State University
Research Foundation
Columbus, Ohio

for

U. S. ARMY AVIATION MATERIEL LABORATORIES
FORT EUSTIS, VIRGINIA

[redacted]

ABSTRACT

An experimental study was conducted using flow visualization techniques to investigate the nature of the boundary layer on a helicopter rotor. Hovering and forward flight data were obtained; however, efforts were concentrated on hovering when unanticipated boundary layer behavior was revealed. The primary flow visualization technique involved the use of ammonia injected into the boundary layer at the leading edge. The blade surface was chemically coated, and as the ammonia moved with the local airflow, it formed a trace on the surface indicative of the boundary layer flow. The hovering traces initially moved chordwise along the surface, and then abruptly turned outward. A short distance later, the traces moved inward and then continued aft along the blade in a somewhat diffuse pattern. Similar traces were found over wide ranges of pitch angles and rotor speeds. It is hypothesized that a standing laminar separation bubble exists on the blade surface aft of the peak pressure position. No indication of any separation bubbles could be found on the forward flight traces.

An exploratory study of the possible use of ordinary claw-type pressure probes was undertaken to determine whether such probes could provide an indication of the flow in the boundary layer of a model rotor.

TABLE OF CONTENTS

	Page
ABSTRACT	iii
LIST OF ILLUSTRATIONS	vii
LIST OF SYMBOLS	xi
INTRODUCTION	1
APPROACH	4
EXPERIMENTAL METHODS OF FLOW VISUALIZATION	5
Boundary Layer Flow Visualization	5
Ammonia-Azo Streak Process	6
Chemical Sublimation Method	9
Rotor Blade Tests	9
Hover Tests With 4-Inch-Chord Blade	9
Tests With 7-Inch-Chord Blade	13
DESIGN OF EQUIPMENT	14
Rotor System	14
Valve System	14
Hover Test Stand	17
Flow Channel	20
Rotor Drive System	24
Forward Flight Ammonia System	24
EXPERIMENTAL PROCEDURE	28
Experimental Procedure for 7-Inch-Chord Rotor Tests (Hovering)	28
Method of Flow Channel Operation	28
RESULTS OF HOVER TESTS	30
Results With 4-Inch Chord-Blades in Hover With Orifice at 72% Radius	30
Chemical Sublimation Test Results	30
Ammonia-Azo Traces	30

TABLE OF CONTENTS (CONTINUED)

	Page
Separation Bubble	34
Boundary Layer Step Studies	40
Discussion of Inverted "V" Traces	45
Spanwise Variation With 4-Inch-Chord Blade	47
Hover Tests With 7-Inch-Chord Blade	55
Discussion of Stall	61
RESULTS OF FORWARD FLIGHT TESTS	65
CONCLUSIONS	76
RECOMMENDATIONS	77
LITERATURE CITED	78
APPENDIX - STUDY OF USE OF CLAW-TYPE BOUNDARY LAYER PROBES	80
DISTRIBUTION	89

LIST OF ILLUSTRATIONS

Figure		Page
1	Stuart Plot	2
2	Formation of Diazo Dye	7
3	Diagram of Small Hover Stand	7
4	Flow Reversal in a Boundary Layer	10
5	4-Inch-Chord, 2-Blade Rotor and Test Rig	11
6	4-Inch-Chord Blade Cross Section	11
7	7-Inch-Chord, Single-Blade Rotor	15
8	7-Inch-Chord Blade Structure	16
9	Valve System Schematic	18
10	Valve Test Rigs on the Plywood Sheet	19
11	Model Rotor Wind Tunnel	21
12	The Assembled Model Rotor Wind Tunnel	22
13	Tunnel, Fan, and Diffuser Assembly	23
14	Schematic of Rotor Drive System for Tunnel Use	25
15	Tunnel Rotor Drive System with Single-Blade Rotor	26
16	Chemical Sublimation Results Showing Location of Transition Versus Radius	31
17	Location of Transition at 72% Radius Versus Pitch Angle	32
18	Ammonia Trace Showing Discontinuity for the 4-Inch-Chord Blade at 72% Radius. L_1 = 13.5%, L_2 = 30% Chord, 400 rpm, θ = 10°	33
19	Traces for the 4-Inch-Chord Blade, 72% Radius at 300 rpm and Various Values of θ A) L_1 = 8%, L_2 = 16.5% B) L_1 = 15%, L_2 = 32 % C) L_1 = 39%, L_2 = 79 % D) L_1 = 76%, L_2 = 97 %	35

LIST OF ILLUSTRATIONS (continued)

Figure		Page
20	Traces for 4-Inch-Chord Blade, 72% Radius at 200 rpm and Various Values of θ . . . . . A) L_1 = 15.5%, L_2 = 38% B) L_1 = 22 %, L_2 = 50% C) L_1 = 36 %, L_2 = 74% D) L_1 = 66 %, L_2 = 91%	36
21	Traces for 4-Inch-Chord Blade, 72% Radius at 400 rpm and θ = 5° Showing Trace Formation With Various Exposure Times . . . . . A) L_1 = 21% B) L_1 = 20% C) L_1 = 21%, L_2 = 43% D) L_1 = 20%, L_2 = 42%	37
22	Comparison of Ammonia-Azo Discontinuity and Transition Point for Various Pitch Angles	38
23	Laminar Separation Bubble on an Airfoil	39
24	Two-Dimensional Pressure Distribution for NACA 0015 Airfoil	41
25	"Dual" Trace for 4-Inch-Chord Blade, 72% Radius at 300 rpm and θ = 10° With Boundary Layer Trip at L_1. L_1 = 13.5%, L_2 = 25% Chord	42
26	Streamlines on a Slender Delta Wing - Reference 13.	43
27	Schematic Streamlines on Airfoils with (A) Cusp, (B) Step and (C) Separation Bubble	44
28	Comparison of Ammonia-Azo Trace With and Without Surface Step at 400 rpm and θ = 5° . . . . . A) L_1 = 21%, L_2 = 43% B) L_1 = 20%, L_2 = 34%	46
29	Possible Factors Involved in the Shape of the Ammonia-Azo Trace	48
30	Effect of an Outboard Fence on a Trace. L_1 = 15%, L_2 = 30%, 400 rpm, θ = 5°	49
31	Traces at Several Radii for the 4-Inch-Chord Blade for Various Pitch Angles and 400 rpm	50

LIST OF ILLUSTRATIONS (continued)

Figure		Page
32	Traces at Several Radii for the 4-Inch-Chord Blade for Various Pitch Angles and 500 rpm	51
33	Traces at Several Radii for the 4-Inch-Chord Blade for Various Pitch Angles and 600 rpm	52
34	Ammonia-Azo Trace for the 7-Inch-Chord Blade at 61.5% R, 74% R and 87% R, $\theta = 8°$, and 200 rpm	56
35	Composite Set of Traces for 7-Inch-Chord Blade for 3 Radii at 400 rpm Showing Effect of Changing Pitch Angle	57
36	Composite Set of Traces for 7-Inch Chord Blade for 3 Radii at $\theta = 5°$ With Varying rpm	59
37	Ammonia-Azo Traces for 7-Inch-Chord Blade at $\theta = 15°$ Showing Effect of Change in rpm	60
38	Pressure Distribution in the Vicinity of the Bubble of Laminar Separation - Ref. 11	62
39	Pressure Distribution in the Vicinity of a Bubble - Ref. 12	63
40	Chordwise Pressure Distribution on a Full-Scale Helicopter Rotor Blade - Ref. 19	64
41	Simulated Forward Flight Traces at 500 rpm and Every 90° Azimuth	66
42	Simulated Forward Flight Traces at 650 rpm and Every 90° Azimuth	67
43	Simulated Forward Flight Traces at 800 rpm and Every 90° Azimuth	68
44	Simulated Forward Flight Traces at 500 rpm, $\mu = 0.3$ and Every 30° Azimuth	69
45	Simulated Forward Flight Traces at 650 rpm, $\mu = 0.3$ and Every 30° Azimuth	70
46	Effect of Ammonia Gas Pressure on the Forward Flight Tests at 650 rpm, $\mu = 0.30$, and $\psi = 270°$	74

LIST OF ILLUSTRATIONS (continued

Figure		Page
47	Forward Flight Trace at High Advance Ratio at 650 rpm and $\psi = 270°$	75
48	Schematic of Claw Probe Installation on Blade.	81
49	Installation of Model With Yaw Probe in Wind Tunnel. .	82
50	Yaw Probe Calibration, $\theta = 0°$, $q_{tunnel} = 0.2''$ H_2O . .	84
51	Modified Calibration Curve for Claw Probe, $\theta = 0$ . . .	85
52	Measured Differential Pressure Using Claw Probe Versus Rotor Speed, $\theta = 0°$, 73.5% R Position	86
53	Variation of Differential Pressure With Speed of Rotation, $\theta = 0°$, 73.5% R Position.	87
54	Flow Direction Deviation With Rotational Speed, $\theta = 0°$, 73.5% R Position	88

LIST OF SYMBOLS

c	blade chord length, inches
C	sonic velocity, fps
L_1	separation point
L_2	reattachment point
M	Mach number
P	pressure coefficient
ΔP	differential pressure from lower to upper surface of airfoil, psf
q	dynamic pressure, psf
r	radial distance to local blade section, ft
R	blade radius, ft
s_1	stagnation point preceding the separation bubble
s_2	stagnation point following the separation bubble
V	flight speed or tunnel air speed, fps
x	distance along blade midchord measured from the leading edge, inches
α	local section angle of attack, degrees
$\dot{\alpha}$	time rate of change of angle of attack, degrees/radian
θ	blade pitch angle, degrees
λ	inflow ratio
μ	advance ratio
ρ	air density, slugs/ft^3
ψ	azimuth angle, measured from the downwind position in a counter-clockwise sense, degrees
Ω	rotor speed, radians/second

INTRODUCTION

A fundamental limitation on the performance and utility of the helicopter is related to the onset of "stall" on the retreating blades. This stall limits the performance of the helicopter because of increased power requirements, aircraft roughness, vibration, and control loads. Blade stall, however, depends upon the nature of the boundary layer which exists on an airfoil. Relatively little information on the nature of the boundary layers on rotor blades has existed until quite recently. The complexity of the rotor blade motion, the flow field, and the fluid mechanic equations involved has tended to discourage research into the nature of the rotor blade boundary layers. The purpose of the investigation reported herein was to initiate study into the physical nature of these boundary layers.

Perhaps the most descriptive means of indicating the limitations imposed upon the helicopter speed potential because of stall is through the use of the Stuart plot.[1] A typical plot is shown in Figure 1. In that figure the shaded area on the left indicates the retreating blade stall limitation; the shaded area on the right, the compressibility limitation. Usually, the stall limit line is established as a certain angle of attack above two-dimensional stall for the particular airfoil considered. If the stall limitation line could be moved upward, then the speed potential of the helicopter could be increased. A second area in which aerodynamic improvements would be important is in the profile drag of the airfoils. Since the profile drag, as well as stall, is the result of the viscous actions in the boundary layer, it is necessary to understand as much detail of the rotor blade boundary layer as possible.

Recently, the validity of the assumptions made in the lift and drag analysis of rotors has been questioned.[2] Ordinarily, in calculating the lift and drag on the rotor, one assumes that only the component of flow normal to the blade span axis is important. Hence, only that component is used in calculating these forces, and all possible influences of radial flow or centrifugal field effects in the boundary layer are disregarded. In the case of lift forces at high angles of attack or drag forces, the neglect of the secondary sections may not be justified.

The scope of the action which may occur in rotor boundary layers is quite broad. The primary action is the chordwise viscous flow in the presence of the given chordwise pressure distribution. Flow components exist in both the chordwise and the spanwise directions. The magnitude and direction of the local velocity vary around the azimuth and along the blade span, as do the spanwise pressure gradients which exist.[3] Tip vortex-induced flows exists.[4] The fluid particles within the boundary layer can experience centrifugal and Coriolis effects. Compressible flow effects can occur on the tips of the advancing blade, and reversed flow occurs in the inboard regions of the retreating blade.

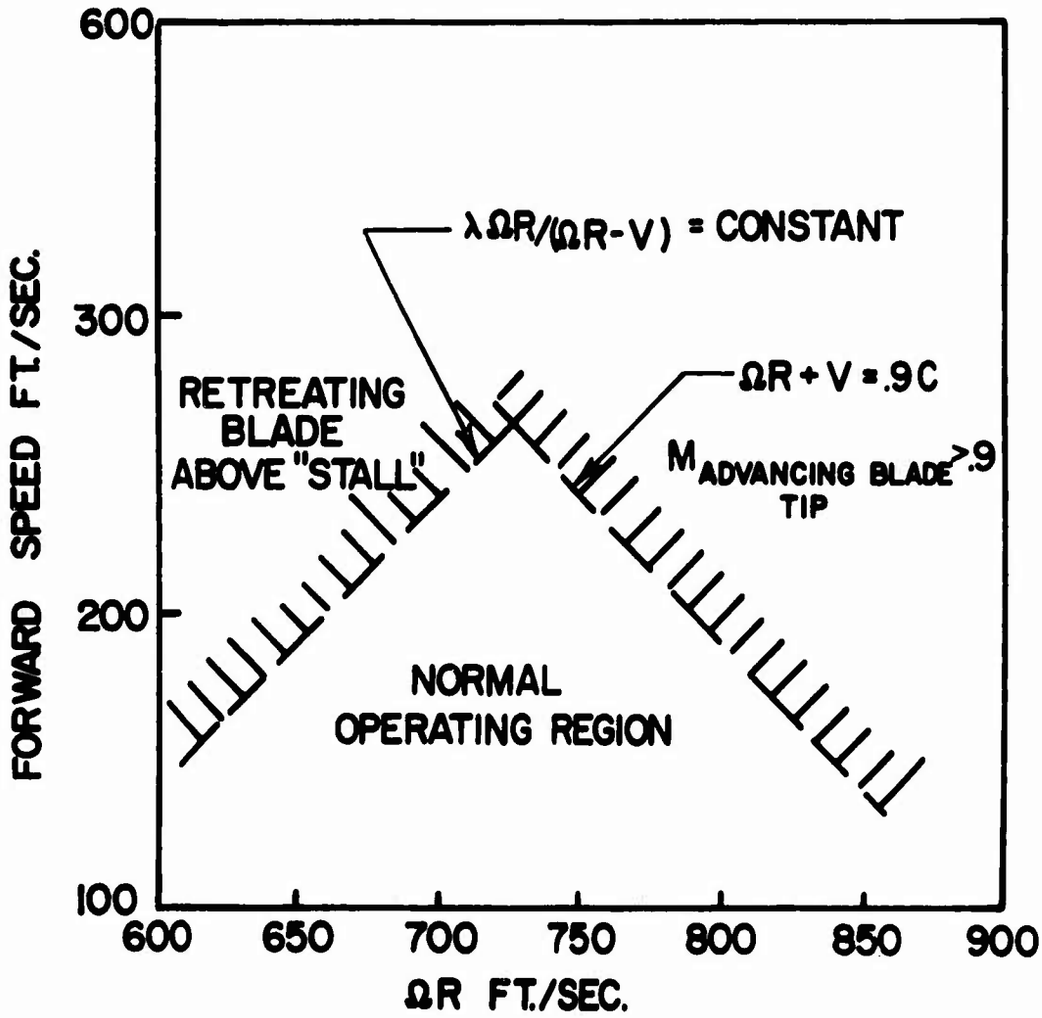

Figure 1. Stuart Plot.

Very rapid angle-of-attack changes occur, which can lead to unusual pressure gradient actions in the boundary layers.[3] Periodic stall flutter on retreating blades has also been subject to recent intensive study.[5]

From the foregoing enumeration of actions which relate directly to boundary layer behavior, it is apparent that many interactions do indeed exist and that detailed studies of rotor boundary layers should prove to be a fruitful field of research. Greater understanding of the boundary layer actions would aid those efforts to produce better airfoils for helicopters, or those programs which seek to use boundary layer control of jet flap devices to increase rotor performances.

APPROACH

The study of the boundary layer behavior on a helicopter blade was initiated by a review of the possible ways to observe the boundary layer experimentally. This review led to the adoption of chemical trace methods of flow study as a logical technique. Concurrently, review of analytical methods for rotating boundary layers was undertaken, and this review led to an attempt to modify available theory. As the studies on flow visualization progressed during the program, design and fabrication of a test stand and flow channel were initiated. Exploratory studies of the chemical trace techniques were conducted in a small low-turbulence tunnel as well as on a rotor hover stand. Subsequent to this effort, extensive tests were conducted on two rotors in hovering and on a model rotor in the flow channel. Detailed consideration of these areas of endeavor will be presented in the following sections.

EXPERIMENTAL METHODS OF FLOW VISUALIZATION

The experimental phase of the work included studies of suitable flow-measuring methods as well as the development of the rotor and flow channel test apparatus. Initial efforts were directed toward obtaining a satisfactory method for flow visualization.

BOUNDARY LAYER FLOW VISUALIZATION

The lack of experimental data on the rotor boundary layer is largely due to the compound problems of boundary layer measurement and instrumentation in a centrifugal field. Meaningful boundary layer measurements must be made at heights on the order of 0.010 inch, thus imposing many practical problems on the experimenter. In addition, large centrifugal forces are present, being as high as 4000 g's at the tip of a typical tail rotor.[4] Many materials used for flow visualization are unsatisfactory for use in centrifugal fields because their densities, quite different from that of air, cause them to experience a greater outward force. Wool tufts, some chemicals, smoke, and oil are common visualization devices, but they may be unreliable for flow visualization in high centrifugal fields. They also tend to average out potentially important actions in the boundary layer. Subliming chemicals, such as acenaphthene, are useful for locating transition lines. Some studies of flow direction have been conducted using these chemicals with vortex or disturbance generators. These vortex generators act by triggering a local turbulence behind the generator, and this turbulence tends to move back with the local airstream. This resulting turbulence causes an accelerated rate of sublimation of the chemical coating. The region from which the coating is removed indicates the direction of the boundary layer flow. In using this method, one must assume that the turbulence zone reveals the direction of the undisturbed boundary layer. The subliming chemicals, however, have molecular weights of more than five times that of air (154:29), and questions can arise as to the proper interpretation of the turbulence trace when they are used to indicate flow direction in high "g" fields.

It was decided to search for chemical trace techniques which might overcome some of the limitations of the various probe methods or the subliming chemical technique. The basic concept involved the injection of a tracer gas into the boundary layer, which would then move with the boundary layer. This tracer gas would, in turn, react with a chemically coated surface of the rotor blade airfoil in such a way that the trace made on the surface, if visible, would provide an indication of the local flow direction. Several chemicals were considered in a preliminary screening process. The following is a listing of some of the chemicals considered. In all these cases the reaction of the chemicals to NH_3 was considered and is listed with the chemical.

Methyl Red - slowly turned yellow

Bromphenyl Blue - turned blue quickly with a very distinct trace

Thymol Blue - turned purple but the trace was not sharply defined

Although these chemicals indicated some promise for use as surface coatings, it was decided to investigate the possible use of the ordinary blue-line or "Ozalid" blueprint reproduction method. In this method the "blueprint" paper has been coated with a chemical which reacts quickly to ammonia vapor. If the paper is exposed to ammonia, its color changes from yellow to a blue-black color. The use of pretreated paper and a technique as proven as the "Ozalid" azo method appeared to be very attractive, and an intensive study was started. In addition, since the molecular weight of ammonia is close to that of air (a ratio of 17:29), it should not be affected markedly by the centrifugal force field.

Ammonia-Azo Streak Process

Literature review revealed that the ammonia-azo method of flow visualization was first used by Ruden in 1937 and more recently (in 1964) by Johnson in the study of centrifugal compressors.[6] The chemistry of the reaction involves the joining of a diazonium salt and a naphthol coupling component to form a diazo or azo dye. The reactants are yellow, and the products are a dark color. For this reaction to proceed, a basic pH is necessary and the ammonia provides this. A typical reaction is shown in Figure 2.

In the actual use of the ammonia-azo process, the chemically coated paper was fastened to the surface of the airfoil being tested. Either rubber cement or double-sided tape was utilized. Ammonia vapor was released through small orifices located at the surface. The paper was pricked at these orifices to allow the passage of the ammonia. During the major portion of the test program, the ammonia vapor was produced by bubbling air through an ammonium hydroxide solution. The vapor was then carried through plastic tubing directly to the airfoil, in the case of the two-dimensional tests, and to a transfer ring, in the case of the tests using the rotor stands.

A diagram of the ammonia-feeding apparatus, the hover stand, and the airfoil is shown in Figure 3. The setup is seen to be a fairly simple one. Metering was used, and the pressure was regulated to assure a low exit velocity of ammonia to prevent disruption of the boundary layer at the ammonia orifice. The pressure level in the reservoir was held, in most cases, to a few inches of water pressure. In the higher rotor speed runs, reservoir pressure of the air supply had to be raised to values as high as 2 feet of water in order to obtain the desired traces on the rotor airfoil; during pulsed valve operations, the line pressure of NH_3 was held at approximately 3 psi.

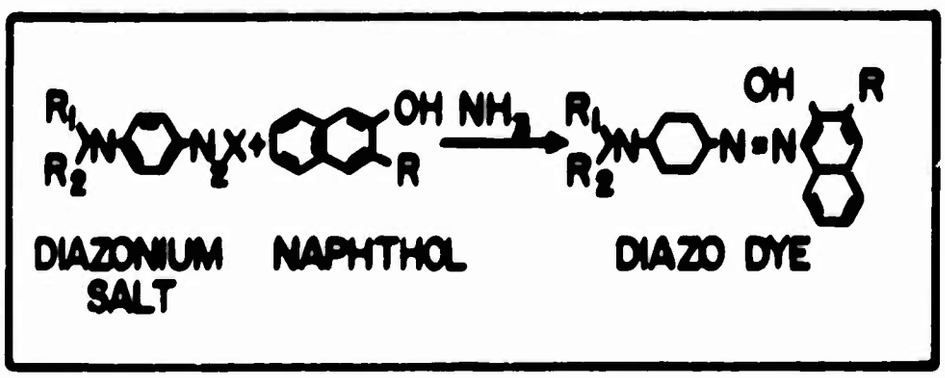

Figure 2. Formation of Diazo Dye.

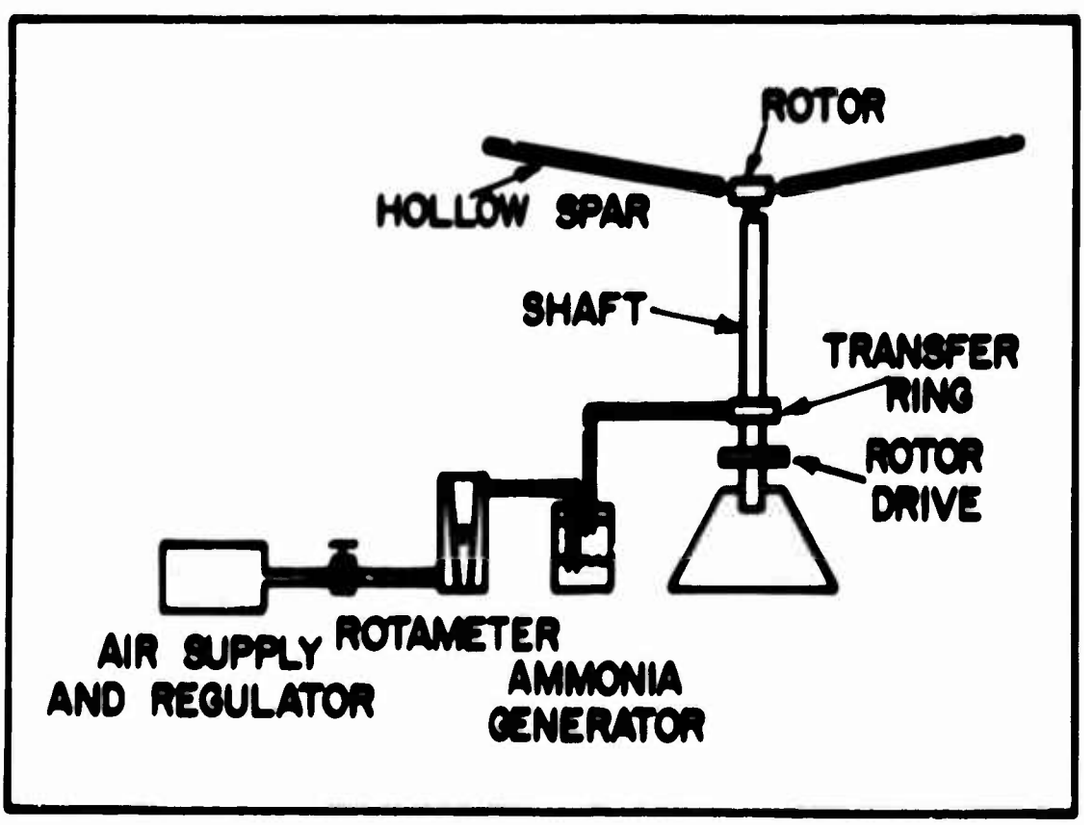

Figure 3. Diagram of Small Hover Stand.

After injection into the boundary layer, the ammonia will mix quickly with the air in the region of the orifice and will be carried along with the local airflow. As it diffuses to the surface, it will leave a permanent trace on the paper, which should be indicative of boundary layer flow. Such a trace also should provide an indication of gross effects of the flow outside the boundary layer. It is interesting to note that if one uses hot wires, pitot tube probes, or other pressure transducers to study the flow field on the surface, data are obtained from only one point at a time. When such probes are used, it is necessary to mount a large number of them in the fluid stream in order to provide data over a complete region. The ammonia trace technique, however, provides information all along the path of the ammonia, and fairly large regions of flow can be studied with a few traces.

Since one of the primary objectives of the study was the boundary layer on the retreating side of the azimuth, short release times were required, and it was necessary to determine the transient response time of the method. To do this, an electric solenoid to control the ammonia efflux was installed underneath an NACA 0012 airfoil. The airfoil and solenoid were mounted in a two-dimensional, low-turbulence wind tunnel with an ammonia generator similar to that shown in Figure 3. Tests were conducted using a Reynolds number of 4.22×10^5 and a free-stream velocity of 90 fps. An oscillograph recorded the time that current was supplied to the solenoid. The ammonia was introduced into the boundary layer through orifices located at the leading edge of the airfoil and at two other positions on the airfoil surface. All preliminary two-dimensional tests were conducted at zero or low angles of attack. A trace obtained under these conditions consisted of a narrow dark line aft of the orifice which tended to become more diffuse toward the rear of the airfoil. No sharp demarcation occurred along the traces in the chordwise direction to indicate the presence of any unusual boundary layer occurrence.

The preliminary tests were run over a wide range of injection times, ranging from several seconds to milliseconds. It was found that good traces could be made in 200 ms without greatly sacrificing the length of a trace. (The average trace length on the 7-inch chord was 3 inches at $\theta = 0°$.) Traces were discernible with valve speeds as great as 50 ms, but these were faint and were not consistently obtainable.

Heat and moisture accelerate the formation of diazo dye, and some tests were run with the ammonia heated to boiling. The necessary time of exposure was noticeably reduced, but the hot ammonia can be extremely irritating.

One pertinent disadvantage of ammonia-azo flow visualization is that no information is obtained about the velocity of the boundary layer flow. However, this could be obtained if high-speed movie equipment were mounted to record the rate of paper development. Another

criticism is that no boundary layer profiles are obtained because only the flow direction immediately next to the surface is recorded. This could lead to confusion if the flow had a reversal, as shown in Figure 4.

In spite of the disadvantages named, this process gives excellent records of flow paths and at a very low cost. Though not sophisticated, the method can prove very useful information and can serve as the preliminary to more intricate testing methods.

Chemical Sublimation Method

To provide for a reference between data taken in this study and data from other investigations, several chemical sublimation tests were run. The use of chemical sublimation in locating the point of transition between laminar and turbulent flow over an airfoil has been well established and documented by researchers in the 40's and early 50's.[7] Chemicals considered during this study included dissolved biphenyl, fluorene, and acenaphthene. The most satisfactory technique utilized a 10-percent solution of acenaphthene $[C_{10}H_6(CH_2)_2]$ dissolved in acetone, which was sprayed on the airfoil surface. Care was exercised to ensure than an even layer of the chemical was deposited over the surface. If the coating is uneven, it is possible that a misinterpretation could result. The sublimation time of the chemical coating is a function of the temperature, humidity, free-stream velocity, and turbulence of the flow. The turbulence is a particularly important factor in the rate of sublimation, and it is this rapid removal of the coating due to turbulence that makes the sublimation technique valuable.

ROTOR BLADE TESTS

Two major series of tests were conducted using the ammonia-azo technique on rotor blades. The first sequence, which was quite extensive, involved rotors in a hovering condition, and the second sequence involved a rotor in forward flight in a large flow channel.

Hover Tests With 4-Inch-Chord Blade

The initial tests using the trace technique were conducted using a two-bladed teetering model rotor mounted on a hovering test rig. Figure 5 shows the test rig with the model rotor mounted. The rotor utilized a 6-foot-diameter NACA 0015 blade section with zero twist, and a 4-inch chord. The pitch angles could be adjusted over a wide range. The blade was constructed using a steel tubular spar as the primary structural member, with a pine leading edge, a 1/32-inch-thick plywood chordwise web in the aft portion of the blade, and balsa wood blocks to fill out the contour. The cross section of the blade is illustrated in Figure 6. The ammonia vapor for the hover tests was generated in a manner analogous to that described previously. Air from the laboratory high-pressure air supply was passed through a commercial-gas regulator

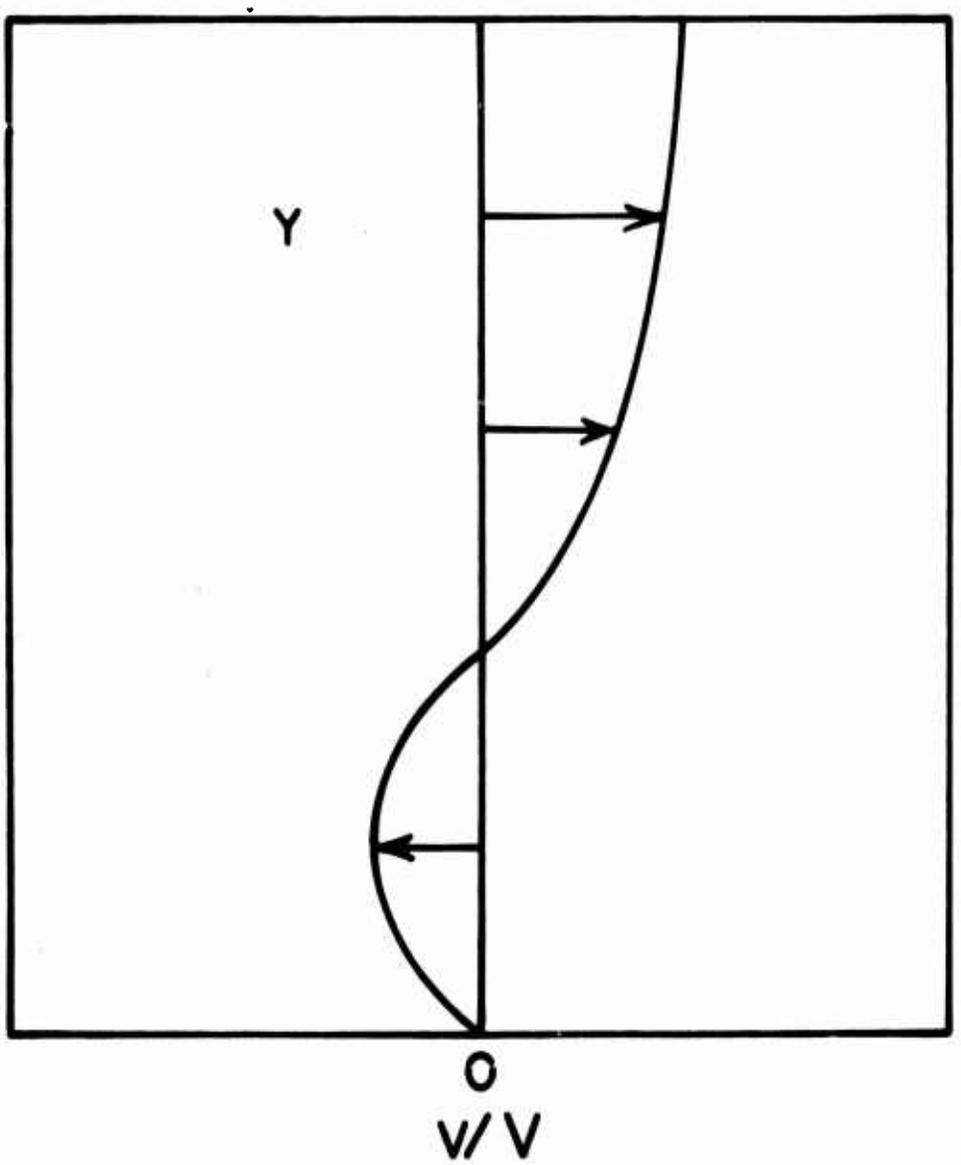

Figure 4. Flow Reversal in a Boundary Layer.

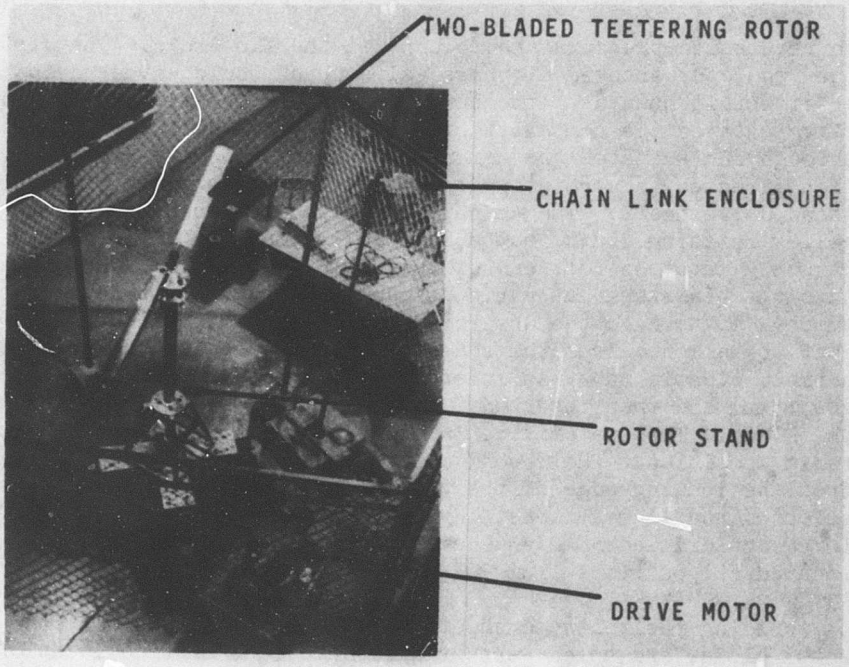

Figure 5. 4-Inch Chord, 2-Blade Rotor and Test Rig.

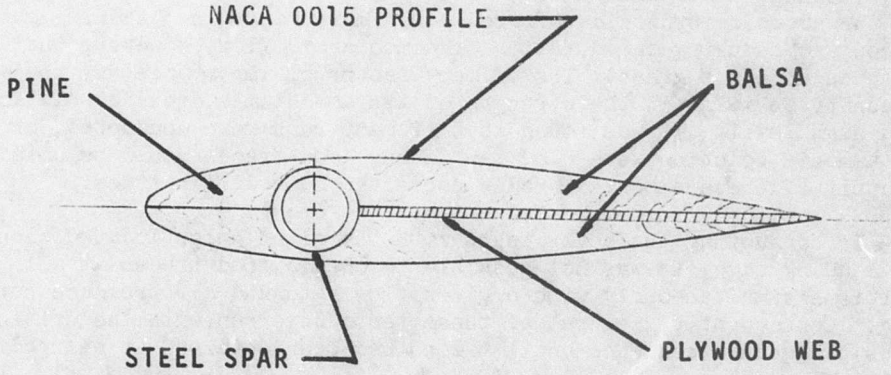

Figure 6. 4-Inch-Chord Blade Cross Section.

to reduce its pressure and to control the flow rate. The air leaving the regulator entered a bypass valve which could either dump the air or direct it onward to the ammonia system. The air leaving the bypass valve entered the container of ammonia hydroxide, where it bubbled through and agitated the ammonia solution. The air-gas mixture was then directed to a rotating transfer ring at the base of the rotor stand drive shaft. The ammonia-air mixture then passed up through the hollow rotating shaft, out a lateral port at the top of the shaft, and directly into the root end of the hollow blade spar. Holes were drilled into the blade spar at various spanwise locations to deliver the air-ammonia mixture to the desired location. Two techniques were used to duct the ammonia from the spar to the orifice. In the initial tests, a small plastic tube was inserted into the spar from the bottom side of the blade and then inserted into a drilled hole to the leading edge of the blade. The one orifice made in this manner was located at the 72% radius position. The second method consisted of drilling holes directly from the leading edge of the blade into the hollow spar at a series of selected radial positions. Hypodermic-needle tubing was then pressed into each drilled hole and cemented in place. These orifices were located at positions from 20% to 90% radius in 10% increments.

During the tests, a sheet of "Ozalid" paper was fastened to the rotor blade, and holes were pricked into each orifice location. The ammonia system was set into operation by opening the pressure regulator and setting a given flow rate, using a standard rotameter. Prior to each data run, the bypass valve was placed in the dump position so that no ammonia would be sent into the blade. When the desired rpm of the rotor had been reached, the bypass valve was actuated and the ammonia-air mixture was allowed to pass out the lines to the orifices in the blades. The time for making the traces was varied from a few seconds to several minutes.

Testing was conducted with both heated and unheated ammonia. Heating the ammonium hydroxide offered some improvement in obtaining good traces and reducing the duration of ammonia-air flow; however, the differences were not great. The primary factor of importance was the necessity to maintain the strength of the ammonium hydroxide solution at a high level. It was found that if many runs were conducted, or the ammonia solution were old, few if any good traces could be obtained. A supply of fresh ammonia usually corrected such difficulties.

In conducting the hover tests with the eight holes located along the leading edge, it was not possible to obtain good traces at all positions simultaneously with a given flow rate and air pressure setting. Consequently, several of these tests were run with the orifice holes plugged in sequence until traces had been obtained at all radial positions.

The rotor speeds used in this sequence ranged from 200 to 800 rpm, and pitch angles from -15° to + 25° were covered.

Tests With 7-Inch-Chord Blades

One of the primary areas of concern with the boundary layer on rotor blades is in the retreating side of the azimuth. Consequently, it was necessary to devise a technique which would provide for ammonia-azo traces on the retreating blade over a limited angle of rotation of the blade.

To accomplish the testing on a retreating blade, it was decided to devise a method of pulsing the ammonia vapor over the selected azimuth. Tests with the solenoid valves in the two-dimensional tunnel had indicated that traces could be obtained for single pulse times as short as 50 ms, but they were faint. It was believed that if suitable valving could be arranged, the ammonia flow could be pulsed in a repetitive fashion at a particular azimuth of the blade to get sufficiently distinct traces to allow interpretation of the boundary layer flow direction. The basic assumption in such a process is that the external airflow and boundary layer flow will be repetitive during each revolution. It was anticipated, nonetheless, that the method would provide an averaged trace over the selected azimuth. This would provide useful first-order data where none had been available. The azimuth angle over which the ammonia would be emitted was planned to be variable.

DESIGN OF EQUIPMENT

ROTOR SYSTEM

The rotor system for the forward flight tests was designed to operate either as a two-bladed teetering rotor or as a counterweighted single-bladed rotor. Figure 7 illustrates the general layout of the rotor considered. It was decided to utilize the single-bladed configuration in the study of the boundary layer in forward flight. The hub and yoke were machined from a solid steel block. Provisions were incorporated for a counterweight whose radial position could be varied to provide proper balance to accommodate various changes in the mechanism installed in the blade. The blade was designed as a built-up structure using a laminated birch leading-edge spar, a full-length steel strap in the leading edge, and a rib with plywood-covered aft section. The blade structure is shown in Figure 8. The blade was attached to the yoke by means of a steel-fork fitting. The spindle of the fork passed through the hub yoke. The blade pitch angle could be set by turning the steel fork into the desired position. A graduated scale was incorporated in the hub yoke to facilitate blade pitch setting.

The rotor blade section used was an NACA 0015 airfoil. The blade chord was 7 inches, and the overall rotor diameter was 6 feet. The design tip speed for this rotor was 300 fps, which corresponded to a rotational speed of 955 rpm. The blade airfoil contour was carefully controlled. A series of computer-developed gage points was established for the airfoil templates, which were then located using a tape-controlled mill. The final templates were then hand-finished to the final shape. The airfoil was milled to shape, where possible, and hand-finished to final contour. Specific attention was given to avoiding any flat spots on the airfoil surface. The airfoil surface is considered to be within ±0.010 inch of the desired airfoil contour and closer than that value over the more critical leading edge. The airfoil surface was finished by spraying a series of base coats on the surface, by final sanding, and by spraying a finish coat of flat black paint. The orifices on this blade were located at the leading edge at 61.5%, 74%, and 87% radius.

VALVE SYSTEM

The valve to pulse the ammonia in the blade must meet some stringent requirements. The desired characteristics for such a valve system include short duration of opening, good sealing when closed, minimum restriction to gas when open, controllable open time, controllable azimuth position of pulse, light weight, and compactness to fit in a small rotor blade. The smallest electrical valve considered and tested had too slow a response time, it was slightly too large and too heavy for the rotor application.

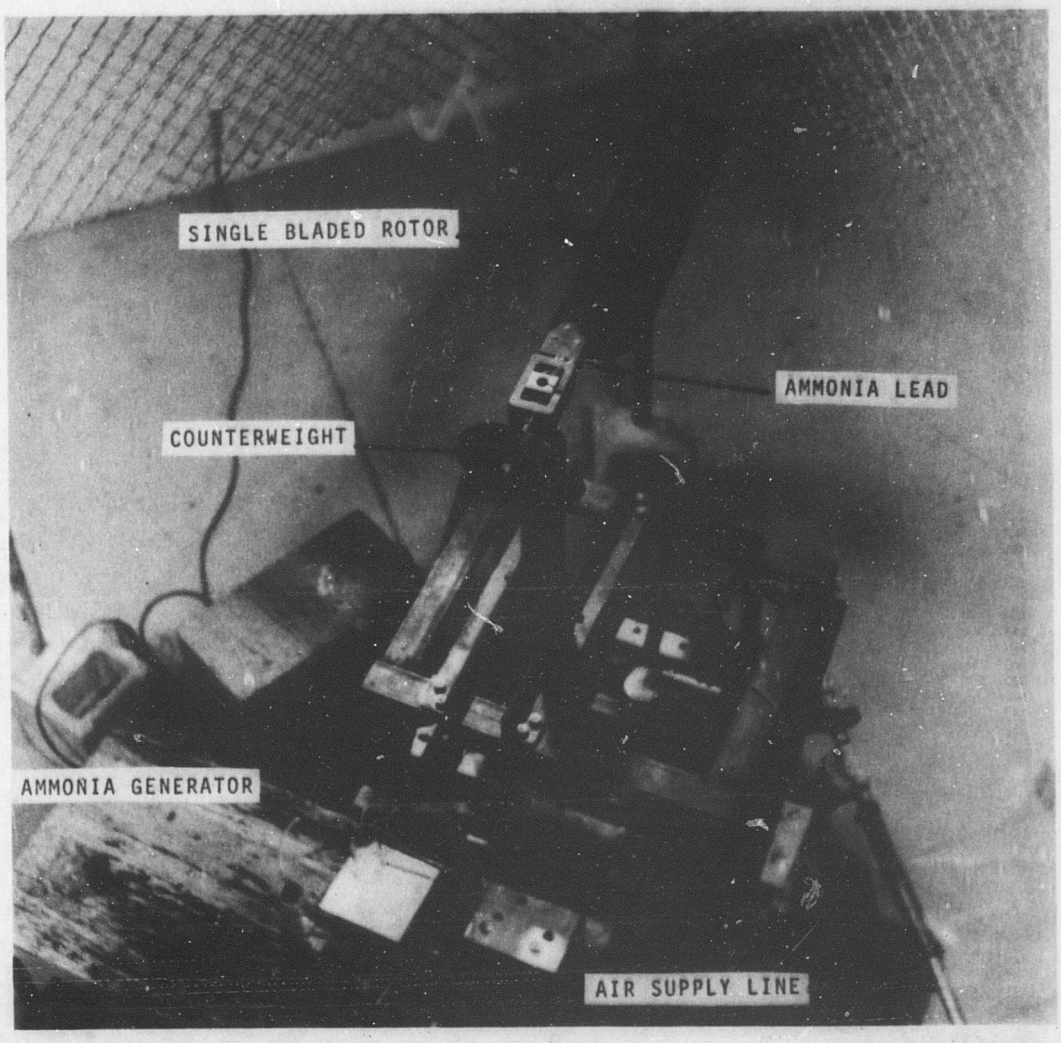

Figure 7. 7-Inch-Chord, Single-Blade Rotor.

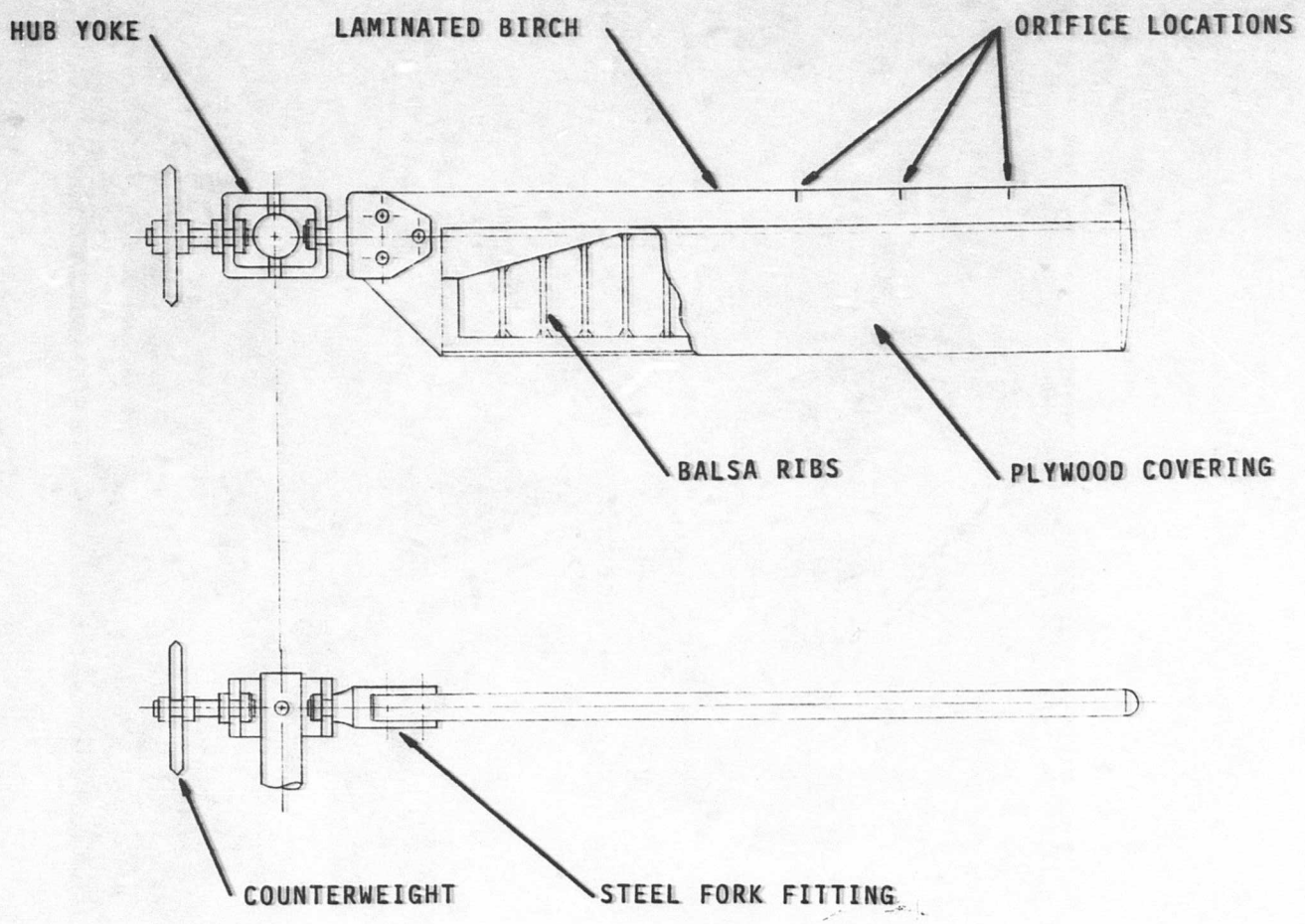

Figure 8. 7-Inch-Chord Blade Structure.

Mechanical valve arrangements were then considered. Two types of valves were designed and tested; i.e., a spool valve and a poppet valve. The poppet valve seemed to provide better results and was used for the majority of the forward flight tests conducted. A schematic of the overall valving arrangement is shown in Figure 9. The valve system is composed of the following elements: a poppet valve in the blade, a pivot link at the center of rotation, and a cam assembly at the bottom of the rotor mast. The operation of the unit can be most clearly seen by study of the actions of the elements shown in the figure. As the rotor rotates, the cam rotates. The cam lobe engages the cam roller follower, moving it outward. The cam roller motion causes the rocking link to push up on the push rod slider, which in turn drives the main push rod upward. The pivot link then acts to pull the blade valve rod inward, which unseats the poppet valve. This in turn allows ammonia vapor to flow through the valve and to the orifices located in the leading edge of the blade.

In order to evaluate the performance of the entire valve system ammonia flow system, a breadboard setup was designed and constructed (see Figure 10). In this test arrangement the actual valve drive components (including the cam, rocking link, all push rods, and the valve itself) were included. As can be seen in the figure, the cam is rotated by the output of the speed reducer. The speed reducer also drives a rotating cylinder by means of the chain. This cylinder is covered with a sheet of "Ozalid" paper, and it translates along its axis as it rotates. As the cam is rotated, the valve is actuated. The ammonia vapor from the ammonia supply is released through the valve each time the cam lobe strikes the follower. The ammonia vapor is carried by a short length of tubing, similar to that used in the model blade, to an orifice which is directed at the "Ozalid" paper on the cylinder. Since the cylinder rotates at 12/25 of the speed of the cam, the short puffs of the ammonia released by the valve describe a helical pattern on the "Ozalid" paper. In operation, cam speeds from 200 to more than 1000 rpm were used to simulate the operating range of the model rotor. It was necessary, however, to replace the steel main push rod with a hollow, large-diameter aluminum tube. Tests using a strobe light had shown that the natural first bending frequency of the steel rod fell within the desired operating range. The breadboard tests of the ammonia valve system indicated that the ammonia vapor pulsed satisfactorily. Study of the traces on the "Ozalid" paper revealed that the traces extended over an azimuth of approximately 25° at 500 rpm to approximately 50° at 1000 rpm. The traces were distinct and very repetitive. Based upon these results, the entire valve system was installed in the model rotor assembly.

HOVER TEST STAND

The hover test stand used in the initial tests of the 4-inch-chord blade and the sublimation tests shown in Figure 5 consists of a heavy

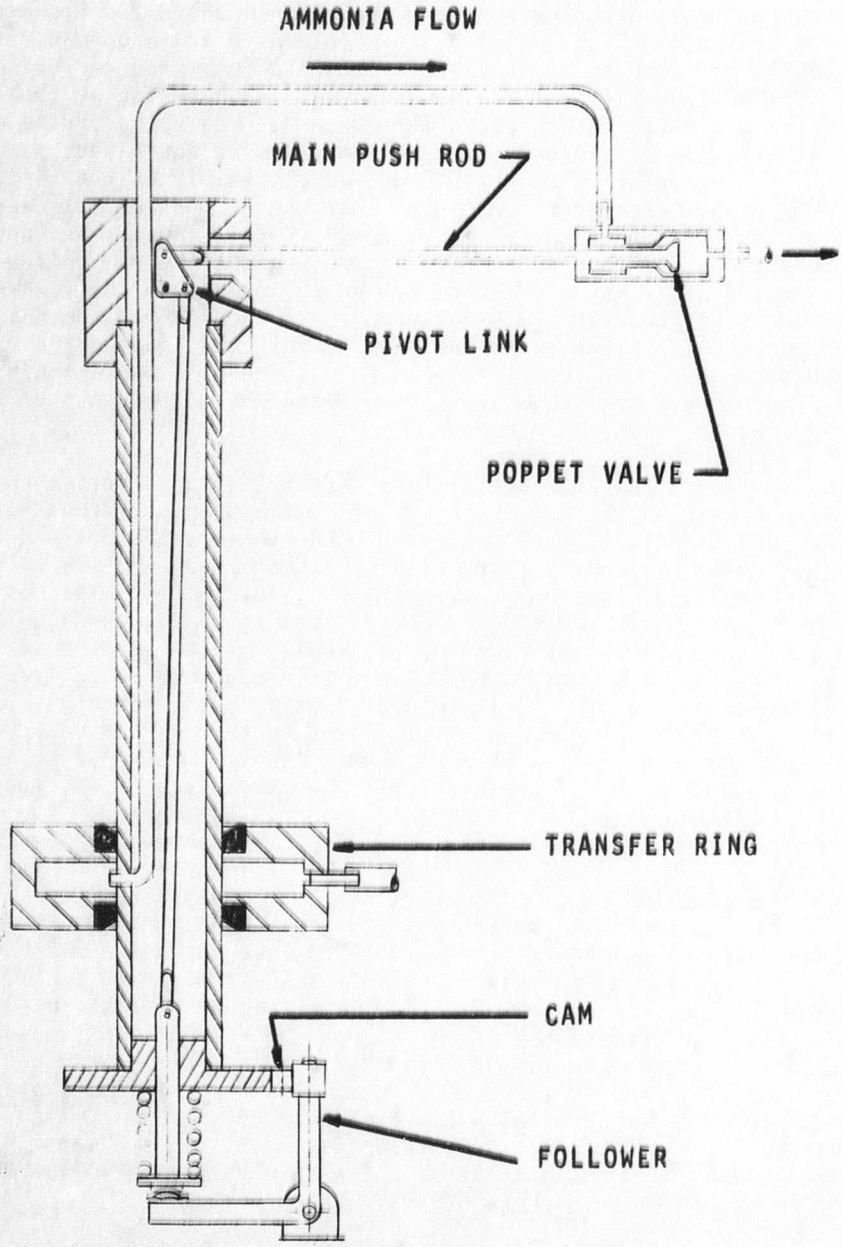

Figure 9. Valve System Schematic.

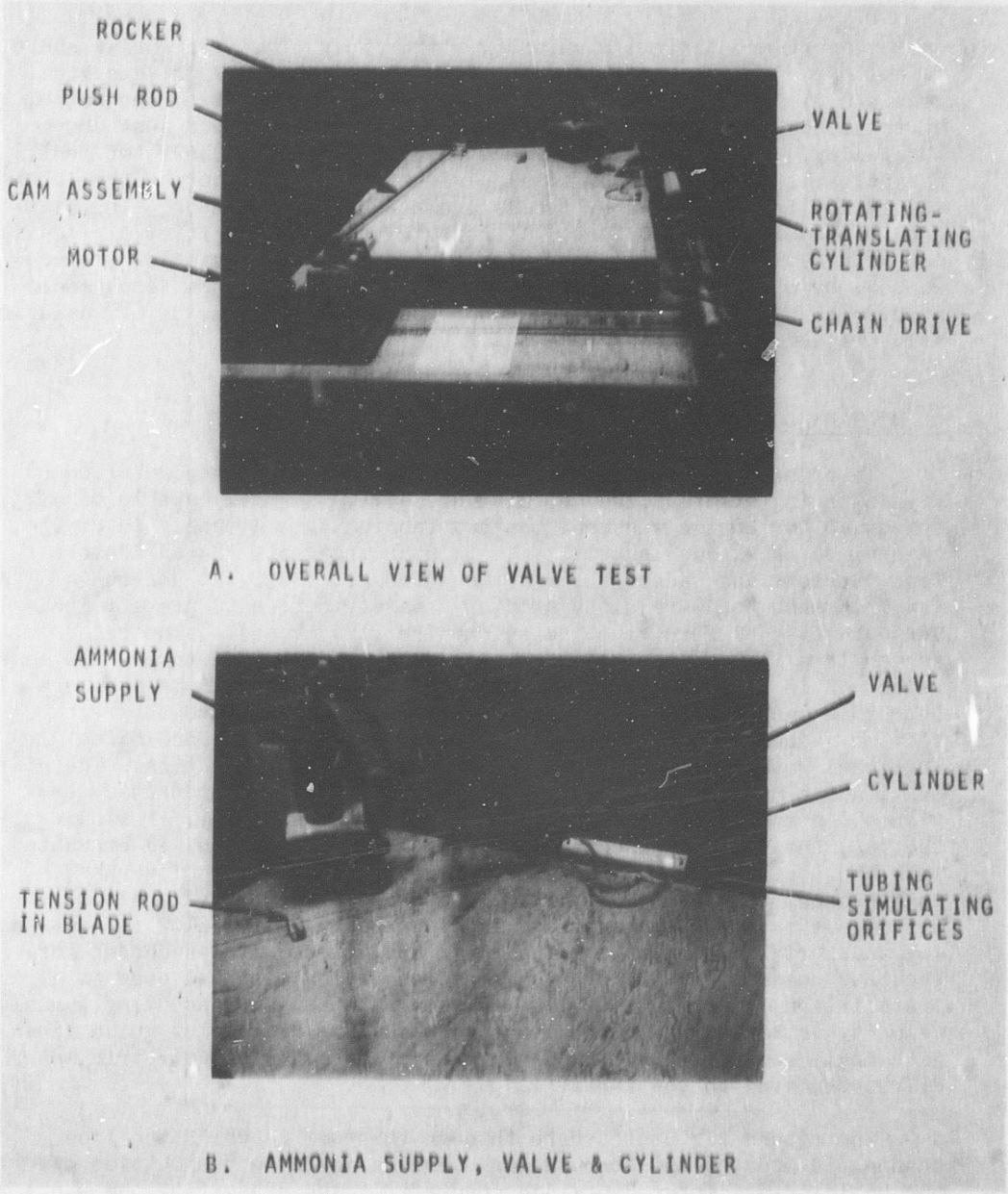

Figure 10. Valve Test Rigs on the Plywood Sheet.

base support and a rigid stationary stand pipe. The rotor drive shaft is hollow and runs through three sets of bearings. The drive system consists of a dc electric motor connected by a "V" belt to the bottom of the rotor shaft. The ammonia transfer ring is located just above the pulley. The tachometer is located at the base of the rotor mast. The rotor is located approximately 7-feet above the floor of the laboratory and is surrounded by two layers of chain-link fence. The diameter of the fence is 10 feet. It is beleived that the rotor airflow is not affected significantly, insofar as boundary layer studies are concerned, by either the ground plane or the presence of the fence enclosure. The speed control of the rotor was achieved by means of variable armature and field resistors.

FLOW CHANNEL

In order to provide the test conditions to study the rotor boundary layer in forward flight conditions, a flow channel capable of air speeds up to 100 fps was designed and fabricated. A schematic of the channel is shown in Figure 11. In this arrangement, the air enters from the left and passes through two screens. The first screen is 1/4-inch mesh hardware cloth used as a safety screen to prevent inadvertent entry of foreign objects into the flow channel. The second screen is a 16-mesh stainless-steel screen incorporated to provide some reduction in the turbulence of the tunnel. The air then is accelerated through a convergent entrance section prior to entry into the test section. The test section is 4 feet high, 8 feet wide, and 8 feet long. The model rotor is located at the center of the test section. The air leaving the rectangular test section passes through a transition section and a safety screen, and then into the fan assembly. Following the fan, the air is passed through a conical diffuser and is exhausted into the test room. The fan assembly consists of a set of variable inlet vanes, the rotor of the fan, a 150-hp ac motor, and a set of stator blades. The fan assembly is a commercial axial-flow fan designed for industrial drying or cooling tower operation. It was chosen for the flow channel because of a combination of low cost and ease of installation and operation. The airflow rate and corresponding tunnel velocity is varied by controlling the blade angle of inlet guide vanes. Such angle control is achieved by means of a reversible electric motor drive connected to the vanes.

The return air passes both through the room in which the flow channel is located and through large double doors to the outside of the building. A large door is opened aft of the exhaust of the tunnel, and large doors are opened near the inlet of the channel. In this manner, an adequate airflow and suitable air exchange are provided. The design test section speed of 100 fps was readily reached with a significant reserve capability in flow rate and power still remaining. The assembled flow channel is shown in Figures 12 and 13.

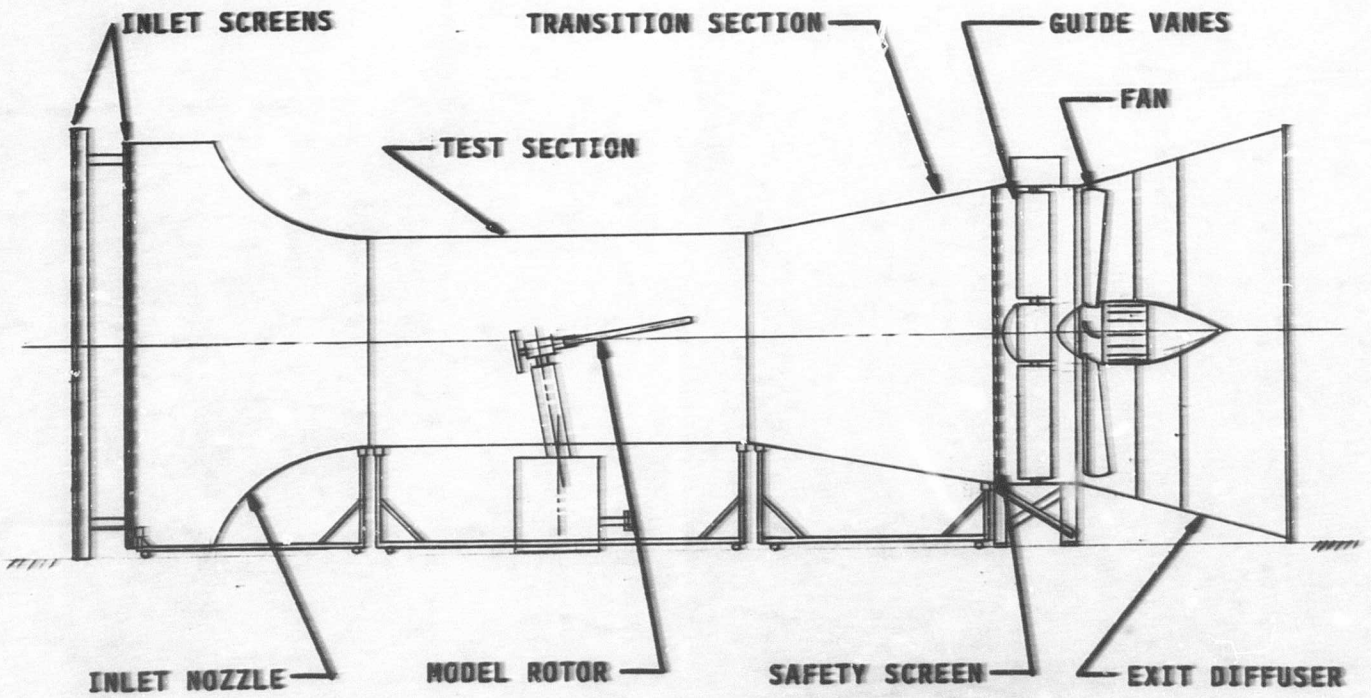

Figure 11. Model Rotor Wind Tunnel.

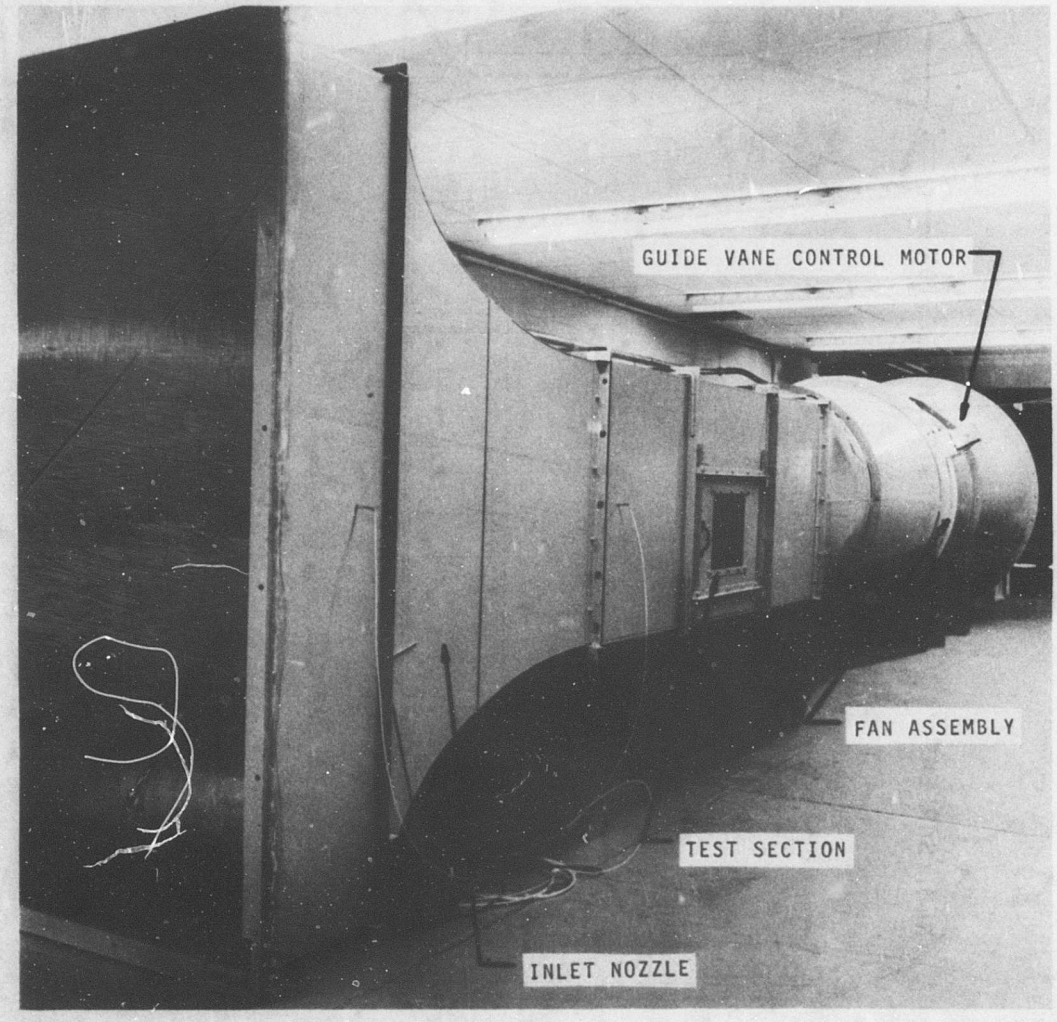

Figure 12. The Assembled Model Rotor Wind Tunnel.

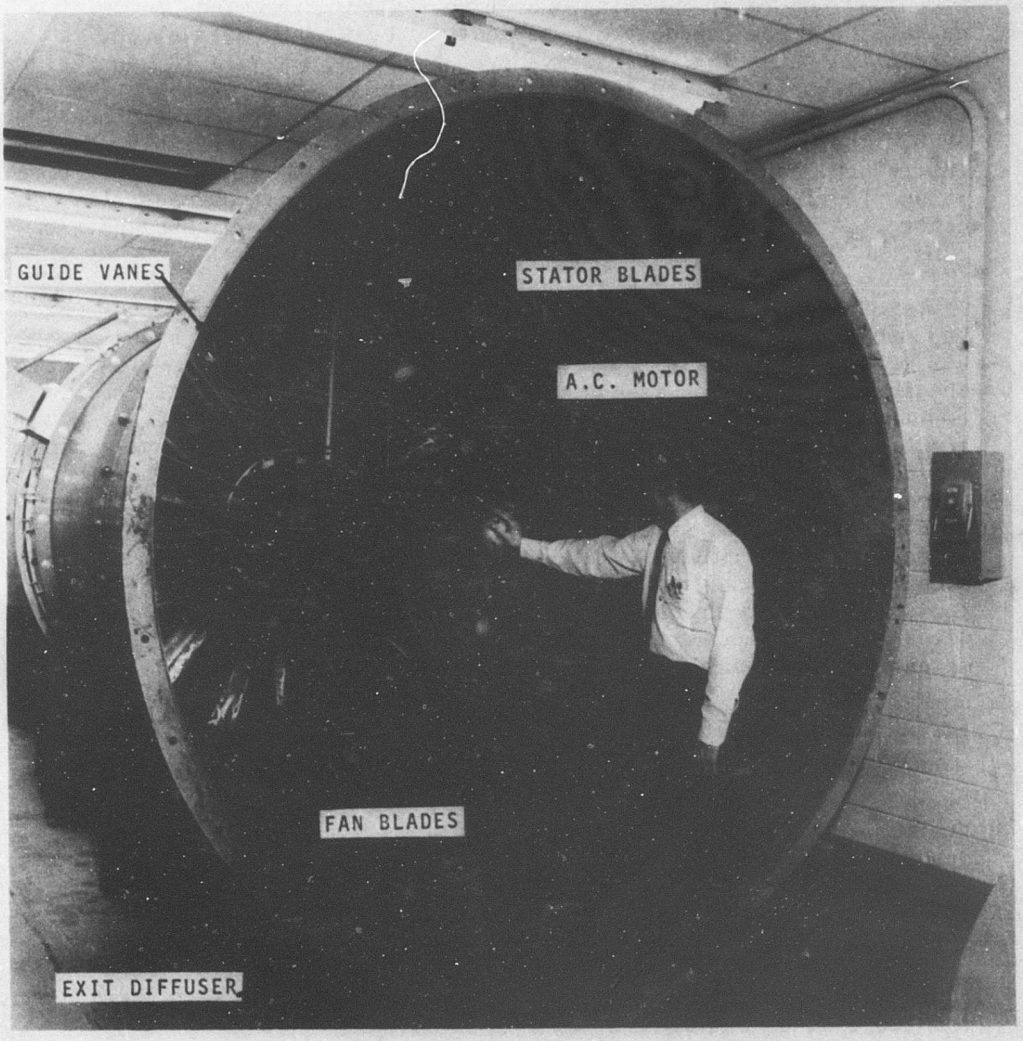

Figure 13. Tunnel, Fan, and Diffuser Assembly.

ROTOR DRIVE SYSTEM

The boundary layer studies in forward flight require a test facility which can properly duplicate helicopter rotor operation over a broad range of conditions. The large flow channel was designed to provide a uniform airflow over a range of velocities up to 100 fps. Likewise, the rotor mounting and drive system must be adaptable to a range of airflow speeds, rotor speeds, and rotor thrust values. To accomplish this, the rotor drive system shown in Figure 14 was designed and fabricated. Figure 15 shows the assembly. The rotor to be tested is mounted atop the drive shaft, which is carried in the stationary mast. The stationary mast is connected to the drive assembly, and this entire unit can be rotated about the mast pivot to achieve the desired value of drive shaft inclination. This inclination, or mast tilt, is controlled by means of a long lead screw and can be adjusted between runs.

The power for the rotor is obtained from a 10-hp air motor which is connected by "V" belts to the rotor drive shaft. The speed of the air motor is controlled by means of a standard air-pressure regulator. The speed of the unit is monitored through the use of an electronic counter and is considered to be accurate to within 1%. The air motor and belt assembly, as well as the stationary mast, are mounted upon the tilting frame. The entire assembly tilts as a unit to the main frame when the lead screw is turned. This tilting frame in turn is mounted to the main frame by means of the mast pivot pin. The main frame in turn is mounted to the floor on rubber blocks. The rubber blocks are so chosen to ensure that the operating frequencies are above the natural frequency of the entire assembly. The proper blocks were chosen during preliminary tests, using various vibration measuring techniques.

FORWARD FLIGHT AMMONIA SYSTEM

The ammonia transfer system is similar to that described for the hover stand. During some runs, the transfer ring was located below the base of the stationary mast. However, because of somewhat erratic behavior of the system, a second transfer ring was designed and fabricated. This second unit was located on top of the rotor. It consisted of a rotating housing, a central nonrotating shaft, and two leather seals to prevent leakage of ammonia. The nonrotating shaft was restrained by means of a cable leading to the sidewall of the flow channel. The ammonia was brought into the transfer ring by tubing from the top of the test section.

In the forward flight tests, two methods of obtaining ammonia were utilized. The initial tests were conducted using the same technique as used in the hover tests; i.e., air was bubbled through a heated NH_4OH solution. Because of the somewhat erratic results obtained with this method during forward flight tests, the system was modified to use

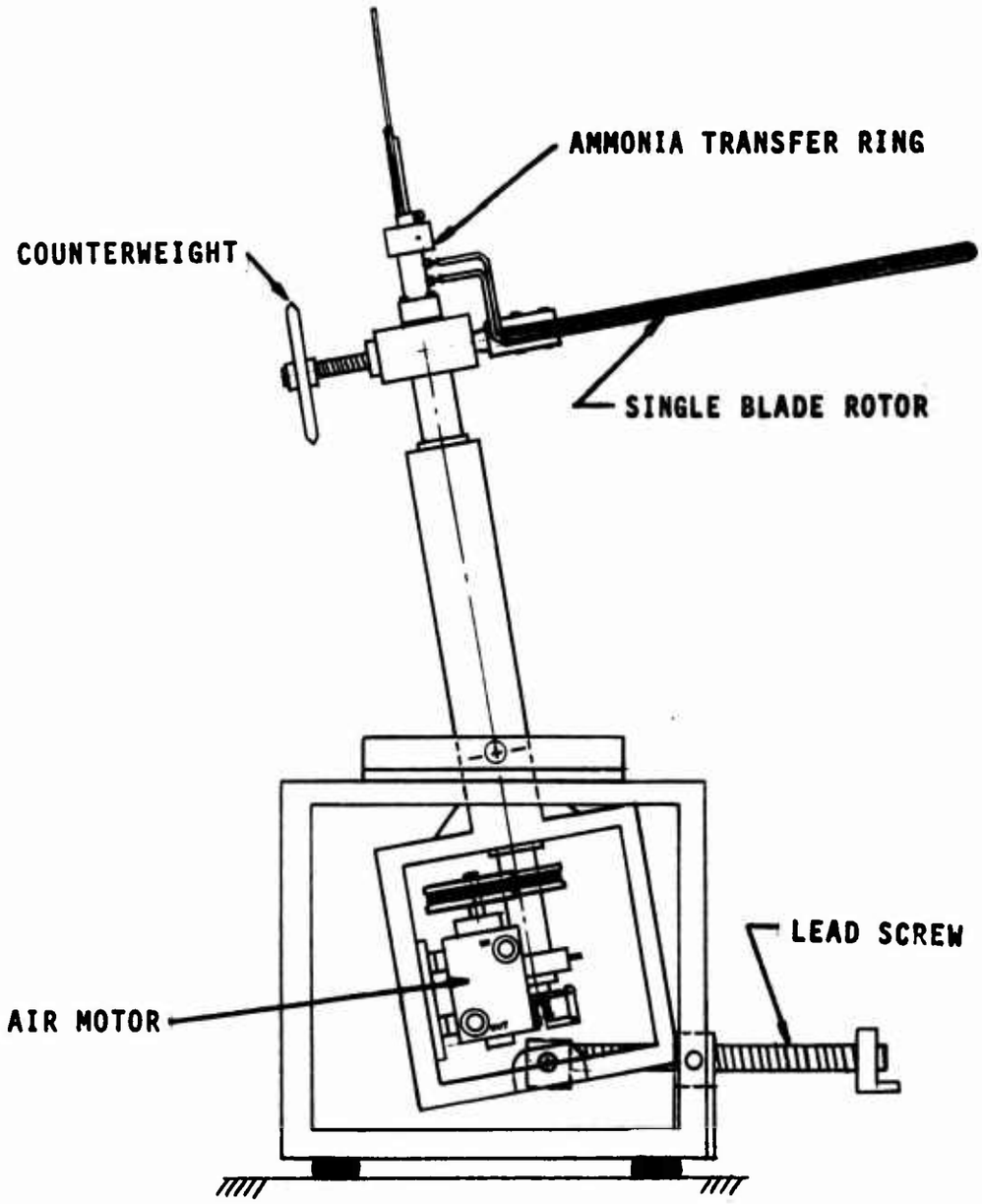

Figure 14. Schematic of Rotor Drive System for Tunnel Use.

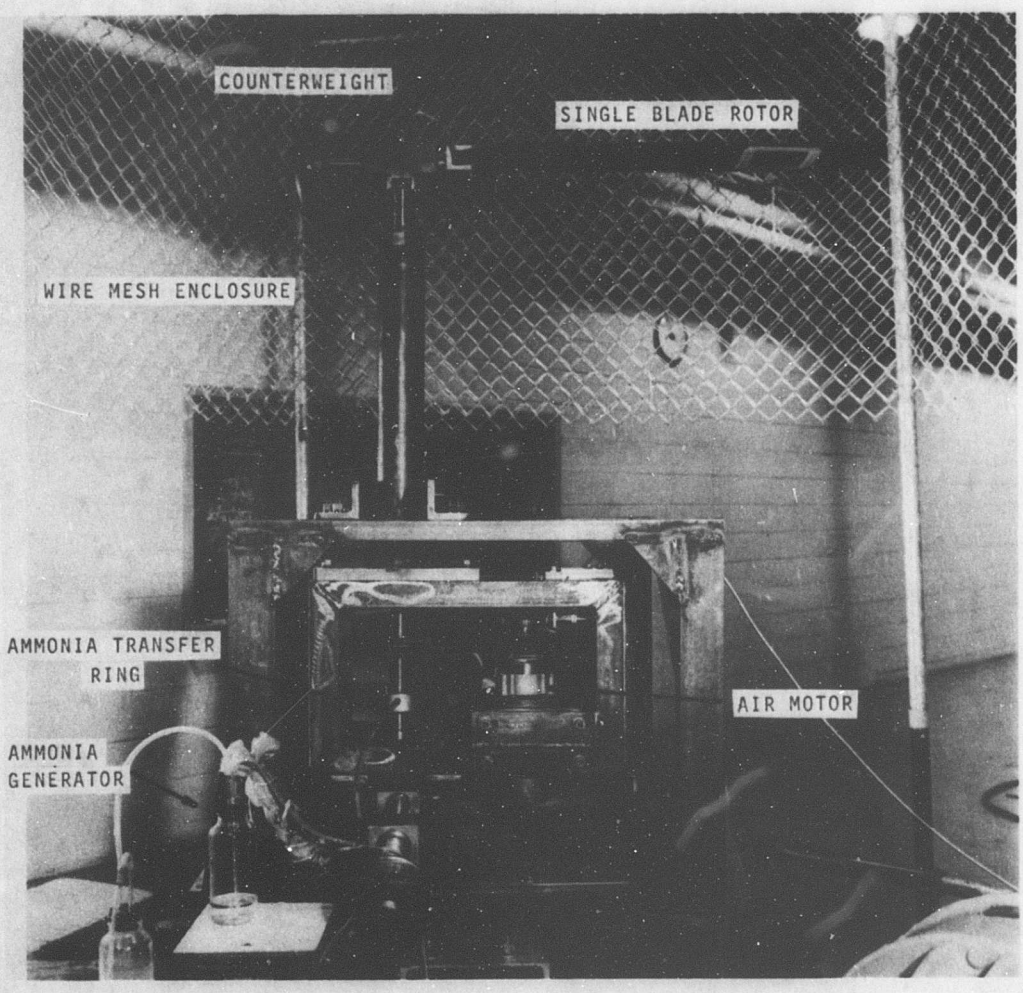

Figure 15. Tunnel Rotor Drive System With Single-Blade Rotor.

ammonia gas directly. In this method a commercial high-pressure tank of NH_3 was produced. A needle valve was installed on the tank to meter the amount of ammonia, which was measured by means of a rotameter. A pressure gage was installed in the line to measure supply pressure to the transfer ring. With the NH_3 gaseous system, the traces were obtained more consistently. In order for the ammonia-azo reaction to proceed properly, it is necessary to have sufficient moisture and relatively warm temperatures of the air stream. It was found that on cold, dry days, traces were difficult to obtain; whereas on warm, humid days, dark and distinct traces could be obtained within 15-20 seconds running time. Typical conditions for the NH_3 gas technique were a flow rate of 0.04 cfm, a pressure of 3 psi, and test times from 30 seconds to 2 minutes. The test times depended primarily on the prevailing weather conditions.

EXPERIMENTAL PROCEDURE

EXPERIMENTAL PROCEDURE FOR 7-INCH-CHORD ROTOR TESTS (HOVERING)

The hovering tests using the 7-inch-chord blades were essentially conducted in a manner similar to that previously described for the 4-inch-chord blades. The tests of the 7-inch-chord rotor, however, were conducted using the rotor drive stand designed expressly for use in the large flow channel. Ammonia traces were run both with the blade valve operating and with the valve bypassed. The purpose of using the valve during the hover tests was to evaluate the overall operating characteristics of the valve system in the rotor. It was quickly found that the initial design using a spool valve was inadequate; this knowledge led to the redesigned poppet valve discussed previously. When the poppet valve was installed and tested in a hovering state, it operated satisfactorily. Good ammonia traces could be obtained on the blue-line paper in a manner of 20 to 30 seconds' time with the valve operating.

A separate sequence of tests was run using the 7-inch-chord blades in hovering with the valve bypassed. The purpose was to ascertain if boundary layer behavior would be similar to that of the 4-inch-chord blade during hovering tests. The techniques of supplying ammonia and applying the sensitive paper and the general conduct of these tests was essentially the same as those with the 4-inch-chord blades. The method used was the bubbling of air through the NH_4OH solution. The outside weather conditions in all of the 7-inch-chord hover tests were hot and humid, and consequently good traces were obtained consistently.

The test sequence included a blade pitch angle range of $\theta = 0°$ to $\theta = 20°$ and a rotor speed range from 200 to 1,000 rpm. It was necessary at the higher operating speeds to selectively plug up some of the holes in the blade and thus obtain a complete set of traces by conducting several runs. The ammonia flow rates ranged from 0.03 cfm to 0.10 cfm, and pressures of up to 24 inches of water were used.

METHOD OF FLOW CHANNEL OPERATION

To obtain traces during the forward flight sequence, the following method was generally used:

First a flight condition was selected. A computer program for various rotor thrusts and gross weights indicated the necessary values of pitch angle and shaft tilt angle. The blade pitch angle was set, and then the mast angle was set using a precision clinometer. The rotor was then brought up to the desired rotor speed. Once the speed was stabilized, the tunnel motor was engaged and the tunnel was brought to speed. When the desired tunnel velocity and the rotor speed were stabilized, the ammonia (NH_3) valve was set to give the desired flow

rate and pressure. A stopwatch was used to determine the time of the ammonia flow. After the predetermined time had elapsed, the ammonia valve was closed. The rotor and tunnel continued to run at the established condition until all the ammonia in the line was cleared. This usually required an additional 20 seconds. At this point, the tunnel was stopped and the rotor speed was reduced to zero. The blade traces were then inspected. In some cases, reruns were necessary to obtain a satisfactory trace.

To obtain information at various azimuth positions at a specific flight condition, the cam lobe was rotated to various positions around the azimuth, and a trace was taken at each position. Usually four azimuth positions (at 0°, 90°, 180°, and 270°) were tested. In some cases, traces were taken at 30° intervals.

RESULTS OF HOVER TESTS

RESULTS WITH 4-INCH-CHORD BLADES IN HOVER WITH ORIFICE AT 72% RADIUS

The hover tests with the 4-inch-chord blades provided some results which directly affected all subsequent work in this study. Consequently, specific emphasis is placed upon the findings with the 4-inch-chord blades and upon the interpretation of the results. The discussions of this section include consideration of sublimation tests, ammonia-azo results, boundary layer step studies, discussion of the mechanisms involved, and possible spanwise flow effects.

Chemical Sublimation Test Results

Sublimation tests were run to provide a suitable reference between this work and that done by others in this field. All sublimation tests were conducted using the rotor that had a constant, 4-inch-chord with no radial twist. The airfoil shape used was an NACA 0015 profile. A 3-foot radius gave a maximum tip Reynolds number of 2.62×10^5. The pitch angle, θ, was varied from -15° to more than 20°. All the chemical sublimation tests were done at 400 rpm. The location of the transition to turbulent flow for three pitch angles is shown in Figure 16. Transition points for a radius of 72% and various pitch angles are compared with those of Tanner and Yaggy[8] in Figure 17. The Reynolds number used in Tanner's tests was 1.1×10^6. In spite of the large difference in Reynolds numbers, the correlation of these tests results with Tanner's is very close for high pitch angles. For pitch angles of less than 8°, there is a greater difference, but the trends of the data are similar. The correlation of the data suggests that the location of transition may depend on the pitch angle more than the Reynolds number. Also plotted in Figure 17 are the results from Ref. 9, showing transition for two-dimensional symmetrical airfoils. In those tests, airfoils with thickness ratios of 9, 12, and 18% were tested, and the data have been interpolated for an NACA 0015 airfoil. The Reynolds number used was 1.7×10^6, and the airfoil had a chord of 6 feet. Although it was predicted by Banks and Gadd[10] that rotation delays the occurrence of transition, data from the sublimation tests did not confirm this.

The results of rotating sublimation tests proved to be useful, since the transition location was shown to correspond with other data in spite of the lower Reynolds numbers used in these tests.

Ammonia-Azo Traces

When the ammonia is released from the leading edge, the resulting traces often show a severe discontinuity. This can be seen in Figure 18 for a pitch angle of 10° and a rotational speed of 400 rpm. The ammonia-azo traces are shown with the leading and trailing edges of

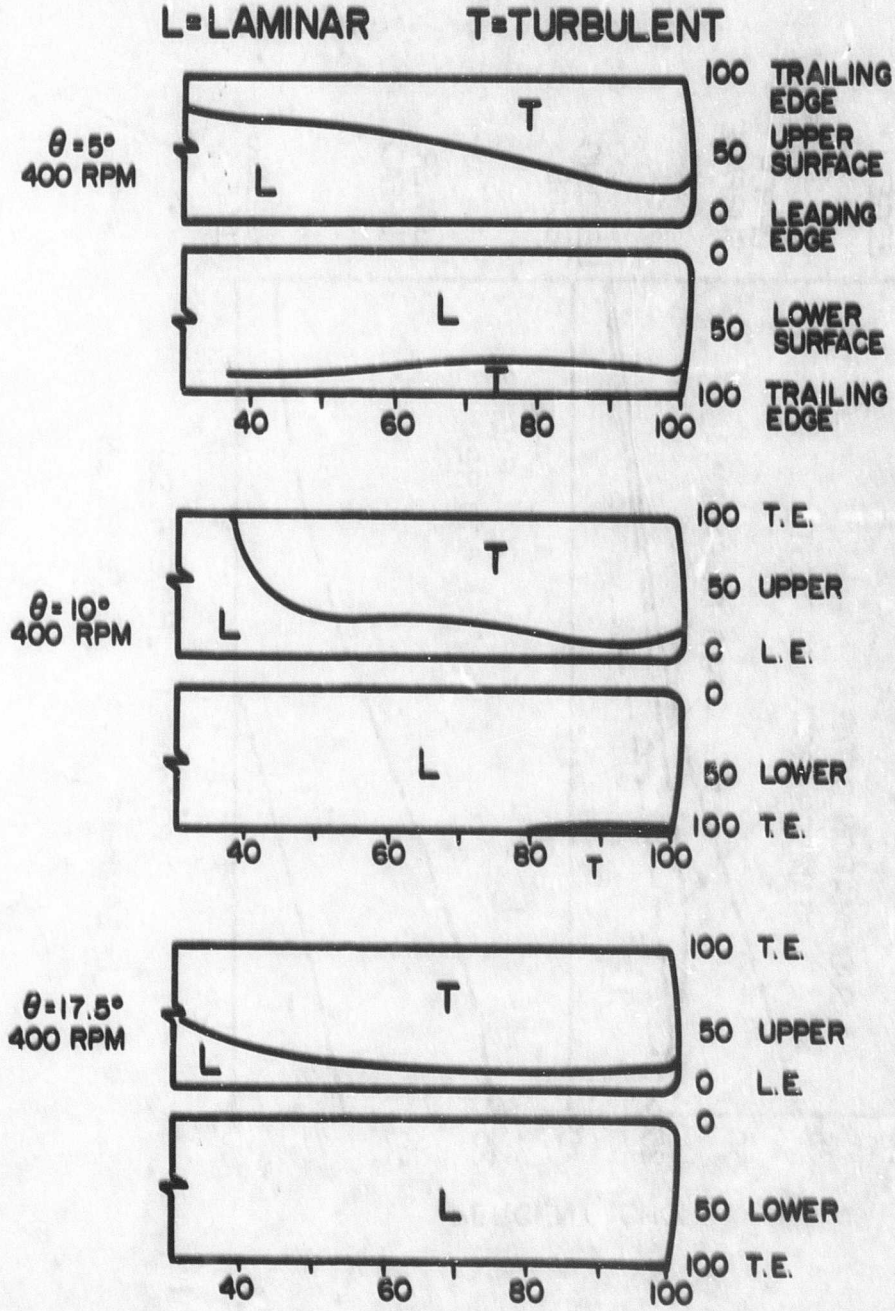

Figure 16. Chemical Sublimation Results Showing Location of Transition Versus Radius.

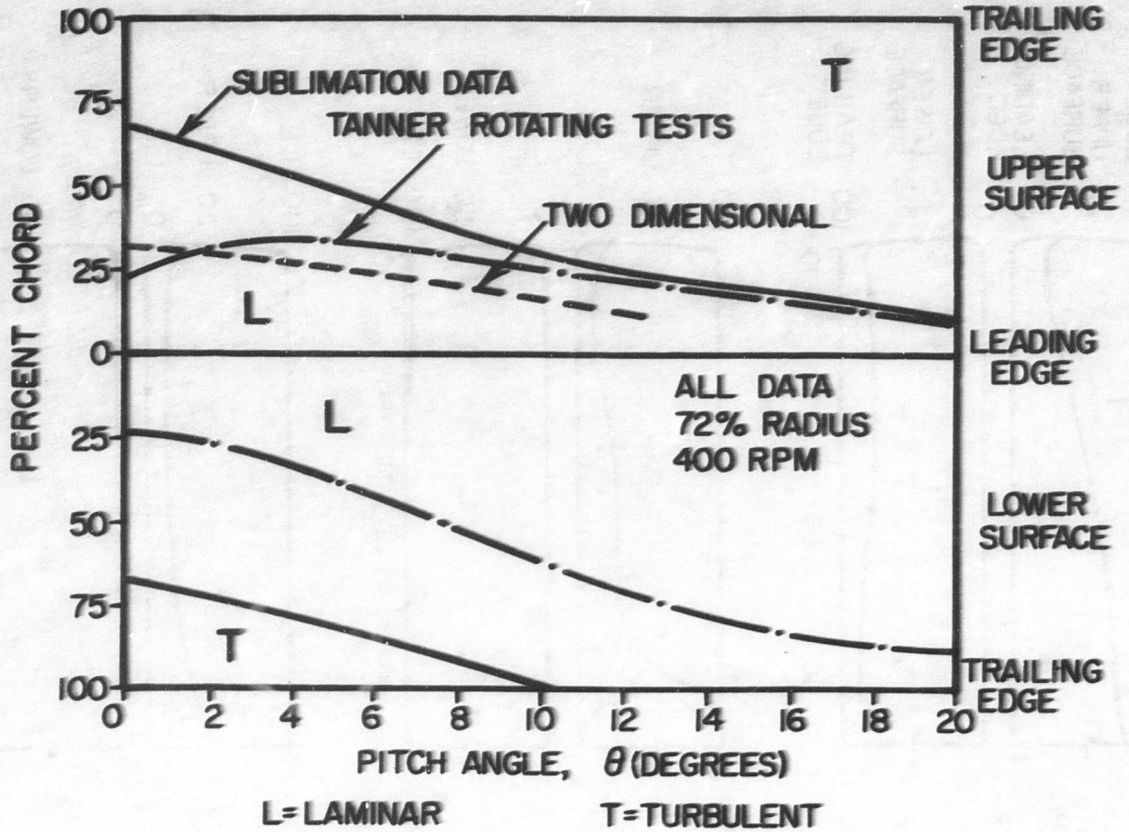

Figure 17. Location of Transition at 72% Radius Versus Pitch Angle.

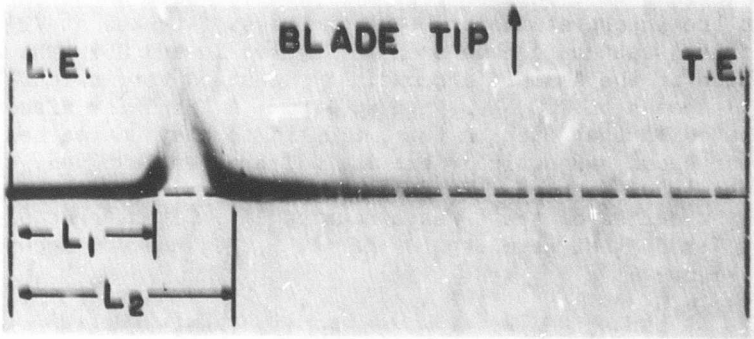

Figure 18. Ammonia Trace Showing Discontinuity for the 4-Inch-Chord Blade at 72% Radius. L_1 = 13.5%, L_2 = 30% Chord, 400 rpm, $\theta = 10°$.

the blade marked and the direction of the blade tip indicated. To attempt to correlate and interpret this unusual trace behavior, the start of a discontinuity was located at the chord length where the flow first starts to deviate from a straight chord line (designated by L_1). Similarly, the end or reattachment was placed at that point where the flow had completely returned to the same straight chord line (designated as L_2). For example, the discontinuity in Figure 18 covers the distance from 13.5 to 30% chord using this criterion. Because of different radii in these discontinuities, it is difficult to locate these points with precision, especially with pitch angles in the 0° to -10° range. However, it is felt that this criterion to locate the discontinuities is useful in the interpretation. Other examples of traces at 72% radius showing this Λ pattern can be seen in Figures 19 and 20. The length and location of the ammonia discontinuity changed very slightly with rotational speeds of 200, 300, and 400 rpm. A trend for discontinuities to be located farther back on the chord and to stay unattached longer with slower speed was noticed, but the differences involved were generally less than 3% chord. To show the time development of an ammonia-azo trace, a series of tests was conducted at a pitch angle of 5° and 400 rpm. Traces that were exposed for 1, 5, 20, and 180 seconds are shown in Figure 21.

There is strong correlation between the reattachment of an ammonia-azo trace and the transition of the boundary layer to turbulence. The point of transition and the length of discontinuities versus pitch angles are plotted in Figure 22 to show this correlation. There is an average difference of only 6% chord between the point of transition and the end of a discontinuity. This difference is extremely small when the error in locating a discontinuity is considered. The reattachment of the ammonia appears to correspond closely with the occurrence of transition.

SEPARATION BUBBLE

Based upon study of the ammonia traces and the sublimation data, it was hypothesized that a standing vortex or separation bubble associated with transition occurs on the blade and causes the discontinuity seen. The occurrence of separation bubbles in two dimensions has been discussed by McCullough and Gault and others.[11,12] The pattern of a separation bubble is shown in a somewhat exaggerated drawing in Figure 23.

The chordwise pressure distribution is an important factor in determining the location of boundary layer transition. Since the end of an ammonia-azo discontinuity corresponds closely with the point of transition, the start of a discontinuity was examined for correlation with the chordwise pressure distribution. The correlation that was used is based upon the location at which the pressure is 90% of its maximum value; the results are also plotted in Figure 22. Correlation is quite good for pitch angles of less than 10°. At higher angles, the start of a discontinuity lags behind the 90% pressure location.

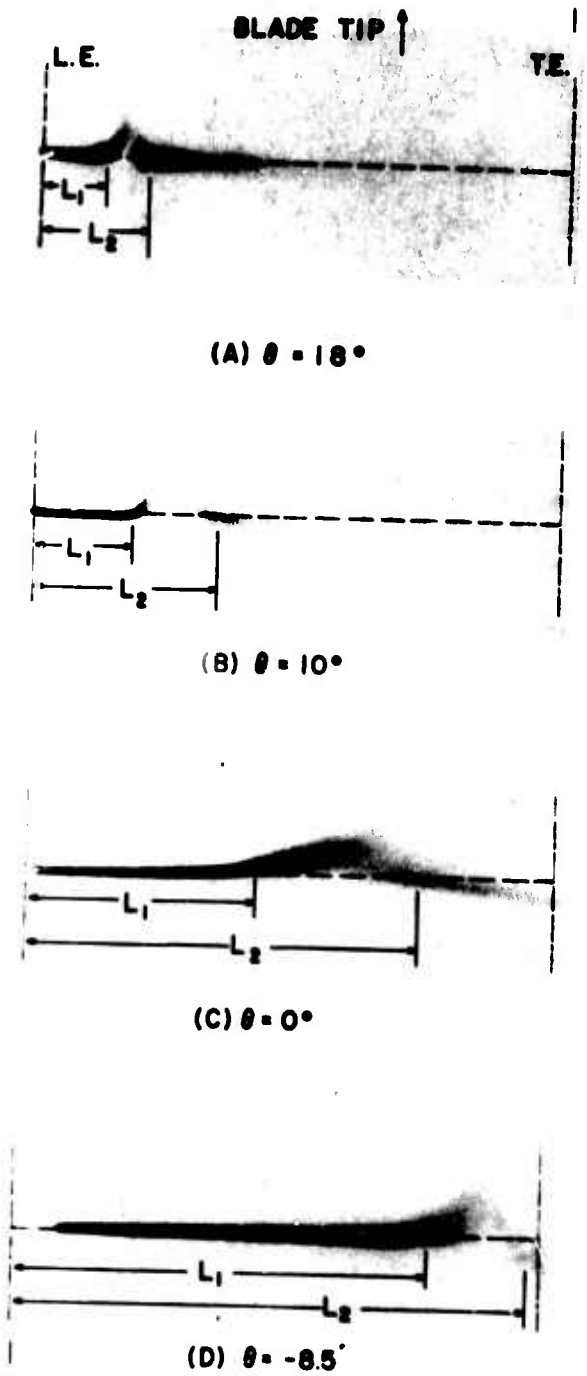

A) L_1 = 8%, L_2 = 16.5%
B) L_1 = 15%, L_2 = 32 %
C) L_1 = 39%, L_2 = 79%
D) L_1 = 76%, L_2 = 97%

Figure 19. Traces for the 4-Inch-Chord Blade, 72% Radius at 300 rpm and Various Values of θ.

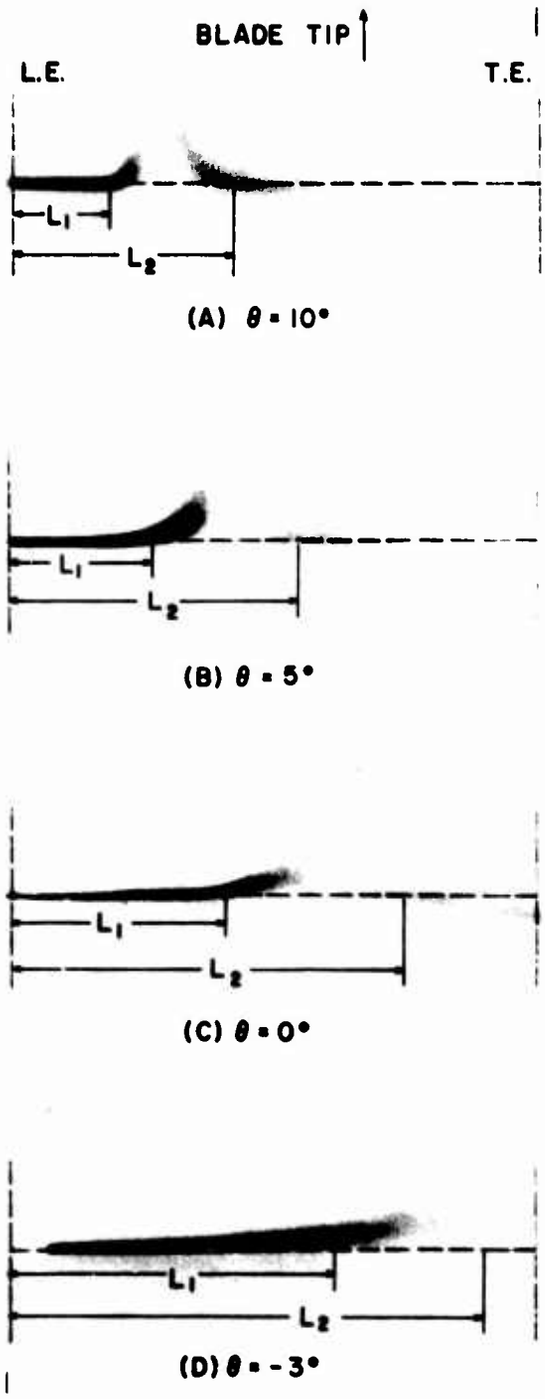

A) L_1 = 15.[illegible], L_2 = 38% C) L_1 = 36%, L_2 = 74%
B) L_1 = 22 %, L_2 = 50% D) L_1 = 66%, L_2 = 91%

Figure 20. Traces for 4-Inch-Chord Blade, 72% Radius at 200 rpm and Various Values of θ.

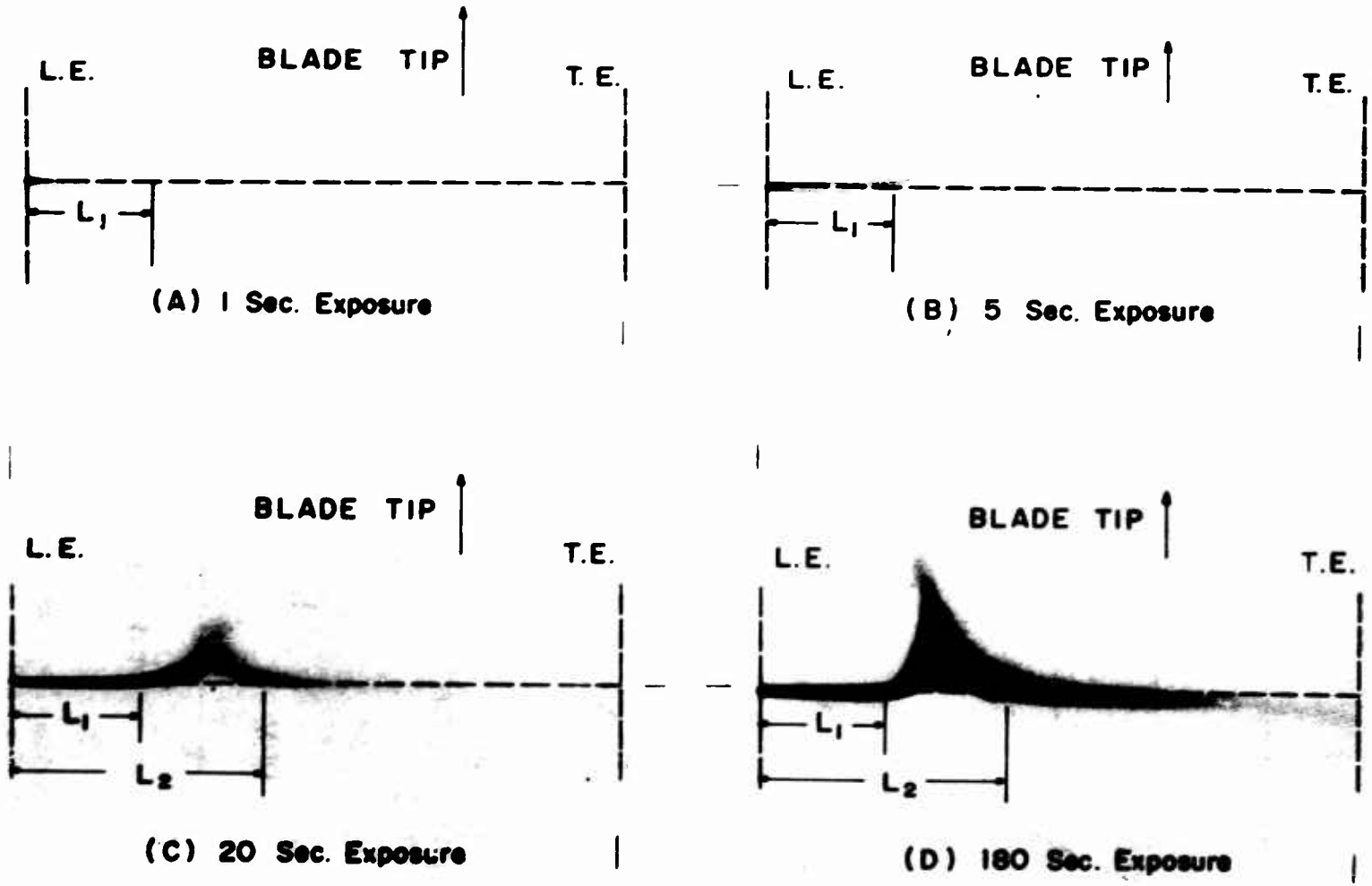

A) L_1 = 21% C) L_1 = 21%, L_2 = 43%
B) L_1 = 20% D) L_1 = 20%, L_2 = 42%

Figure 21. Traces for 4-Inch-Chord Blade, 72% Radius at 400 rpm and $\theta = 5°$ Showing Trace Formation With Various Exposure Times.

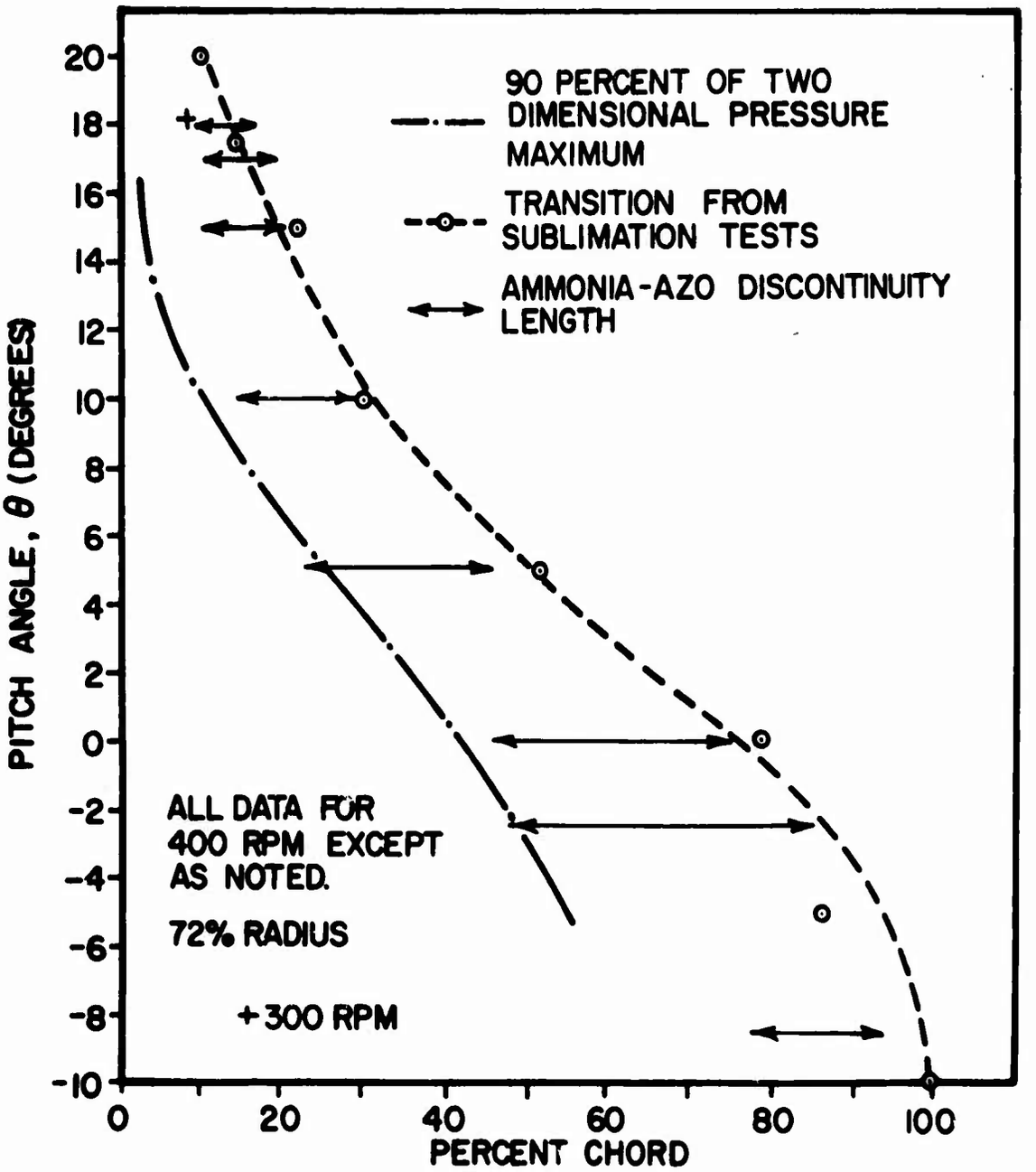

Figure 22. Comparison of Ammonia-Azo Discontinuity and Transition Point for Various Pitch Angles.

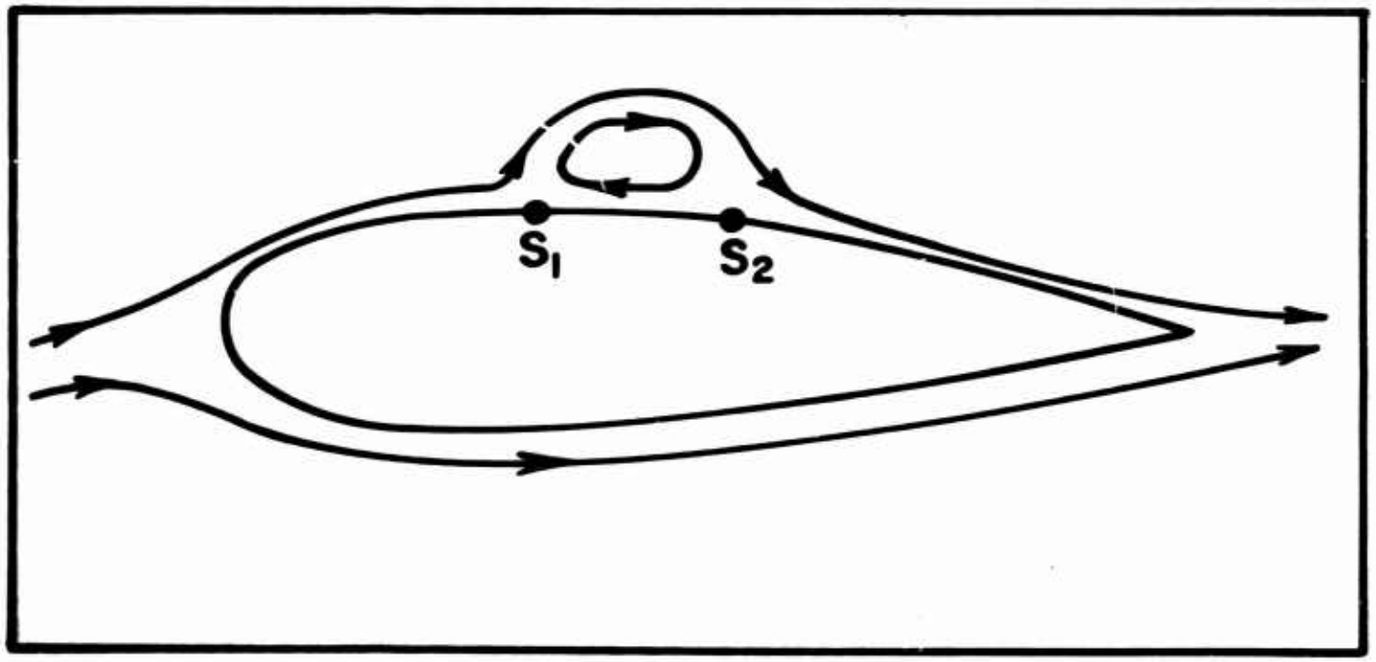

Figure 23. Laminar Separation Bubble on an Airfoil.

The chordwise pressure distributions for 5° and 10° pitch angles are plotted in Figure 24. The locations of transition (based on sublimation tests), of ammonia-azo discontinuities, and of 90% of the maximum pressure are superimposed on these plots.

If a separation bubble is present, the majority of the fluid will go over the vortex and be reenergized by gaining momentum from the free stream, the presence of an accelerating profile caused by the bubble, and the absence of surface friction over the length of the bubble. As a result of these three factors, the flow will reattach to the surface and a turbulent boundary layer will exist.[13] The bubble causes two stagnation points, s_1 and s_2, to be present at either end of the vortex. They should not be confused with the stagnation point which occurs at the leading edge of the airfoil. It should be noted that s_1 corresponds to the initial separation point, and s_2 corresponds to the point of reattachment.

By virtue of a defective orifice, an important confirmation of the presence of a separation bubble was made. The orifice split the trace into two distinct lines as the ammonia left the leading edge. The fluid went through the expected discontinuity, but when it reattached, the trace was still split (see Figure 25). The main stream of air could not have been involved with the outward flow at the discontinuity because it would have been mixed in the process. The fluid turning outward is not from the main airflow, but rather from a smaller amount associated with the stagnation points at either end of the vortex.

The authors of Ref. 14 have indicated that the flow over a rotor is mathematically similar to that on a delta-shaped wing. This wing, however, is known to have standing vortices near its leading edge under certain conditions (Figure 26).[13] Thus, it seems possible that under rotation, separation bubbles are present on the NACA 0015 rotor which may be similar to those found on swept wings.

BOUNDARY LAYER STEP STUDIES

As the fluid approaches a separation point in the boundary layer, it decelerates and eventually leaves the airfoil. Such a separation can be avoided by changing the shape of the surface on which the separation occurs. If a cusp is put on the surface, the fluid will leave the wall tangentially with a finite velocity, and one stagnation point will be eliminated from the usual standing vortex flow pattern Figure 27). A stable vortex is formed behind the cusp and prevents the separation of the flow elsewhere on the blade. In this manner, the position of laminar separation and transition can be controlled.

The flow over an aft facing step is an approximation to the flow over a cusp and has been studied by Tani.[15] The flow is not actually tangent when it leaves the surface and there may be several vortices,

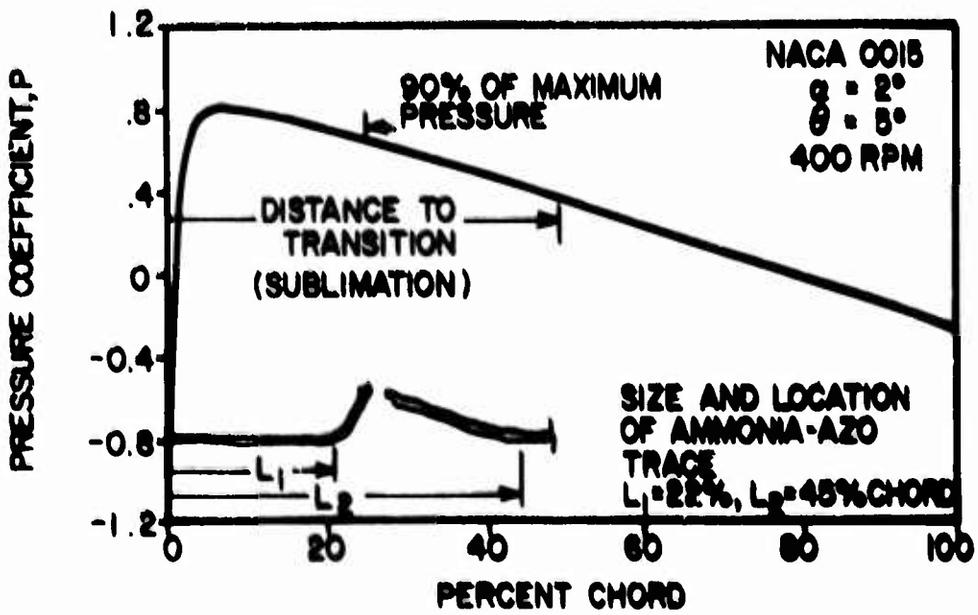

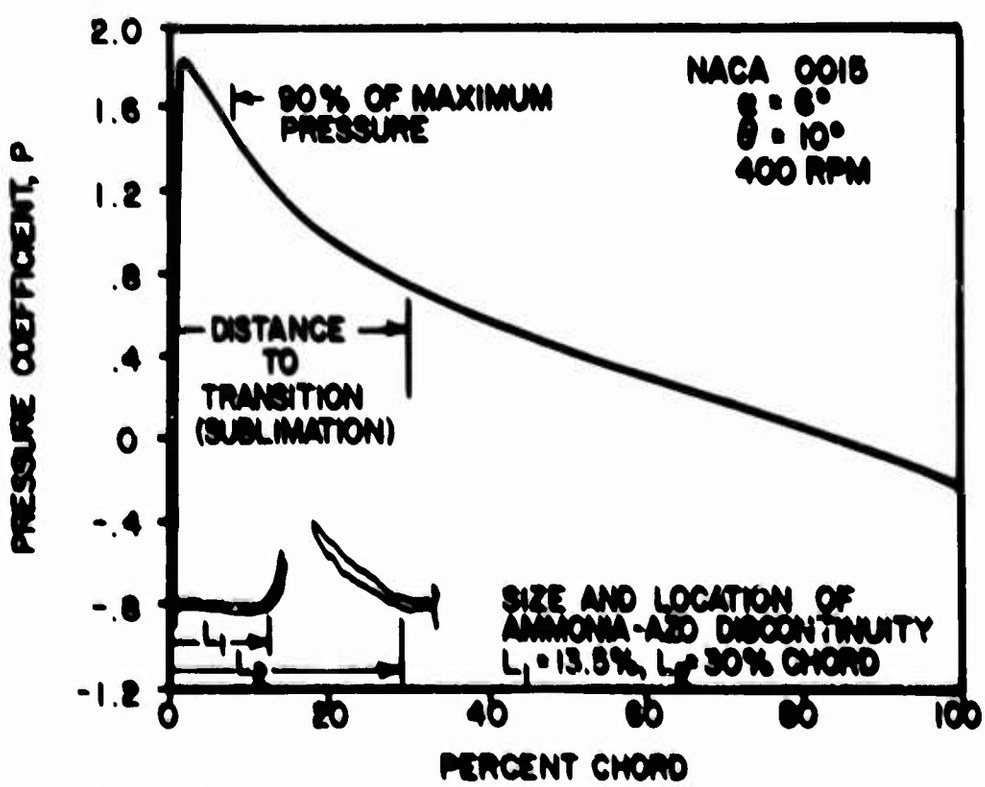

Figure 24. Two-Dimensional Pressure Distribution for NACA 0015 Airfoil.

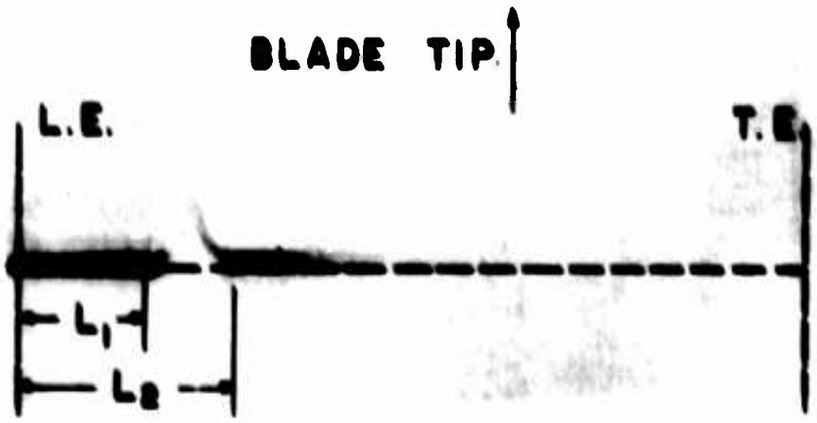

Figure 25. "Dual" Trace for 4-Inch-Chord Blade, 72% Radius at 300 rpm and θ = 10° With Boundary Layer Trip at L_1. L_1 = 13.5% L_2 = 25% Chord.

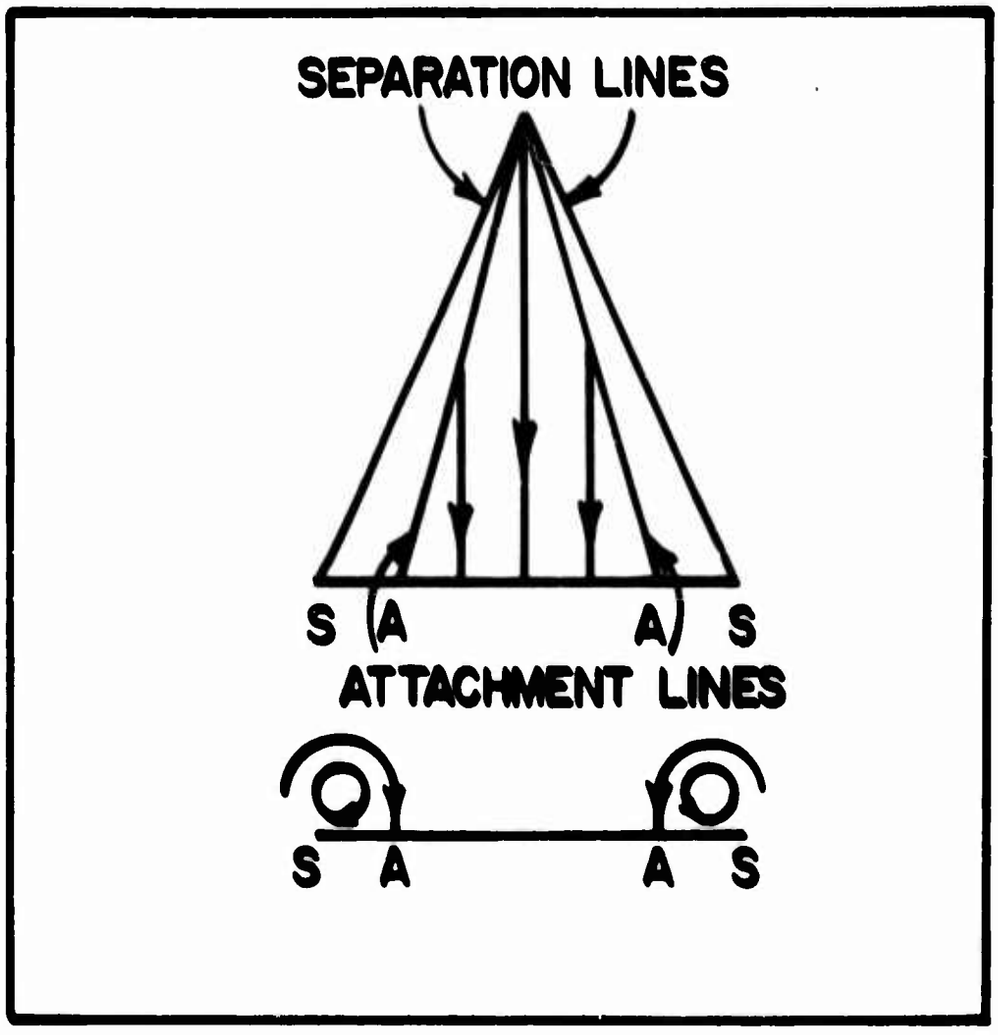

Figure 26. Streamlines on a Slender Delta Wing (Reference 13).

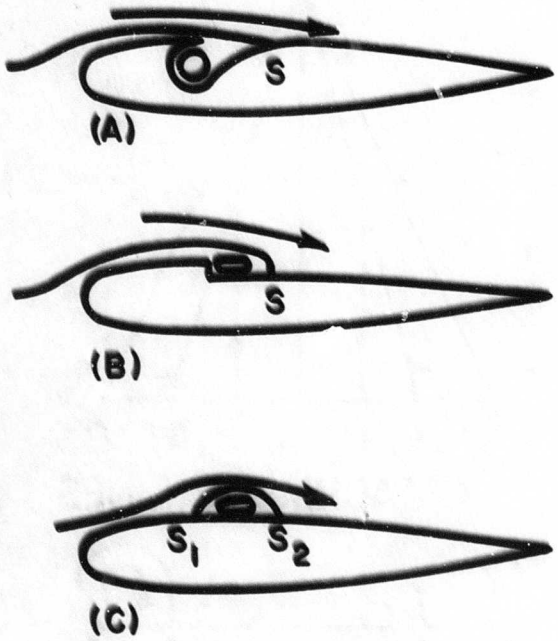

Figure 27. Schematic Streamlines on Airfoils With (A) Cusp, (B) Step, and (C) Separation Bubble.

but the step has the important characteristics of the cusp; that is, there is only one stagnation point of the main stream, the standing vortex is present, and separation can be controlled by the step. The cusp and step are compared with the normal airfoil shown in Figure 27.

To study the action of the ammonia trace technique with a known separation, a step of 0.013-inch height was located at 20% chord on the blade. Both ammonia-azo and chemical sublimation tests were run at 5° and 10° pitch angles. A comparison of the ammonia-azo traces for 5° and 400 rpm, with and without the step being present, is shown in Figure 28. For no step, the "outward flow" trace begins gradually at 21% chord and reattaches at 43% chord. The step causes separation at 20% chord; the trace reappears at 34% chord. This indicates that the step produces a standing vortex with one reattachment stagnation point, moves the discontinuity from its original position, and alters its shape. The first part of the "Λ" discontinuity is gone because no stagnation point is there to produce outward flow. A spanwise trace similar to the second half of a regular discontinuity does occur after the step. The distance that the flow is unattached was shorter, probably because the step produces a more concentrated vortex. The results of the tests with the step give strong assurance that separation bubbles are responsible for the discontinuities seen.

Chemical sublimation tests with a pitch angle of 5° and 400 rpm were run to find the transition point behind a step. The step was again located at 20% chord and was 0.013 inch high. Chemical sublimation did not occur before the step or for the 6% chord just after the step. Aft of the 26% chord point, sublimation did occur. The flow before the step is in the laminar regime. In the 6% chord region after the step, the flow may not be laminar; but because the reverse flow in a standing vortex is about one-fourth of the free-stream velocity,[15] the chemical does not sublime. The primary flow then reattaches, with the turbulent boundary layer causing the chemical to sublime over the rest of the airfoil.

DISCUSSION OF INVERTED "V" TRACES

The shape of the discontinuity that occurred can best be described as an inverted "V" or a Λ. The following mechanism is hypothesized for the shape seen. As the ammonia vapor is injected into the boundary layer at the nose of the airfoil, it is carried aft by the main stream of the flow. At first it forms a dark, distinct, and narrow trace. As the flow in the boundary layer with the ammonia passes the peak pressure position, it feels the adverse pressure gradient. The fluid particle velocity decreases, and the velocity profile changes rapidly to that of a "separation profile." Then the forward separation point is reached, and at this point the fluid velocity and shear stress near the surface are essentially zero. In this reduced velocity region ahead of the separation point, the fluid particles containing the

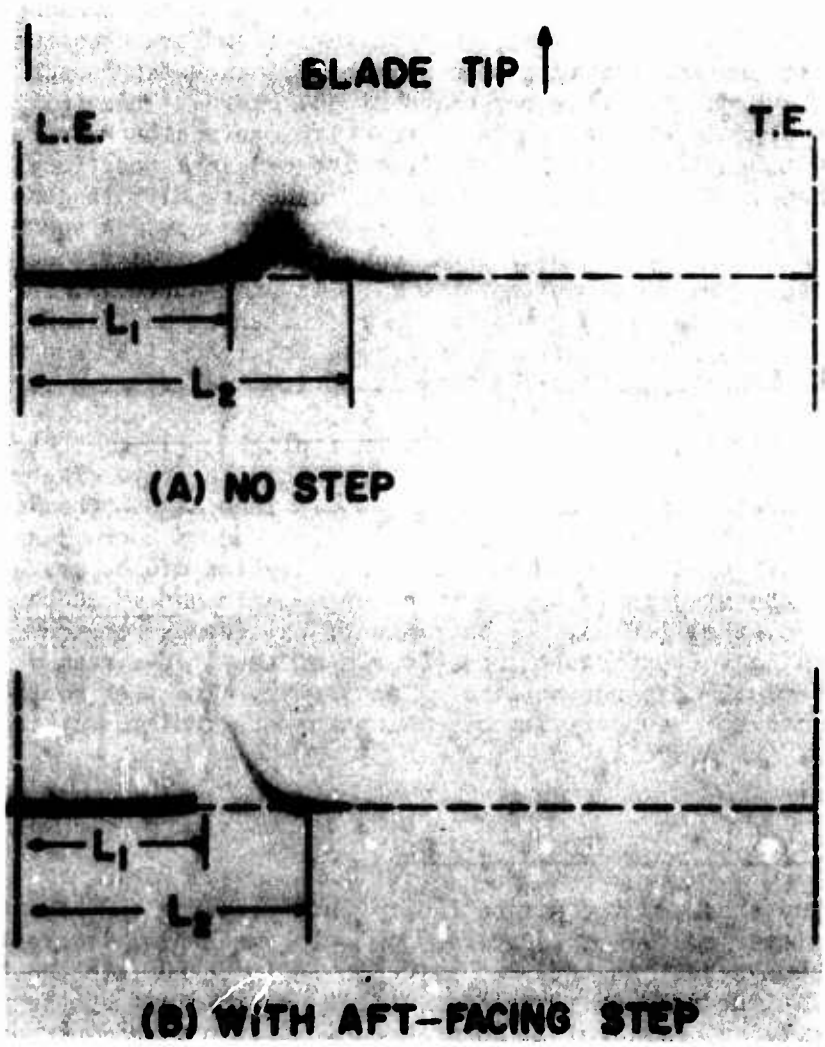

(A) L_1 = 21%, L_2 = 43%
(B) L_1 = 20%, L_2 = 34%

Figure 28. Comparison of Ammonia-Azo Trace With and Without Surface Step at 400 rpm and $\theta = 5°$.

ammonia are subject to both the outward spanwise pressure gradient and the centrifugal force. The inner layers of the boundary layer tend to move outward under the actions of these forces. As they do so, the ammonia diffuses to the surface and leaves the forward portion of the discontinuity--an outward-moving trace.

It is considered, however, that a significant portion of the ammonia in the upper layers of the boundary layer or in the potential flow just above the boundary layer is carried by the main stream over the separation bubble in a chordwise direction. This flow then returns to the surface aft of the bubble at the reattachment point, where again the chordwise fluid velocities are quite low. The local surface flow includes some forward or reverse flow toward the bubble, as well as some outflow which results from the action of either centrifugal force or spanwise pressure gradients. The combined effects of outflow and reverse flow could account for the shape of the aft portion of the discontinuity. This situation is depicted in Figure 29.

A limited amount of testing was done with boundary layer fences on the rotor to determine if significant spanwise flow was involved in the discontinuity patterns.[16] One-inch fences, similar to fences used in swept wings, were placed both inboard and outboard of the ammonia orifice. It was found that with the fences on the blade, the traces retained the same inverted V pattern as found previously (Figure 30). However, a change was noted in the trace after the discontinuity. Those runs made with the fence located on the outside had a noticeable effect on the trace path. With a fence placed 1-inch outside the orifice, the flow after a discontinuity was parallel to the chord line instead of curving inward, as had been found with the traces from the 4-inch-chord blade. More tests are necessary to reach any precise conclusion, but it is believed that the straight fence acting in the curved streamline flow may cause the change. Tests could be made in which the fence had the same curvature as the circular streamlines.

SPANWISE VARIATION WITH 4-INCH-CHORD BLADE

To determine the boundary layer flow in hovering at various positions along the blade, tests were conducted with the 4-inch-chord blade with orifices located at 10% radius positions along the leading edge. Typical results are shown in Figures 31 through 33. Each figure presents data for a specific rotor rpm at five pitch angles. Study of all traces at $\theta = 5°$ reveals that the Λ pattern is evident in most traces from 40% R through 80% R. The increased speed from 400 rpm to 600 rpm seems to have little effect on the form of the corresponding traces at the various radius positions. The evidence indicates the presence of a standing separation bubble at approximately the same chordwise location for a given radius station and θ as the rpm is changed.

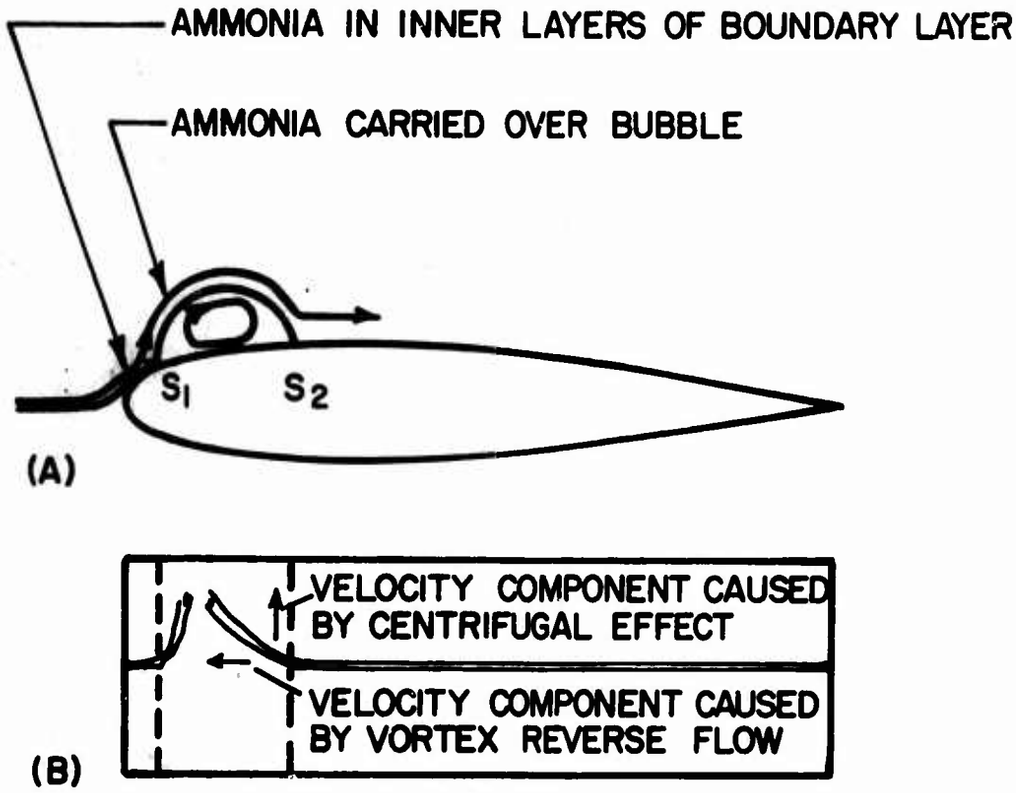

Figure 29. Possible Factors Involved in the Shape of the Ammonia-Azo Trace.

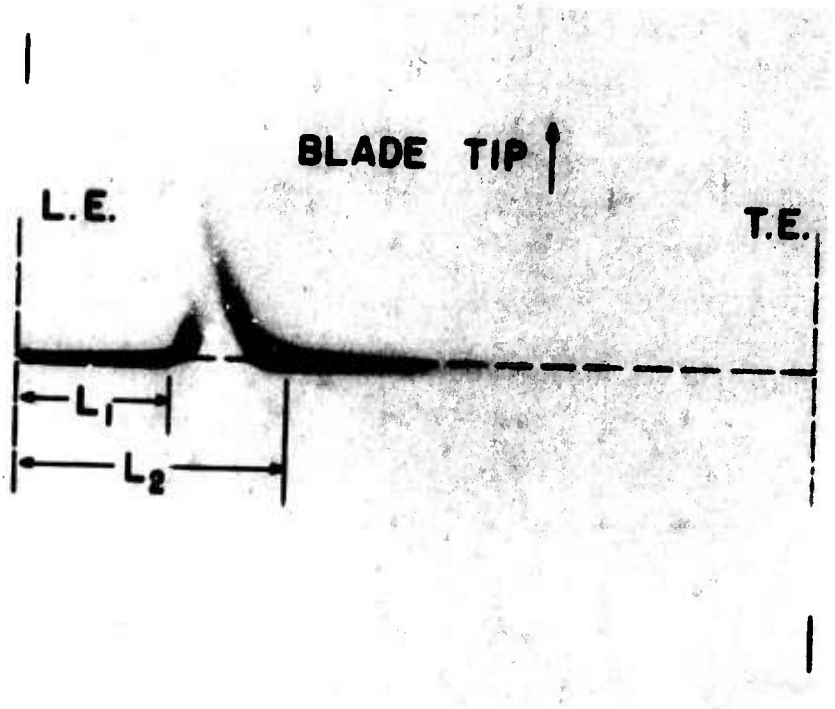

Figure 30. Effect of an Outboard Fence on a Trace. L_1 = 15%, L_2 = 30% 400 rpm, θ = 5°.

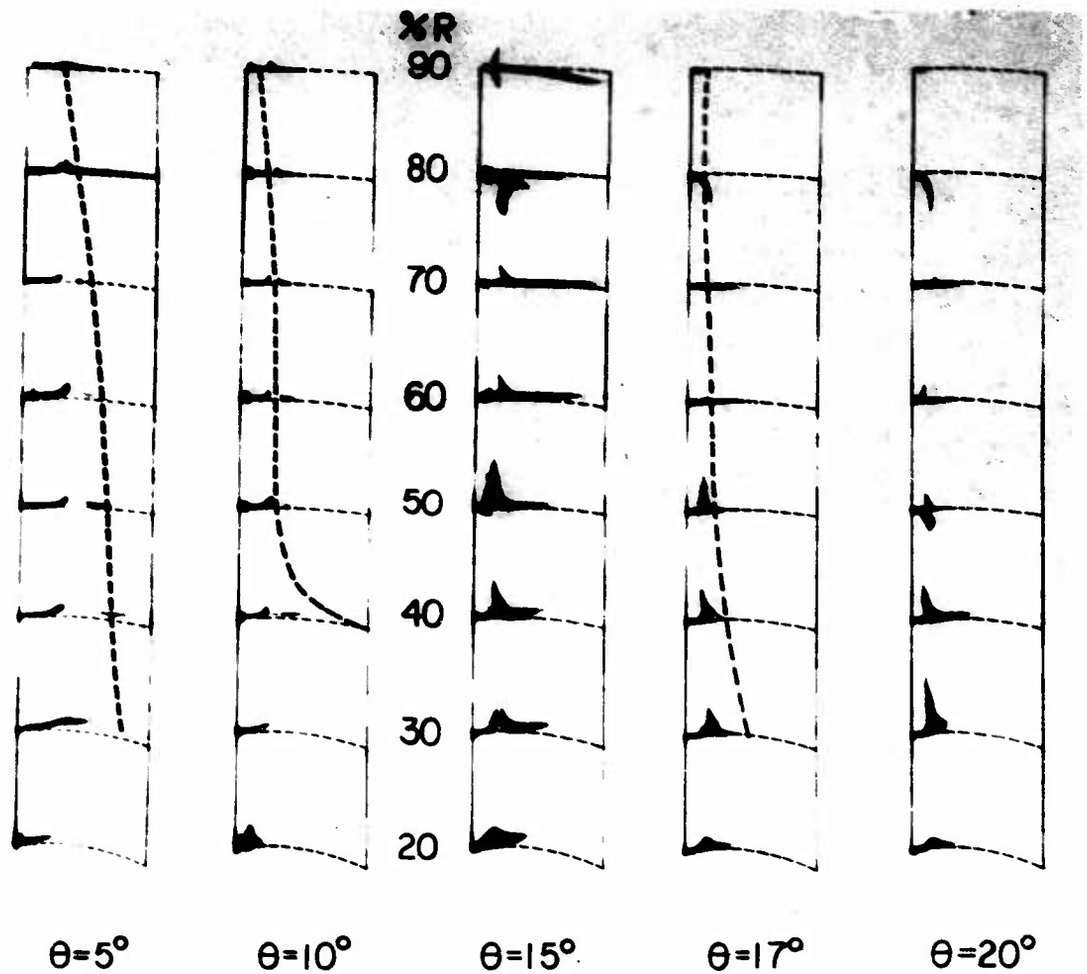

Figure 31. Traces at Several Radii for the 4-Inch-Chord Blade for Various Pitch Angles and 400 rpm.

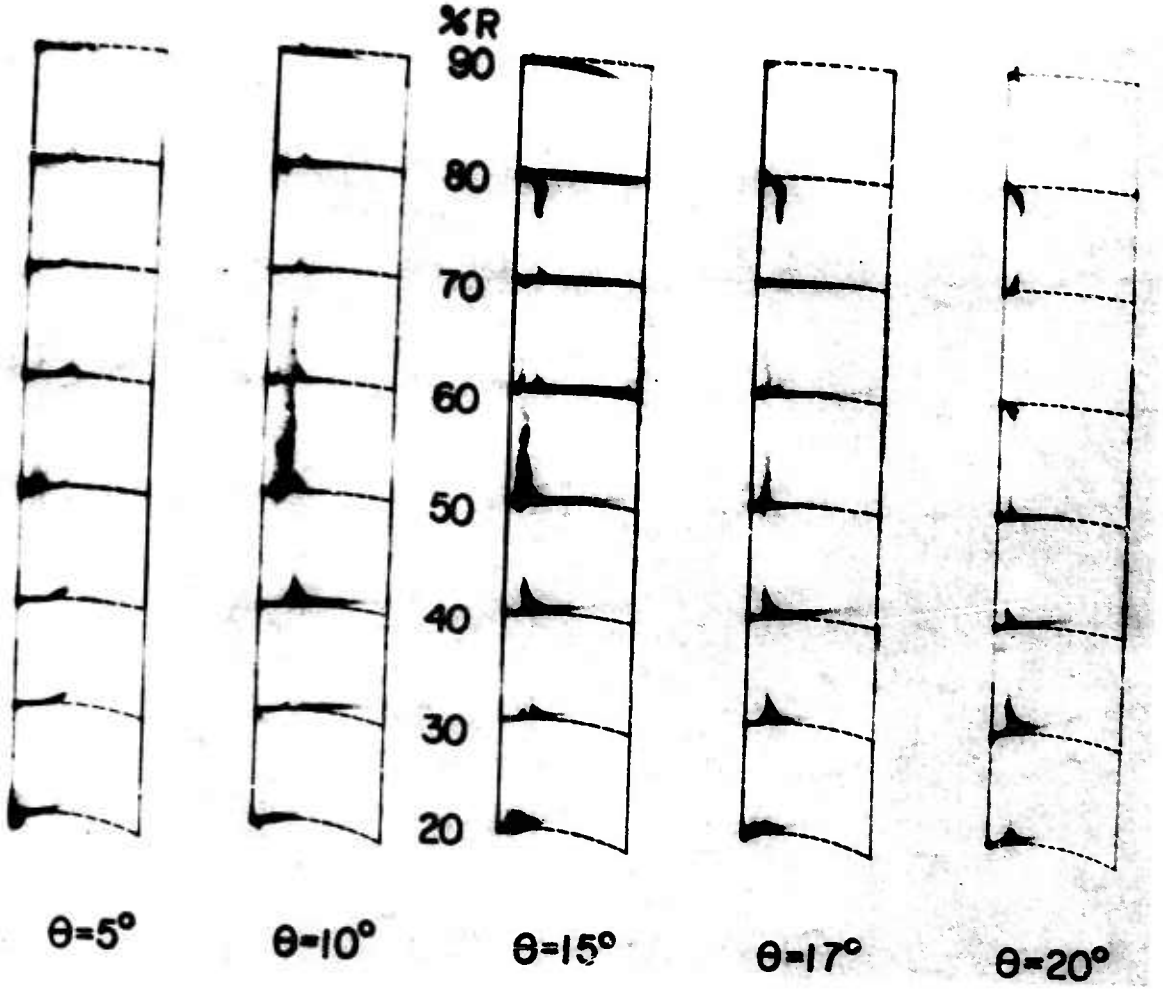

Figure 32. Traces at Several Radii for the 4-Inch-Chord Blade for Various Pitch Angles and 500 rpm.

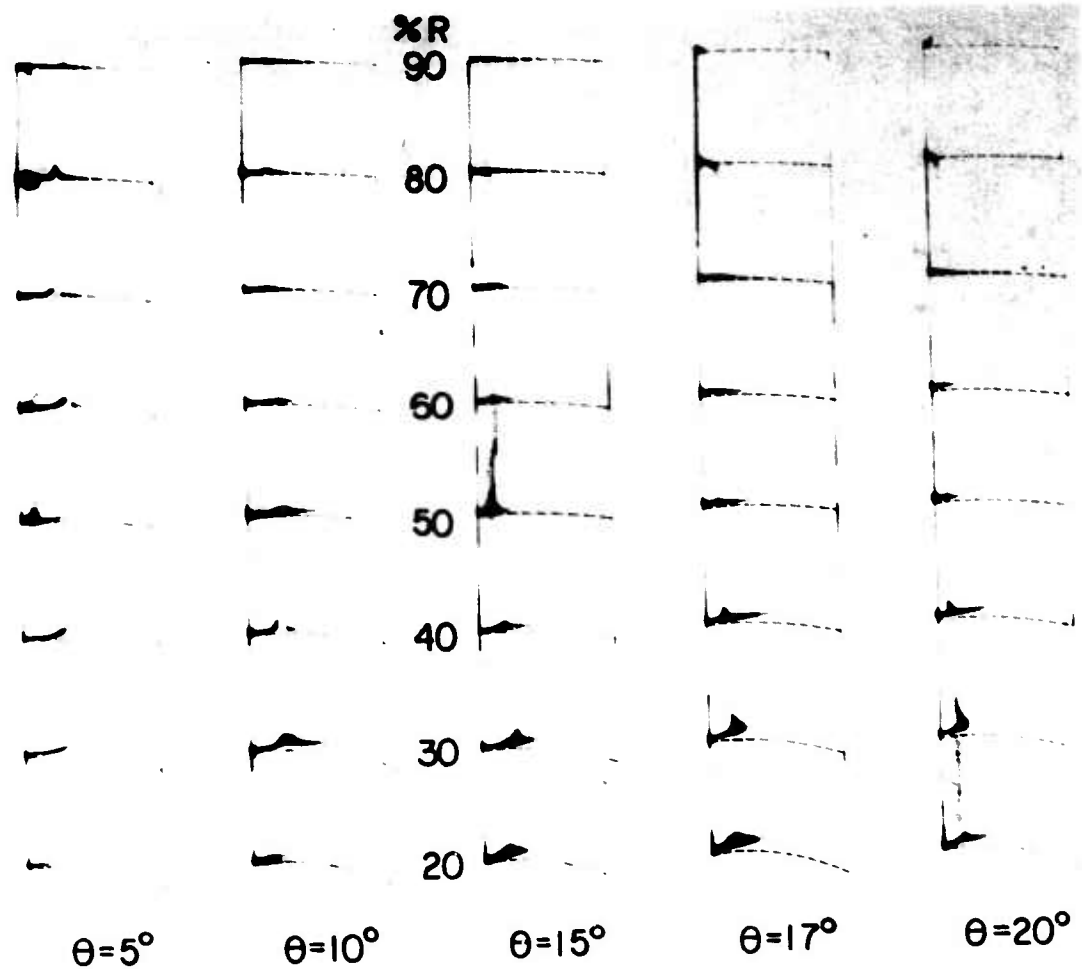

Figure 33. Traces at Several Radii for the 4-Inch-Chord Blade for Various Pitch Angles and 600 rpm.

If one examines the $\theta = 5°$ set of traces at any of the values of rpm, it can be seen that a fairly regular change in the discontinuity exists from the inboard to the outboard region. The width of the Λ pattern is generally wider and slightly farther aft in the inboard region of the blade. The Λ pattern is quite narrow and distinct in the outboard traces. In the 400 rpm, $\theta = 5°$ set of data, the transition line as obtained from the sublimation tests is shown. Reasonably good agreement is achieved. Transition occurs just aft of the discontinuity, as had been indicated by the comprehensive tests at 72% radius.

The changes in the pattern with radius can, however, be the result of two separate actions. First, the tangential velocity and Reynolds number are increasing linearly with radius; this fact could result in the slight movement forward and the somewhat shorter bubble as indicated previously. Secondly, at a fixed θ and rpm, because of a varying downwash angle for an untwisted blade, a slightly different local angle of attack will exist along the blade span. For example, in the case of $\theta = 5°$, the angle of attack at 80% R will be 2.5° and the angle of attack at 40% will be 1.5°. These angles have been calculated using a simple hovering strip analysis. Thus, it can be seen that the changes in the pattern may be due to both velocity and angle of attack influences.

The existence of the discontinuity in the ammonia-azo boundary layer traces is also evident at the other pitch angles. Considering the three sets of data at $\theta = 10°$, it can be seen that the Λ shapes are still evident. The Λ has moved forward and is sharper, as would be expected with the increased angle of attack. At the higher angles, the peak pressure near the nose of the airfoil is closer to the leading edge and is greater in magnitude; thus, laminar separation can occur sooner. In general, comments similar to those for the $\theta = 5°$ case can be made for the $\theta = 10°$ traces. The correlation of the acenaphthane transition line for the $\theta = 10°$ and 400 rpm case is reasonable, although in this case the transition line passes near or through the bubble at most positions.

Considering the $\theta = 15°$ set of traces, it is readily apparent that the discontinuities have moved farther forward on the airfoil, where they tend to show up as a single spike. In the inboard regions of the blade, the spike is located outboard of the main trace. In some of the outboard traces, the spike extends inward. Aft of the spike, the traces from 40% R to 70% R tend to move on a straight line in a direction away from the circular streamlines. Similar patterns can be seen in the traces at other values of θ. One would normally expect that the flow would tend to follow the external potential flow lines. For a hovering rotor, these would be the circular arcs drawn through each leading edge orifice location. The reason for this large outflow aft of transition is not clear at this stage of the investigation. Some possible factors come to mind. It is possible that the steeper velocity profiles of

turbulent flow could be more affected by centrifugal force. It is also possible that the presence of the rotor hub could cause some radial outflow velocity because of its action as a crude centrifugal pump. This latter action, however, should be confined to the innermost traces, and it is doubtful whether the hub influence could extend out as far as the 50 or 60% radius positions.

Particularly interesting traces are those at 80% R for 400 and 600 rpm. These indicate that a dual action exists. First, some ammonia tends to move inward shortly aft of the nose, and the remainder moves aft. It is apparent if a bubble exists, some new action is occurring in the region near the bubble. Secondly, since the trace continues aft, the flow must still be reasonably well attached to the surface and full "stall" has not yet occurred. Because of the wide, rather fuzzy nature of the aft trace, it would appear that a turbulent boundary layer exists. The trace in this region tends to follow the circular streamline.

For several test conditions, the traces near the tip move inwardly relative to the reference circular streamlines. This action is considered to be similar to that reported by Tanner and Yaggy;[8] that is, the motion is the result of the radial inflow on the upper surface induced by the tip vortex. Substantiation comes from considering the 90% R traces at 500 rpm. As θ increases from 5° to 15°, the inward motion of the tip trace increases markedly. At low pitch angles, the tip vortex is weak; and with increasing θ, the vortex strength and the corresponding spanwise inflow should also increase.

If we now consider the traces at the highest values of θ, 17° and 20°, it is evident that a fairly regular trace pattern exists in the more inboard traces. These traces are similar to traces at lower values of θ. The outboard traces, however, are more unusual and are not consistent in their pattern. It appears that some type of "stall" pattern has developed at the higher angles, although it does not seem to be regular. As discussed previously, somewhat lower angles of attack should exist in the inboard regions of the rotor blade, and hence the stall may be delayed. It is also possible that actions similar to those reported by Himmelskamp for propellers may be active.[17] In those tests, it was found that steady-state lift coefficients which exceeded the values that normally would be expected could be reached in the inboard regions of the test propellers.

The outboard patterns of the traces at the high values of θ indicate both inboard and outboard movement of the ammonia tracer gas. It can be seen that some traces move directly aft along the blade chord, indicating that the boundary layer may still be attached over that particular spanwise region of the blade. A possible explanation for the various inward and outward spikes lies in the nature of the spanwise pressures near the nose of the blade. If one would consider

the 60% R, 70% R, and 80% R traces at $\theta = 17°$ and 500 rpm, it can be seen that the middle trace at 70% R goes directly aft and apparently the flow is attached over a large distance of the chord. Likewise, at 60% R the flow seems attached. The trace at 80% R is discontinuous and moves inward in a marked fashion. The flow near 70% R appears to be attached; and with a high angle of attack, very high peak negative pressures will exist on the airfoil. Consider now the flow at the 80% R radius position. If "stall" has occurred, the peak pressures near the nose are drastically reduced. Thus the fluid particles containing ammonia feel the effects of the low pressure inboard in the region of 70% R. This pressure differential causes a radially inward motion of fluid particles along the edge of the separation line, and the inward moving trace at 80% R results.

A similar argument can be used to explain the apparent unrelated directions of the traces in the outboard regions of the blades at other positions and test conditions. Local regions of stalled and unstalled flow will exist simultaneously. It should be noted, however, that the effects of the pressure gradient at these high angles of attack are more significant than the influence of centrifugal force. The similarity of the inward-moving traces and the outward-moving traces, even in the presence of a very strong centrifugal field, tend to indicate the predominant influence of the spanwise pressure gradient under conditions close to stall.

Before concluding this section on the spanwise actions of the 4-inch blade in hovering, it is necessary to interpret some of the traces where ammonia leakage occurred. A typical situation can be seen on the traces for 500 rpm, $\theta = 10°$, and at 50% R and 60% R. Long, gray, diffuse smears can be seen that appear to emanate from the actual boundary layer traces. These smears are, unfortunately, the result of leakage of ammonia vapor under the blue-line paper. The ammonia vapor would then tend to diffuse through the paper and develop the upper side of the paper. Wherever such long, very diffuse smears exist, they should be discounted since they do not represent boundary layer behavior.

HOVER TESTS WITH 7-INCH CHORD BLADE

The series of tests of the 7-inch-chord blade in the hovering condition revealed ammonia-azo traces that were quite similar to those found with the 4-inch-chord blade. Data from a typical run are shown in Figure 34, which depicts the trace at $\theta = 8°$ and 200 rpm. The orifices are located at the leading edge and at 61.5% R, 74% R, and 87% R. The similarity to previous results is apparent. However, a comparison should be made with a higher rpm condition for the 4-inch blade in order to maintain similar Reynolds numbers.

Figure 35 illustrates the effect of increasing angle of attack for the 7-inch chord-blade at 400 rpm. The general trends resemble those found at 600 rpm with the smaller chord. The discontinuity moves

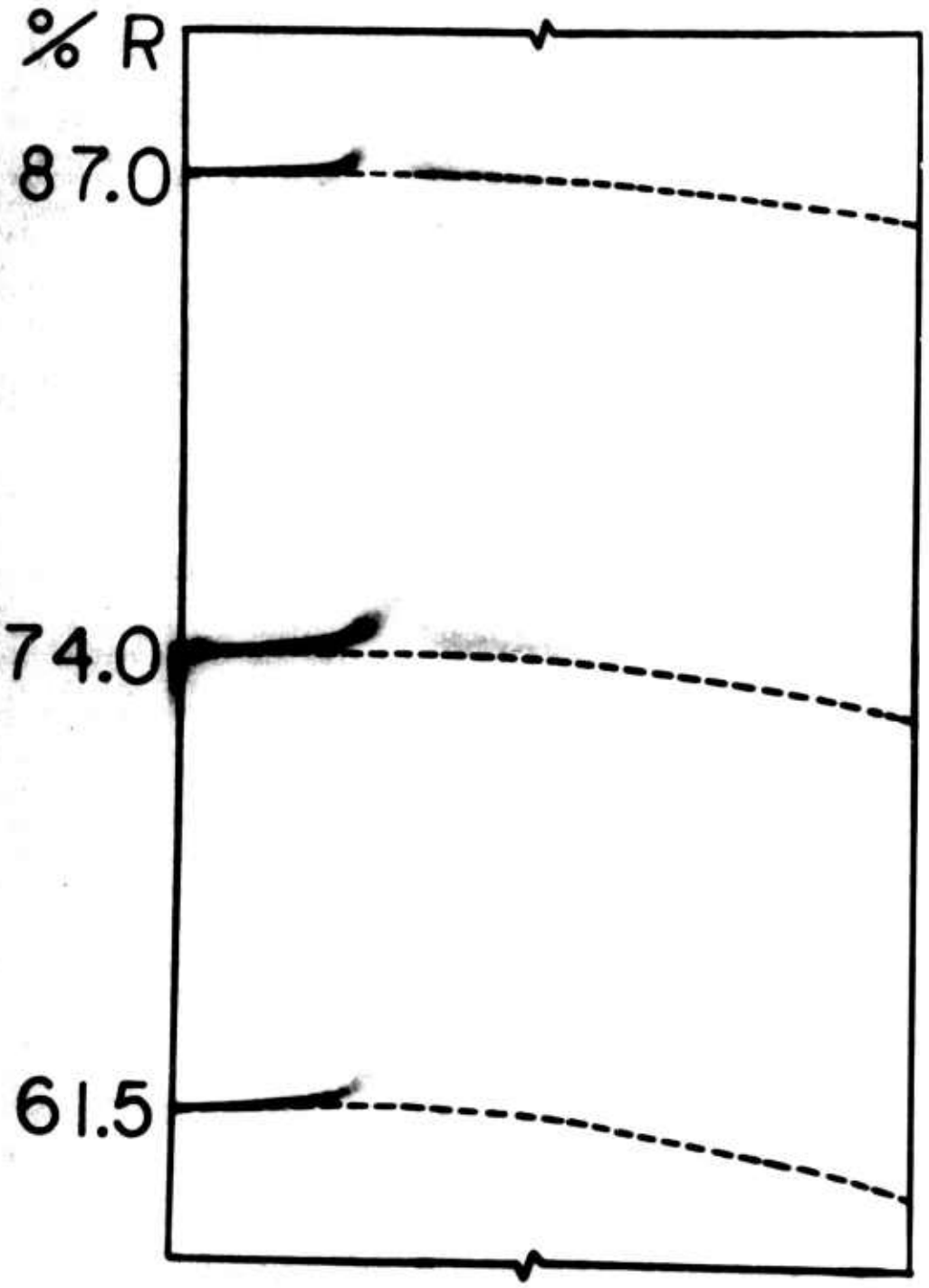

Figure 34. Ammonia-Azo Trace for the 7-Inch-Chord Blade at 61.5% R, 74% R, and 87% R, $\theta = 8°$, and 200 rpm.

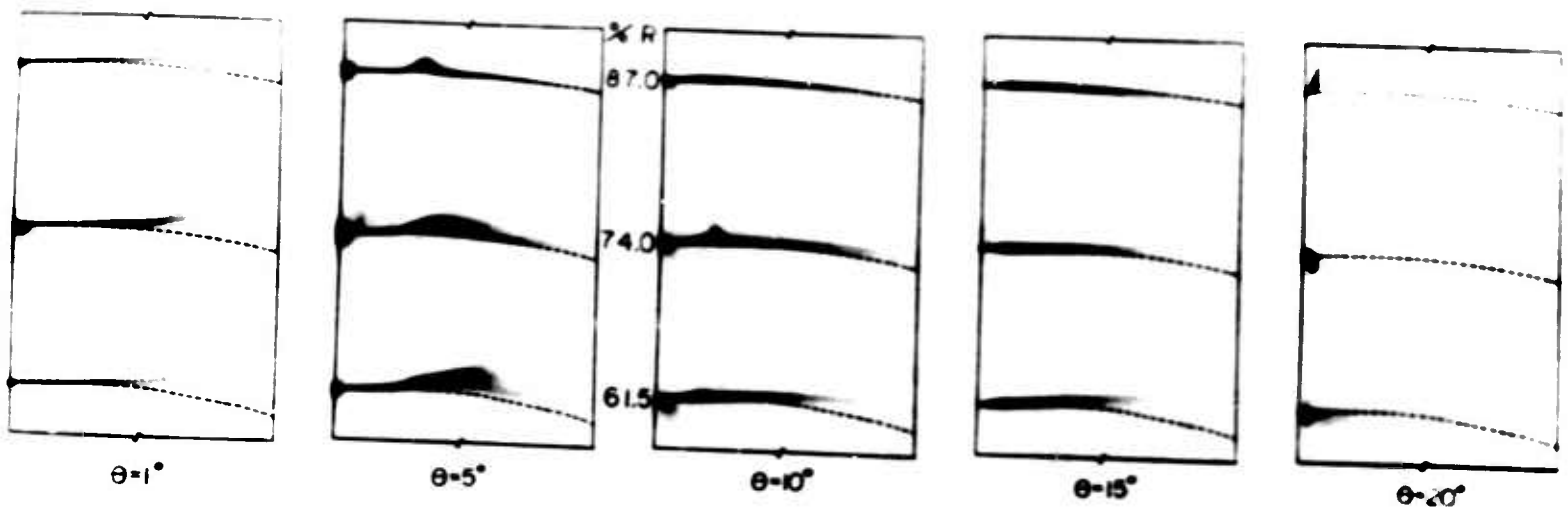

Figure 35. Composite Set of Traces for 7-Inch-Chord Blade for 3 Radii at 400 rpm Showing Effect of Changing Pitch Angle.

forward, and the width of the discontinuity becomes very short or disappears completely as the angle of attack is increased.

It is interesting to note that at a θ of 15°, no outward or radial spike appears near the nose. Apparently, the transition to turbulent flow occurs quickly without a significant bubble forming. The trace in the laminar region extends only about $\frac{1}{2}$ inch and is narrow and quite dark. Then suddenly the trace becomes much wider and traverses the surface toward the trailing edge in an increasingly diffuse pattern. The traces after transition display another characteristic similar to that found with the 4-inch-chord blades. The outboard trace tends to move gradually inward in the aft region, while the most inboard trace tends to move outboard of the circular arc streamline direction. At 400 rpm and a θ of 20°, it can be seen that traces exist only in the region close to the nose of the airfoil. The traces at $\theta = 20°$ indicate a full chord separation.

In order to illustrate the effect of a change in speed on the traces, Figure 36 presents data for $\theta = 5°$ at 200, 400, 600, 800, and 1000 rpm. The traces at 200 and 400 rpm are quite similar to each other, although some evidence exists that the outward deflection of the trace moves forward with the higher speeds. Above 400 rpm, the aft portions of the traces become less and less distinct. Attempts to obtain better defined traces in the aft region of the chord were generally unsuccessful. Various airflow rates and pressures of the ammonia system were tried, and ammonia solution temperature was raised to boiling values. The length of time of ammonia exposure was increased to several minutes in some cases. The traces near the nose of the airfoil became quite dark, but the aft traces in almost every case seemed to be relatively unaffected by the variations in procedure. If the data shown in Figure 36 had been taken in the region of high α, and if full trailing-edge separation had occurred, then the lack of effect on the aft traces might be readily explained. At present, it can only be speculated that at the higher speeds, sufficient turbulent diffusion is taking place to carry the ammonia into the free stream rather than to the surface.

The final data to be considered from the 7-inch-chord hover tests illustrate the influence of a change in speed at a high pitch angle. Figure 37 presents traces for $\theta = 15°$ at 200 rpm and 400 rpm. It can be seen that distinct Λ patterns are formed near the leading edge at 200 rpm, whereas the patterns are not present at 400 rpm. It would seem that at the higher speed, the Reynolds number has increased sufficiently to allow transition to turbulent flow to take place just ahead of, or just at, the bubble. Thus no pattern appears. In such a case it would be expected that stall should tend to occur in a classic fashion with gradual turbulent separation progressing from the trailing edge. Examination of Figure 35 for $\theta = 20°$ reveals, however, that the separation is complete across the entire chord. Because traces are not available for small step increments of θ between 15° and 20° for this airfoil, a better determination of the nature of stall during rotation for this case can not be made.

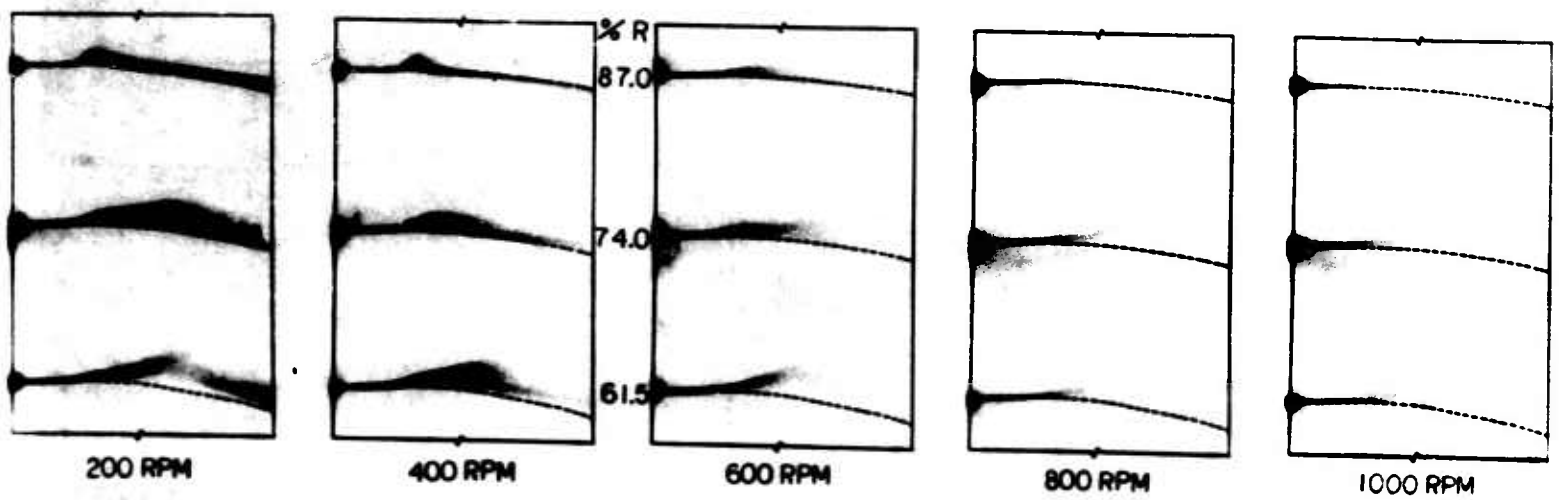

Figure 36. Composite Set of Traces for 7-Inch-Chord Blade for 3 Radii at $\theta = 5°$ With Varying rpm.

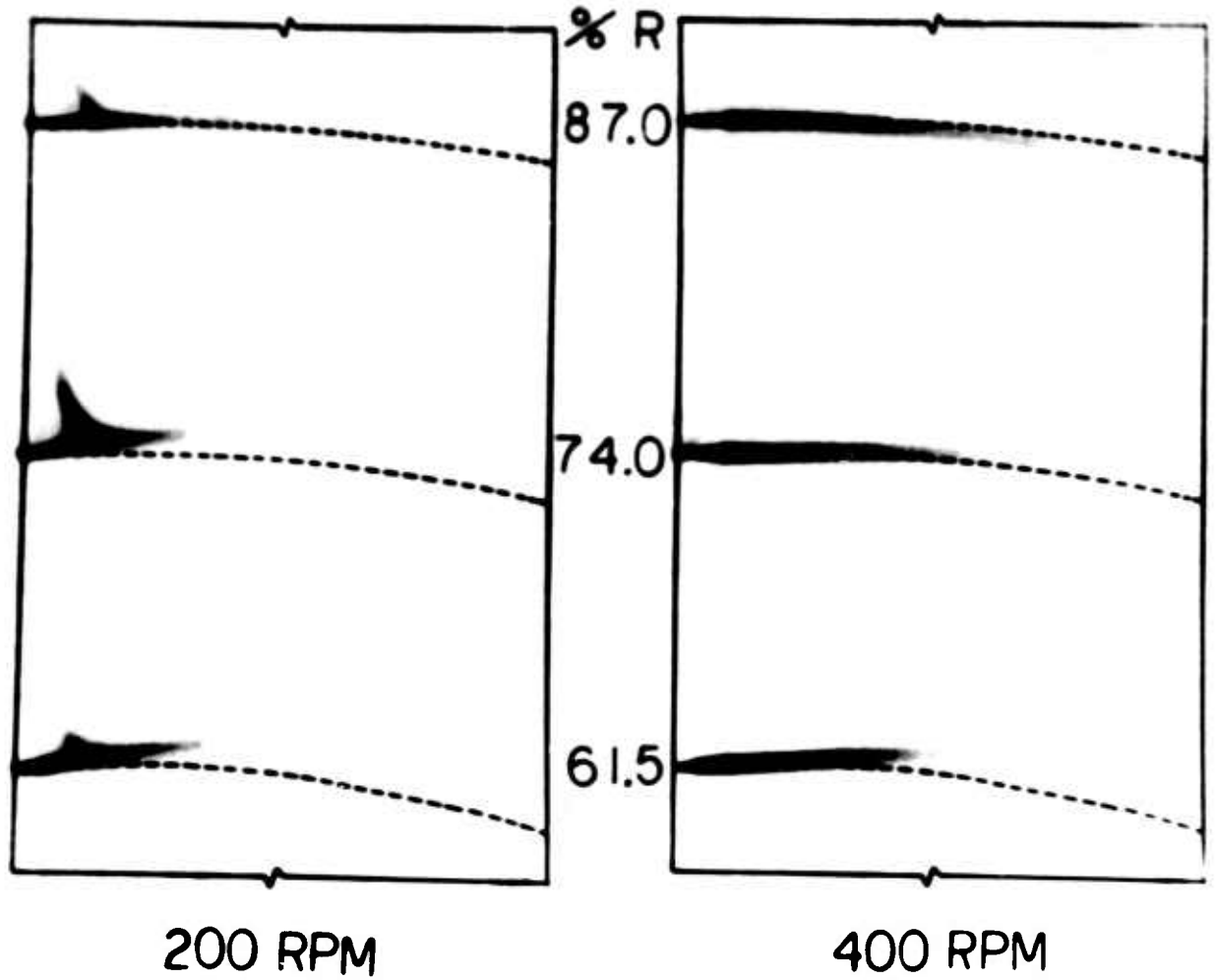

Figure 37. Ammonia-Azo Traces for 7-Inch-Chord Blade at $\theta = 15°$ Showing Effect of Change in rpm.

DISCUSSION OF STALL

In view of the nature of the ammonia-azo traces found and the possible existence of a standing bubble, it is considered logical to examine the nature of ordinary two-dimensional stall. Three types of stall are considered to exist.

1. Trailing-edge stall (preceded by movement of the turbulent separation point forward from the trailing edge with increased incidence).

2. Leading-edge stall (abrupt flow separation near the leading edge, generally without subsequent reattachment).

3. Thin-airfoil stall (preceded by flow separation at the leading edge with reattachment at a point which moves progressively rearward with increasing incidence).

The sequence of events preceding "leading-edge stall" is of interest since, according to Crabtree, this type of stall is associated with a "short" bubble.[18]

At a fixed free-stream Reynolds number, "leading-edge stall" occurs when, as the angle of incidence is increased, the bubble gradually contracts. However, upon further increase in incidence the bubble suddenly "bursts" and the flow may or may not reattach to the airfoil surface. Reattachment further downstream will create a much larger bubble than before. Close examination of Figures 31 through 33 reveals that, as the pitch angle increases, the discontinuity moves toward the leading edge and its length tends to decrease until eventually, at the outboard location, the trace abruptly ends very near the leading edge.

Reexamination of Figure 22, which correlates the discontinuity length with pitch angle, reveals that the decrease in discontinuity length with increased pitch is very suggestive of the events preceding leading edge stall. Recently, Crabtree[18] and Gaster[12] have given evidence that one of the controlling factors of bubble behavior is that of the pressure difference across the bubble. It is generally known that a characteristic of most separated flows is that of a constant pressure region. The pressure difference referred to by these investigators is that which would occur along the length of the bubble in the absence of the bubble. Typical pressure distributions with the presence of a bubble are shown in Figures 38 and 39. The chordwise location of these bubbles can be detected from the small step in the pressure distribution where the pressure remains approximately constant aft of the pressure peak. Direct comparison with the ammonia

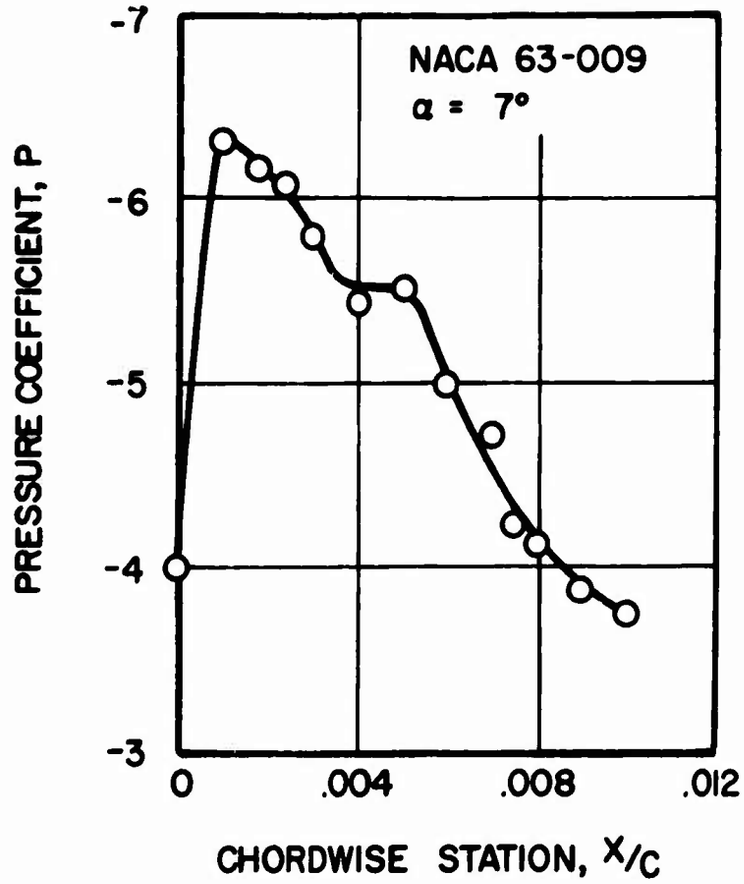

Figure 38. Pressure Distribution in the Vicinity of the Bubble of Laminar Separation - Ref. 11.

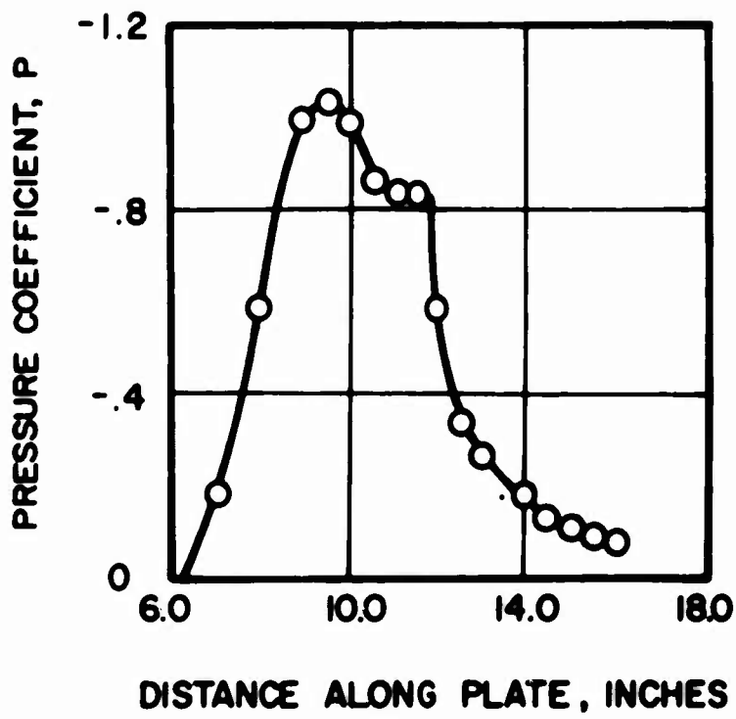

Figure 39. Pressure Distribution in the Vicinity of a Bubble - Ref. 12.

traces cannot be made since the airfoil section, Reynolds number, and incidence angles are not the same and since no pressure data were taken in this study. However, the pressure distribution across the trace discontinuity is expected to follow the same trend as that seen in previous figures.

One of the major concerns in this study was the low Reynolds numbers attained. The maximum Reynolds number at which a discontinuity in the flow was observed was about 6.3×10^5. This is much smaller than that found on typical full-scale helicopters near the rotor tip. However, in Figure 40, the pressure distribution at the 75 and 55% radial positions of the UH-1A helicopter in hovering is presented.[19] The results show a pressure-step pattern very similar to those in Figures 38 and 39. The free-stream Reynolds number at the blade tip for this flight test was 5.8×10^6.

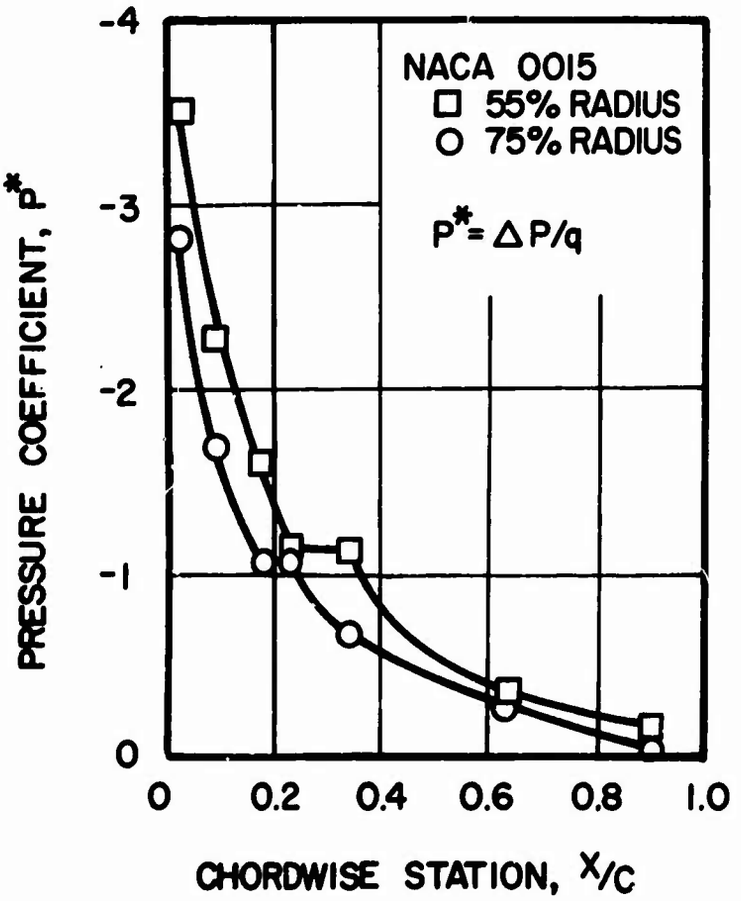

Figure 40. Chordwise Pressure Distribution on a Full-Scale Helicopter Rotor Blade - Ref. 19.

RESULTS OF FORWARD FLIGHT TESTS

The 7-inch-chord blade was operated in the flow channel at three advance ratios to determine the nature of the ammonia-azo traces in a simulated forward flight condition. Advance ratios of $\mu \cong 0.2$, 0.25, and 0.30 were run. Rotor speeds included 500, 650, and 800 rpm. The ammonia valve was set to operate at various positions around the azimuth. The azimuth angle at which the poppet valve was open was the same throughout the series of tests and corresponded to that used in the static evaluation of the ammonia valve system. Runs were made on days of high humidity. The ammonia flow conditions for almost all the traces were: a flow rate of 0.04 cfm, 2-3 psi line pressure of the NH_3 gas, and 2 minutes duration. In some cases, repeat runs were made to verify the traces obtained. The data obtained are presented in Figures 41 through 45, which summarize the traces obtained; the conditions are listed in the table on page 71. All test conditions listed utilized a mean hover lift coefficient of $C_{L_M} = 0.6$, and the flat plate area for the equivalent helicopter was adjusted for each rotor speed used. It should be noted that only the outer two traces were active. The inboard orifice line became disconnected within the blade during the forward flight runs and could not be repaired without major rework.

Consider Figure 41, the 500 rpm case, and the $\mu = 0.20$ condition. It can readily be seen that the traces for $\psi = 0°$, 90°, and 180° are regular and indicate attached flow. No clearly delineated Λ patterns or spikes appear in the traces to indicate the presence of any boundary layer bubble. At 0°, the two traces indicate a slightly outboard motion. This is expected since the crossflow at this azimuth is radially outward. Some small indication of a change in the shape of the trace is evident at about the 20% chord position of the airfoil, but no clearly defined discontinuity exists. At 90°, the long traces are regular and indicate some increased inward curvature near the trailing edge. It is of interest to note at this position (90°) that additional short traces emanate from the orifice which do not seem to be related to the main trace. The exact reason for these additional traces is not clear. At the 180° position, the two main long traces at 74% and 87% indicate an orderly, well-defined flow over the blade surface. It should be noted that these traces, particularly the more inboard trace at 74%, show a strong tendency to turn more rapidly inward near the trailing edge of the blade. The large inward curvature of the entire trace is considered to result from the combined effect of the forward velocity plus the rotation. That is, it simply reflects the usual net flow in the form

$$V_R = \Omega r + V \sin \psi$$

The reference trajectory based on this equation is shown with each trace.

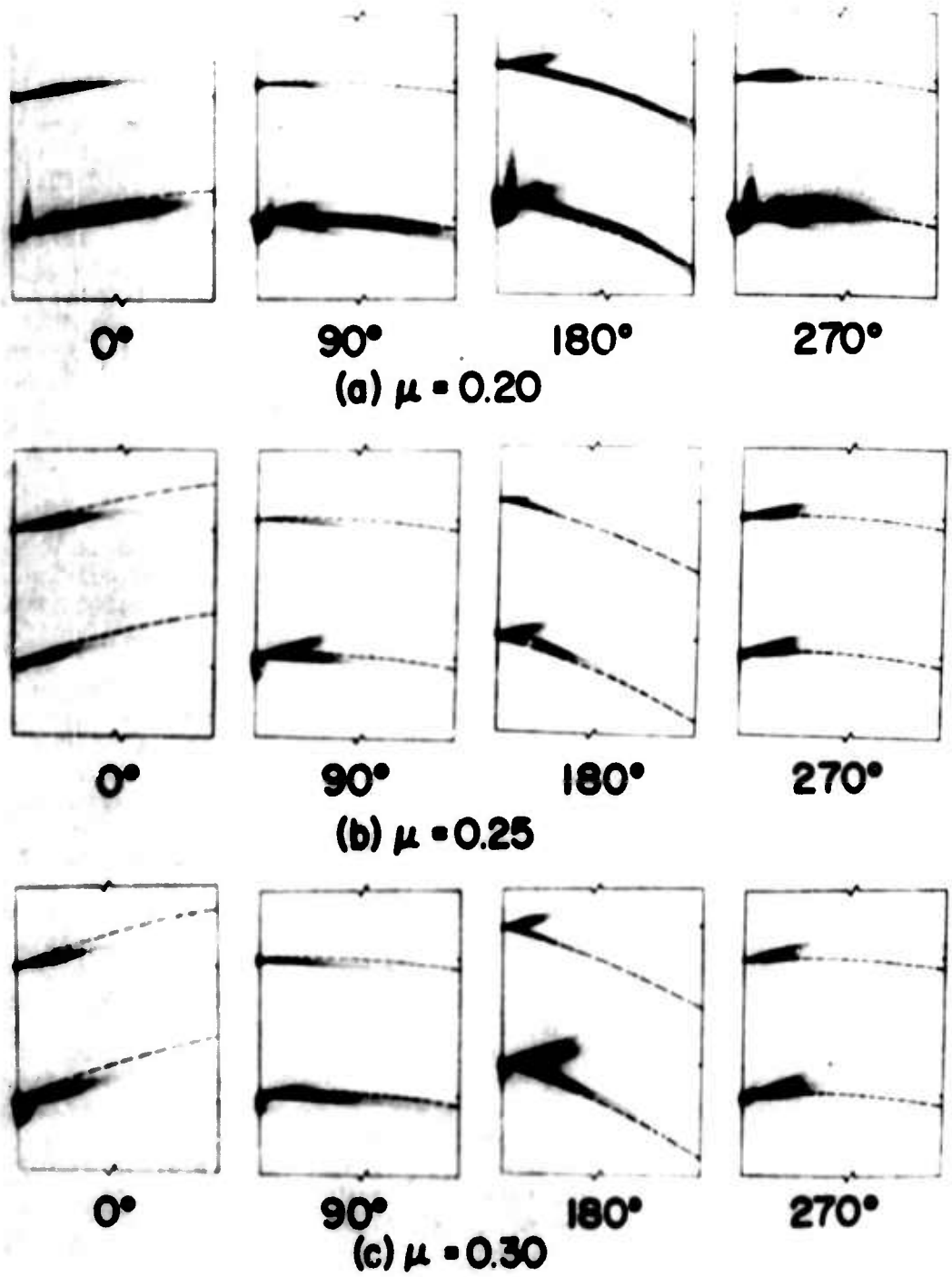

Figure 41. Simulated Forward Flight Traces at 500 rpm and Every 90° Azimuth. r/R = .74 and .87

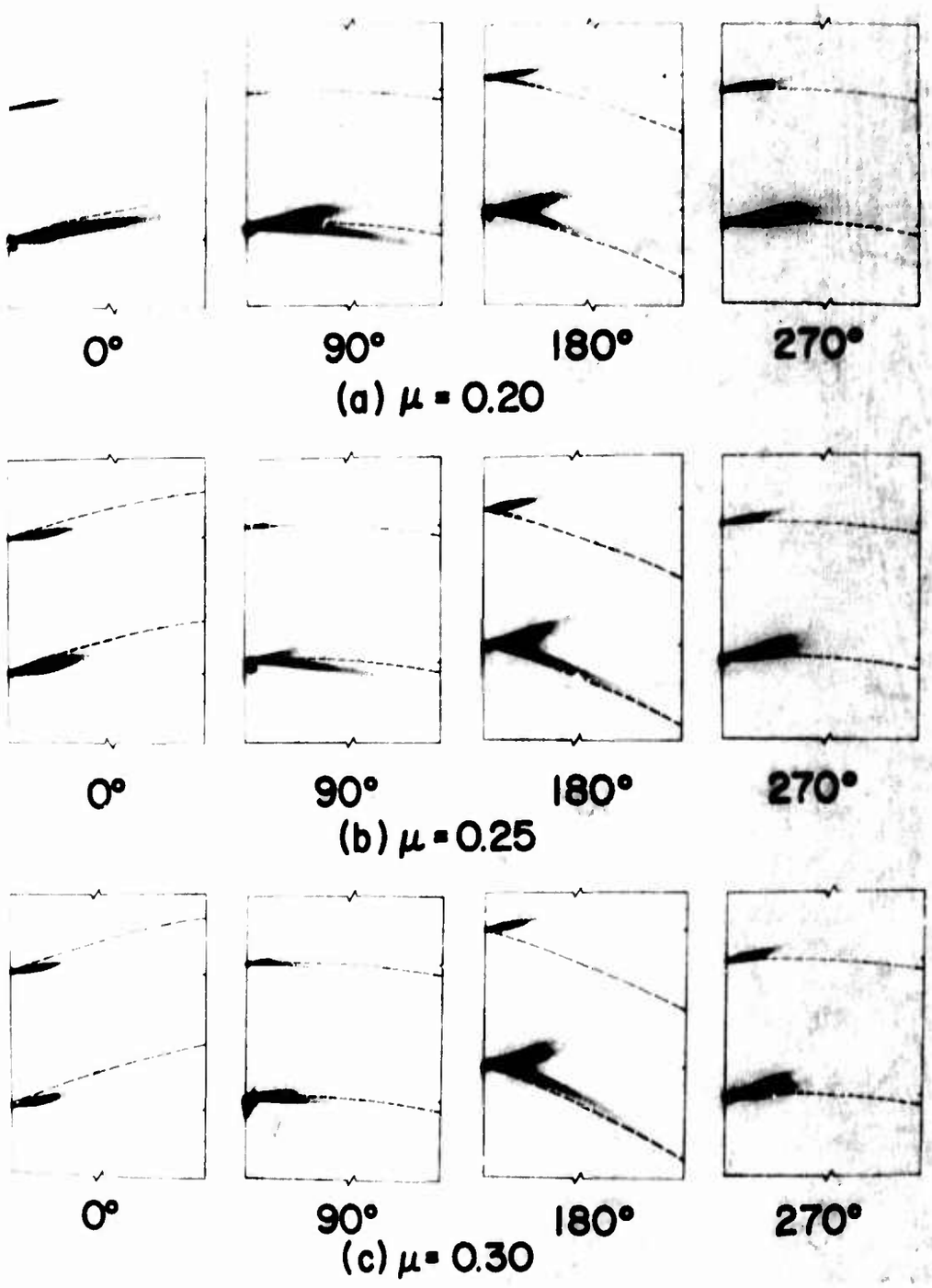

Fig. 42 - Simulated Forward Flight Traces at 650 rpm and Every 90° Azimuth. r/R = .74 and .87

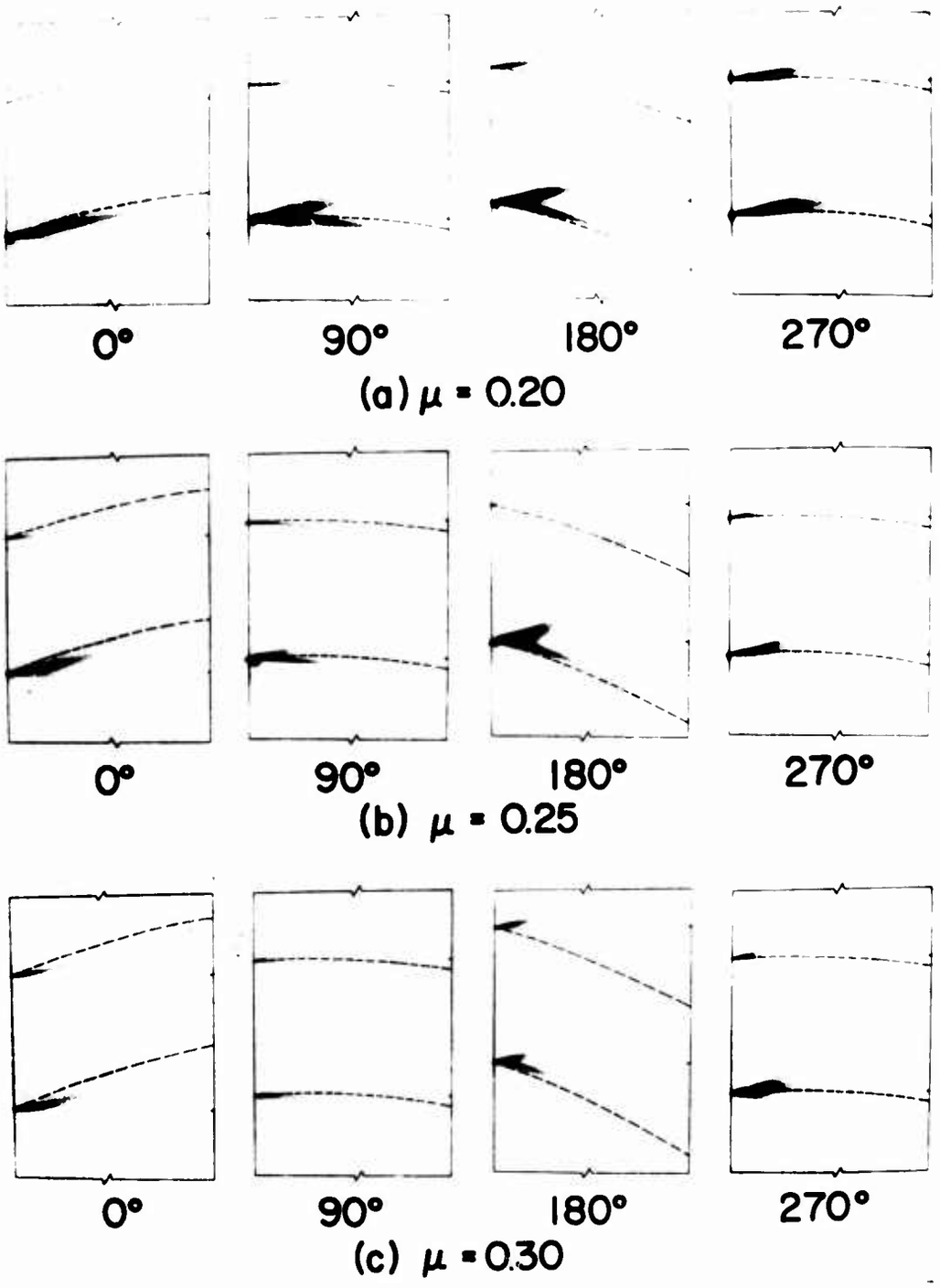

Figure 43. Simulated Forward Flight Traces at 800 rpm and Every 90° Azimuth. r/R = .74 and .87

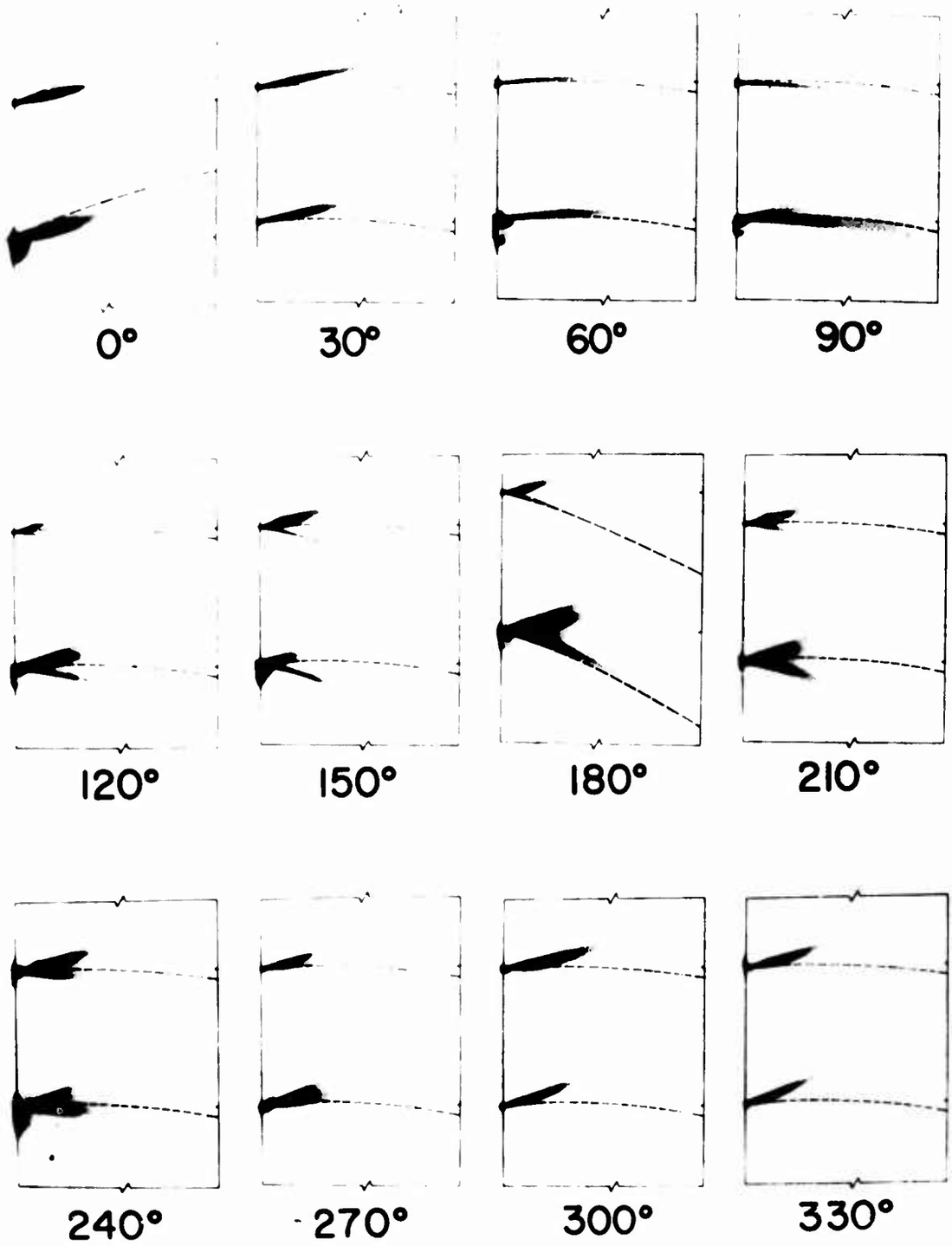

Figure 44. Simulated Forward Flight Traces at 500 rpm, $\mu = 0.3$, and Every 30° Azimuth. $r/R = .74$ and $.87$

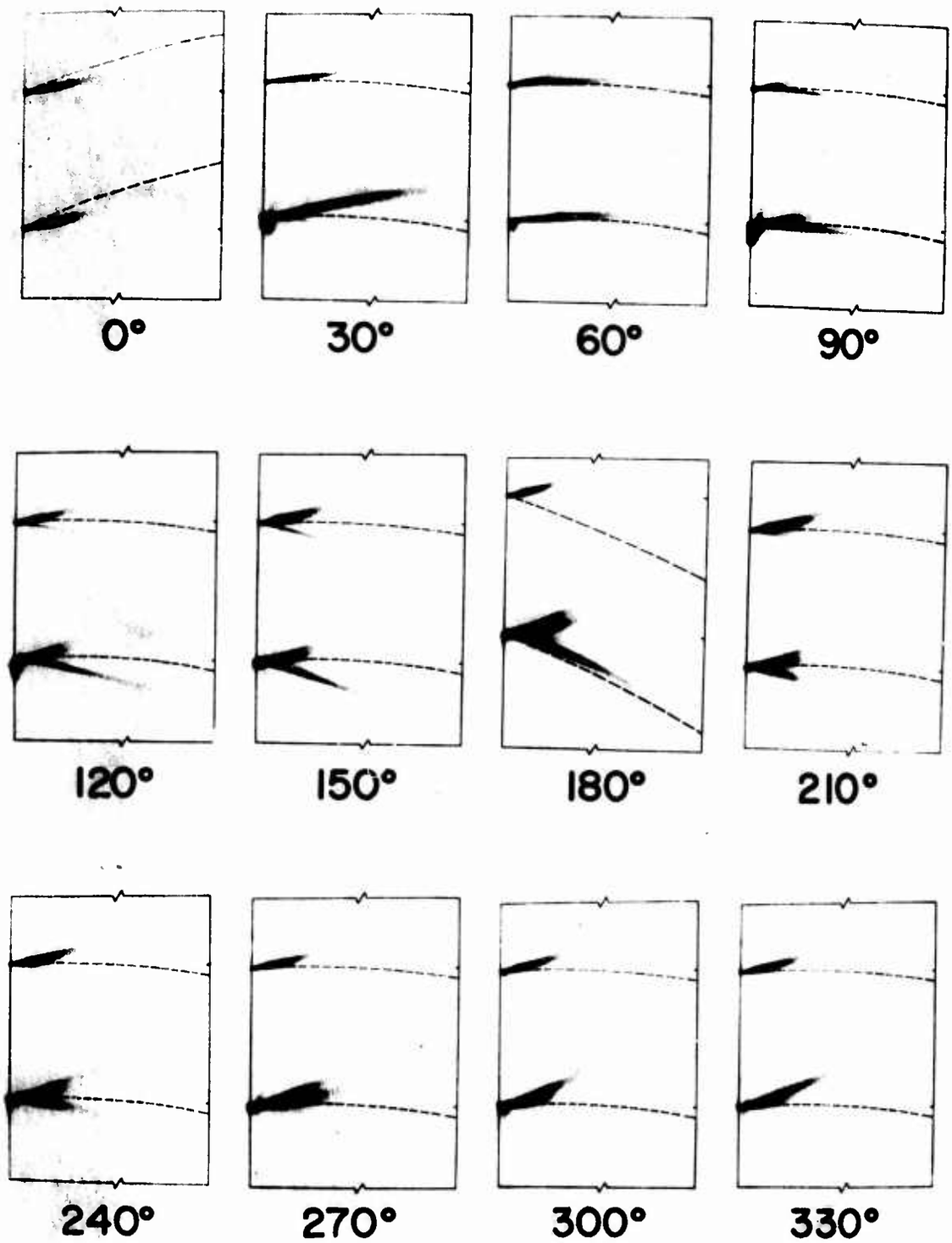

Figure 45. Simulated Forward Flight Traces at 650 rpm, $\mu = 0.3$, and Every 30° Azimuth. $r/R = .74$ and $.87$

FORWARD FLIGHT TEST CONDITIONS			
Figure	Rotor Speed (rpm)	Advance Ratio	Azimuth of Pulse (degrees)
41	500	0.20, 0.25, 0.30	0, 90, 180, 270
42	650	0.20, 0.25, 0.30	0, 90, 180, 270
43	800	0.20, 0.25, 0.30	0, 90, 190, 270
44	500	0.30	0 to 360 in 30° increments
45	650	0.30	0 to 360 in 30° increments

If one considers one of the primary results of McCroskey's analysis of rotor boundary layers (i.e., that the boundary layer direction is largely dominated by the potential flow), then the traces obtained are reasonable and consistent with McCroskey's conclusions.[14] That is, the long, continuous traces mark the direction of the local potential flow above the boundary layer. NH_3 gas that has been injected into the airstream at the nose of the airfoil may penetrate into the free stream. As this gas is carried along by the free stream, and as the blade moves by at Ωr, the free stream particle motion (the particle contains some NH_3) describes the trajectory due to the net velocity, $\Omega r + V \sin \psi$. If the flow is attached to the surface of the blade, some of the NH_3 can diffuse to the surface of the blade, react with the coated paper, and leave the trace. Thus, it appears that the long, continuous traces are indicative of the trajectories of the free-stream particles as well as the attached flow. Based on the foregoing reasoning, it is suggested as a preliminary hypothesis that the additional short traces may be due to NH_3 gas which remains in the boundary layer aft of the point of injection.

A more obvious possible explanation of the secondary traces at the nose would be that they are caused by valve leakage. If that were indeed the case, then similar traces would have been found at the 0° position, where none can be seen. Also, other tests with the valve open continuously indicated that a more fanlike trace exists.

If we next consider the 500 rpm, $\mu = 0.20$ trace at $\Psi = 270°$, it is obvious that the trace at 74% R is no longer similar to the preceding traces. Instead of being relatively continuous and well defined to the trailing edge, it exhibits the tendency to spread rapidly from the orifice as it moves aft. The trace then becomes very diffuse and does not reach the trailing edge of the blade. If one now examines the corresponding 270° traces for increased advance ratios in this same figure ($\mu = 0.25$ and $\mu = 0.30$), it is apparent that these traces also do not extend aft in the consistent fashion shown previously. Additional runs using longer exposure times did

not provide any well-defined traces over the aft portion of the blades at the various advance ratios.

In considering these retreating blade traces, one notes immediately the absence of the circular arc shape found in the trace at 90°; in addition, the traces at the higher advance ratio show rather clear tendencies to move outward along the blade span. All traces seem to be reasonably well defined over the forward portion of the chord and extend to at least the 50% chord point; at $\mu = 0.20$, they extend further aft than this. If one recalls the trace stall patterns on these blades in the hovering condition as indicated in Figure 35 or those for the 4-inch-chord blades, it was found that at high angles the traces were discontinuous. The traces turned sharply inward or outward near the leading edge. Such stall trace patterns would tend to predict a "leading edge" stall with fully separated flow over the blade surface. Generally no traces, diffuse or otherwise, appeared after the "stall discontinuities" in hovering. Examination of the retreating blade traces in Figure 41 reveals that the traces move aft in a rather orderly though diffuse fashion. This indicates that the airflow remains attached over the forward portion of the blade chord on the retreating side, even though high angles of attack were reached. The angles of attack for the retreating blades in Figure 41 ($\mu = 0.3$), as calculated from simple theory, are 12.5° at 74% and 13.6° at 87%.

It appears that the nature of "stall" is different in the retreating blade case from what it appears to be for the hovering case. At the Reynolds numbers used in the tests, stall in hover seems to result from a leading-edge separation, analogous to a sharp-edged airfoil stall. In the retreating blade case, the stall may be similar to the "soft" stall which occurs with gradual separation of the turbulent boundary layer from the trailing edge. It is not possible with the data available from the present work to comment on the possible effects of high $\dot{\alpha}$ on the nature of the ammonia-azo traces.

If one next considers the traces in Figures 42 and 43, it can be observed that the general patterns of all the traces at any particular azimuth are quite similar to those at the $\mu = 0.20$ and 500 rpm case. The curvatures and secondary traces may change somewhat, but no markedly different actions are found. Plotted on the traces are the free-stream trajectory lines. It can be seen that the ammonia traces tend to follow these trajectories.

Figure 44 for 500 rpm and Figure 45 for 650 rpm present traces for $\mu = 0.30$ taken at 30° increments around the azimuth. No really new phenomena are indicated, but the figures serve to provide a picture of how the traces vary around the azimuth. Considering Figure 45, following the 74% trace and starting at $\psi = 0°$, it can be seen that at $\psi = 0$ the trace is relatively short and well defined and moves outward. At $\psi = 30°$ it is located somewhat outward from a circular arc. The traces from 30° to 180° are regular and consistent. There appears a gradual onset of the secondary short trace from the orifice. In the forward quadrant, the secondary trace becomes more predominant; by $\psi = 240°$, it is of equivalent magnitude to the original primary trace. The

retreating side of the disk tends to show only short diffuse traces tending to move outwardly. The pattern of the traces around the azimuth when viewed as a whole seems to be consistent.

To study the possible nature of the actions at 270° for higher advance ratios, tests were made at 650 rpm with the pitch angle increased to 15.5° and with a negative (forward) shaft tilt of 15.5°. Figure 46a utilized an ammonia gas pressure of 3 psi for 3 minutes, and Figure 46b illustrates the trace for a pressure of 0.5 psi for 3 minutes. The high-pressure trace is darker and more diffuse in the aft portion of the trace, but there is little significant difference between the two traces. These traces closely resemble the previous $\psi = 270°$ traces for lower blade loadings. The primary reason for using the two flow pressures was to determine if a change in the ammonia flow out of the orifice would result in a substantial change in the trace pattern. At least from these tests it did not.

Figure 47 illustrates the trace obtained by using the same pitch angle and tilt as in the last figure but for an advance ratio of 0.34. This trace has the same appearance as the others taken at $\psi = 270°$. It seems likely that the flow is attached near the nose of the airfoil and may possibly be separating on the aft portion.

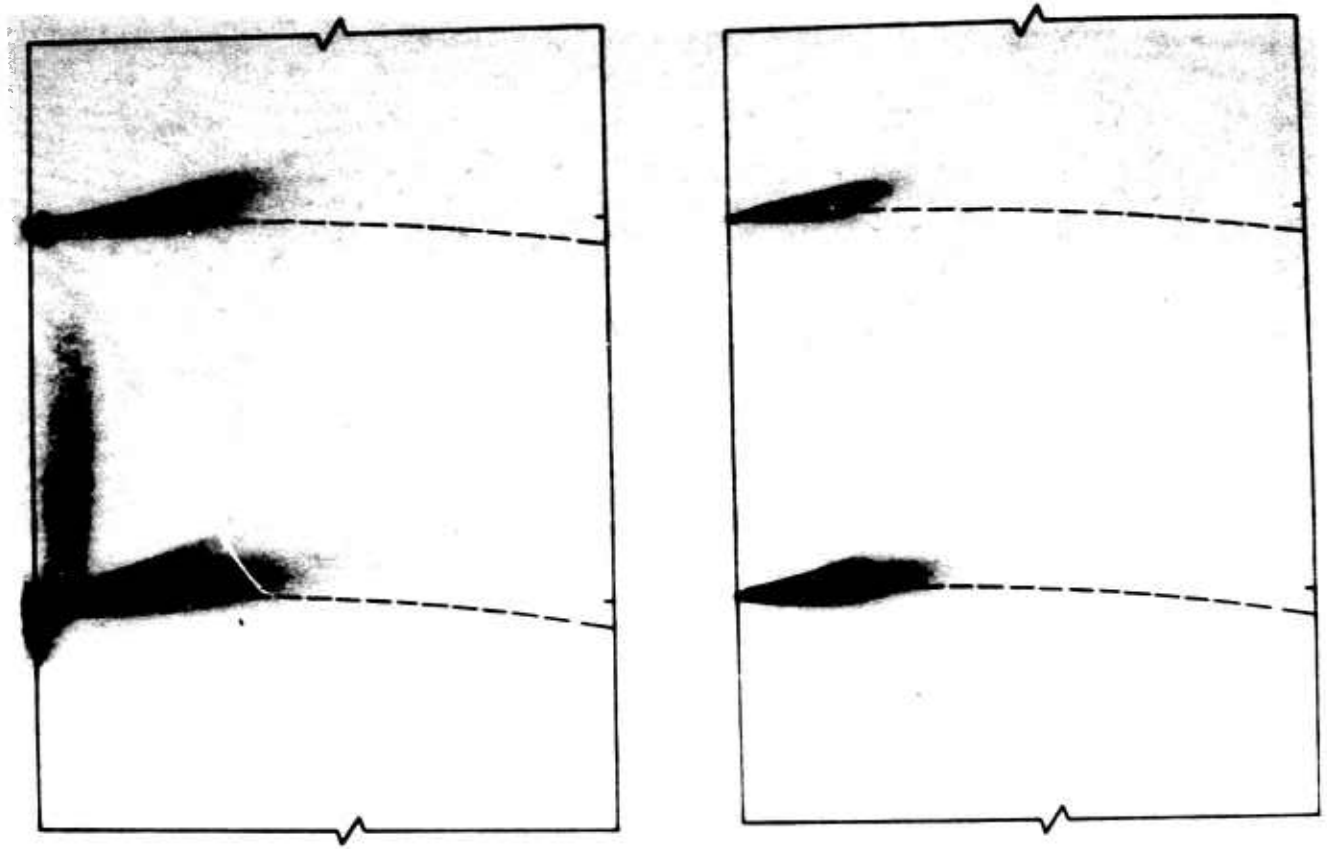

a) 3 PSI b) 0.5 PSI

Figure 46. Effect of Ammonia Gas Pressure on the Forward Flight Tests at 650 rpm, $\mu = 0.30$, and $\psi = 270°$. $r/R = .74$ and $.87$

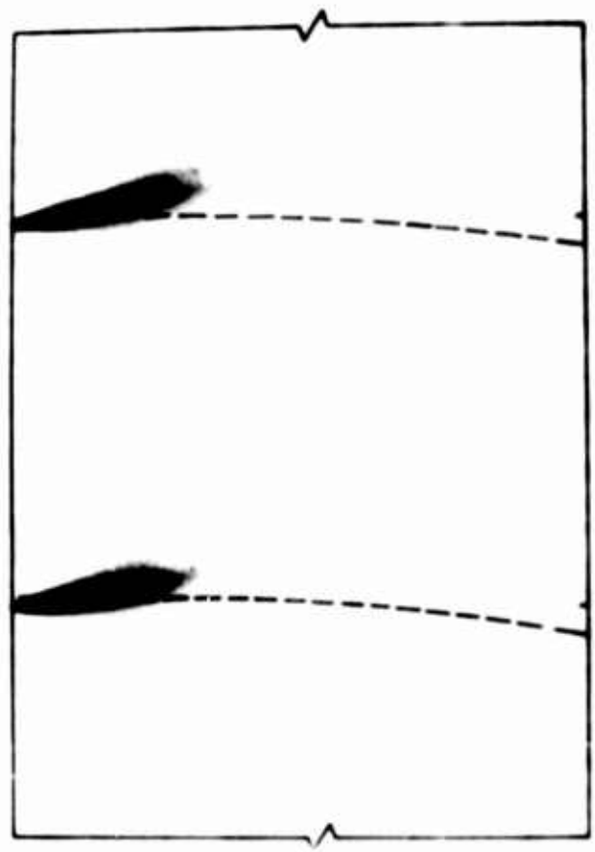

$\mu = 0.34$

Figure 47. Forward Flight Trace at High Advance Ratio at 650 rpm and $\psi = 270°$. r/R = .74 and .87

CONCLUSIONS

The use of the ammonia-azo trace technique provided a valuable insight into the nature of the boundary layer of a hover rotor. The technique itself is simple and inexpensive to use and could well be applied to other fluid flow visualization needs. The particular discontinuities found in the traces are believed to indicate the presence of a standing "bubble." The discontinuities were found to move forward with increasing Reynolds number, and their width would decrease with increased pitch angle. This behavior is similar to that expected for bubbles on two-dimensional airfoils. Of particular interest is the fact that such bubbles may exist over a wide range of Reynolds numbers, since evidence was found which indicates the presence of such a bubble on a full-scale helicopter rotor in hovering. The ammonia-azo traces at high pitch angles indicate that the stall of the NACA 0015 airfoil in hovering tends to become similar to the "sharp leading edge" type of stall.

On the other hand, the forward flight traces on the retreating side indicate that the flow remains attached over the front side of the airfoil, even at high angles of attack. Thus, it would appear that retreating blade stall initially, at least, occurs as a classic trailing edge gradual separation. In a qualitative way, then, this finding tends to agree with the concept that the stall of the retreating blade is delayed because of α effects. It is also very interesting to note that no indication of any separation bubbles could be found from close examination of the forward flight ammonia traces. Whether this absence of a bubble is a result of the short characteristic time involved in the boundary layer around the rotor or of some gross turbulence effects is not known at this stage of investigation.

RECOMMENDATIONS

Because of the utility of the ammonia-azo trace method, it is believed logical to use the technique at significantly higher Reynolds numbers in hovering. The existence of standing bubbles and their nature is sensitive to Reynolds number, and thus the study should attempt to reach Reynolds numbers approaching those used on actual full-scale rotors. Concurrent with such work, more precise instrumentation using boundary-layer probes or hot-wire probes should be used in conjunction with the ammonia technique to determine the local flow patterns in the neighborhood of the trace discontinuity. Surface pressures should also be measured to determine if the expected "flat spot" on the chordwise pressure distribution occurs near the discontinuity, as would be expected for a two-dimensional bubble.

The range of advance ratios used in any future testing should be increased up to at least a value of $\mu = 0.4$, and higher if possible. Coupled with this should be higher blade loadings.

A particularly important facet of any new ammonia trace work should include releasing ammonia out of a matrix of surface holes distributed both spanwise and chordwise. If short ammonia release times were used, a picture of the velocity direction over an entire region of the blade surface could be obtained.

The ammonia trace technique could also be applied to the evaluation of airfoils other than the NACA 0015. Typically, airfoils such as the NACA 0012 and NACA 23012, or modifications to them, could be studied to determine whether standing bubbles exist. Of specific interest to the airfoil designer would be the effect of nose droop on the existence of the bubble.

The ammonia trace technique could also be useful in studies of the flow near the tips of rotor blades. If the ammonia is injected into the surface flow, it will be carried along by the vortex roll-up and could leave a trace of the direction of the local flow. This could provide a useful tool in the study of the flow around various tip shapes.

LITERATURE CITED

1. Legrand, F. L., "Structural Behavior of the Super Frelon in High Speed Flight," Proc. Am. Helicopter Soc., Washington, D. C., May 1964.

2. Harris, F. D., and Pruyn, R. R., "Blade Stall, Half Fact, Half Fiction," Preprint, 23rd Annual Forum, Proc. Am. Helicopter Soc., May 1967.

3. Blaser, D. A., and Velkoff, H. R., "Pressure Distribution and Angle of Attack Variation on a Helicopter Rotor Blade," J. Am. Helicopter Soc., 13:2, April 1968.

4. Tanner, W. H., and Buettiker, P., "The Boundary Layer of the Hovering Rotor," CAL USAAVLABS Symposium Vol. III, Cornell Aero Laboratory, Buffalo, New York, June 1966.

5. Ham, N. D., and Young, M. I., "Torsional Oscillation of Helicopter Blades Due to Stall," J. Aircraft, 3:3, May-June 1966.

6. Johnson, J. P., "A Wall Trace, Flow Visualization Technique for Rotating Surfaces in Air," ASME J. Basic Engr., December 1964.

7. Main-Smith, J. D., "Chemical Solids as Diffusable Coating Films for Visual Indication of Boundary Layer Transition in Air and Water," British R & M 2755, 1954.

8. Tanner, W. H., and Yaggy, P. F., "Experimental Boundary Layer Study on Hovering Rotors," J. Am. Helicopter Soc., 11:3, July 1966.

9. Silverstein, A., and Becker, J. V., "Determination of Boundary Layer Transition of Three Symmetrical Airfoils in the NACA Full-Scale Wind Tunnel," NACA Report No. 637, 1939.

10. Banks, W. H. H., and Gadd, G. E., "Delaying Effect of Rotation on Laminary Separation," AIAA J., 1:4, April 1963, 941-2.

11. McCullough, G. B., and Gault, D. E., "Examples of Three Representative Types of Aerofoil-Section Stall at Low Speed," NACA TN 2502, 1951.

12. Gaster, M., "On the Stability of Parallel Flows and the Behavior of Separation Bubbles," Proc. AGARD Conf., 4, May 1966.

13. Lachmann, G. V., Boundary Layer and Flow Control, Pergamon Press, New York, New York, 1961.

14. McCroskey, W. J., and Yaggy, P. F., "Laminar Boundary Layers on Helicopter Rotors in Forward Flight," J. AIAA, 6:10, October 1968.

15. Tani, I., "Experimental Investigation of Flow Separation over a Step," Boundary Layer Research, Springer-Verlag, Berlin, 1958, 377-386.

16. Schlichting, H., Boundary Layer Theory, McGraw-Hill, New York, New York, 1969, 198.

17. Himmelskamp, H., "Profilunterschungen an einem umlaufendem Propeller," Mitt. Max-Planck Inst. No. 2, 1950.

18. Crabtree, L. F., "The Formation of Regions of Separated Flow on Wing Surfaces," ARC R & M No. 3122, 1959.

19. Anon. "Measurement of Dynamic Air Loads on a Full-Scale Semirigid Rotor," U. S. Army TRECOM Report, TCREC 62-42, December 1962.

APPENDIX

STUDY OF USE OF CLAW TYPE BOUNDARY LAYER PROBES

An exploratory study of the possible use of ordinary claw type pressure probes was undertaken to determine whether such probes could provide an indication of the flow in the boundary layer of the model rotor blade. Figure 48 illustrates the experimental installation of the probe. The claw probe itself was fabricated of 0.040" O.D. and 0.030" I.D. stainless-steel tubing. The two forward-facing arms of the probe are simply open-end, total head tubes whose axes are at 90° to each other and 45° to the main axis of the probe. During installation, the main axis was carefully aligned in the chordwise direction of the rotor blade. The arms of the probe were connected by means of small-diameter tubing to a differential inclined manometer. If the air flow moves directly aft along the blade chord and along the main axis of the claw probe, then the impact pressure in each arm is the same and no differential pressure will exist. If the airflow is inclined from the axis of the probe, a differential pressure will occur and this can be read on the inclined manometer. The probe itself was located directly in contact with the surface of the blade and hence would tend to give an indication of flow at a height of 0.020". It must be recognized that any boundary layer probe of finite dimension will be subject to errors due to shear flow at low Reynolds numbers. However, it is believed that differential readings can provide valid data on the nature of flow inclination relative to the chordline of the blade.

A question may arise as to the effect of centrifugal force on any readings taken with a pressure gage located out on a rotor blade. In this present work, the ends of the arms of the probe are essentially at the same radial position, and the centrifugal pressure change in each pressure lead will be the same. Thus, by measuring differential pressure, the effects of centrifugal force are essentially cancelled out.

Because of the inherent time lag, such as that found in a pressure system of this kind, valid data can be taken only in a hovering condition where steady-state conditions can be reached. Consequently, no attempts were made to take pressure measurements under forward flight conditions.

In order to use the claw probe, it was necessary to calibrate the probe as mounted on the blade surface. This calibration was accomplished by mounting the blade on the rotor drive stand in the rotor wind tunnel and yawing the blade through a series of positions. The arrangement is illustrated in Figure 49. The tunnel speed was established, the blade angle was set to 0°, the blade was positioned in yaw relative to the air system, and a reading of differential manometer pressure was taken. In order to allow the data to be useful at various air speeds, the data obtained were nondimensionalized by dividing by the dynamic pressure. The calibration curve of the claw probe is shown in

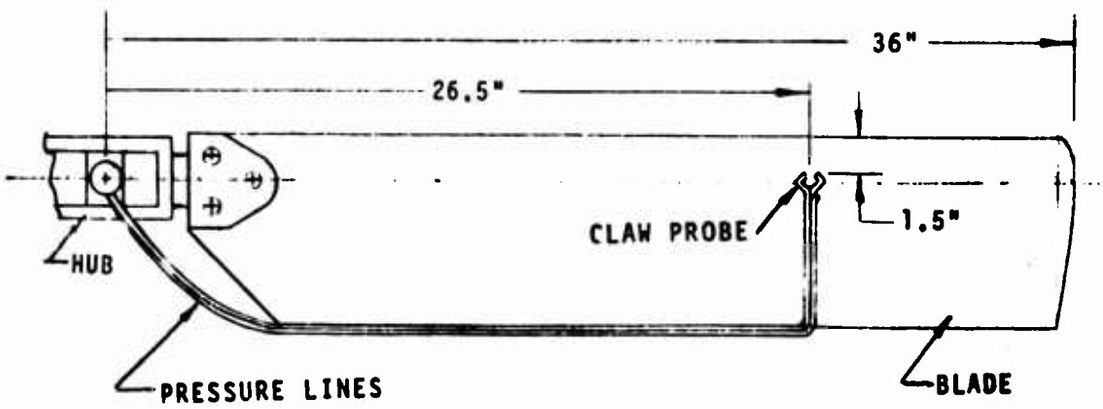

Figure 48. Schematic of Claw Probe Installation on Blade.

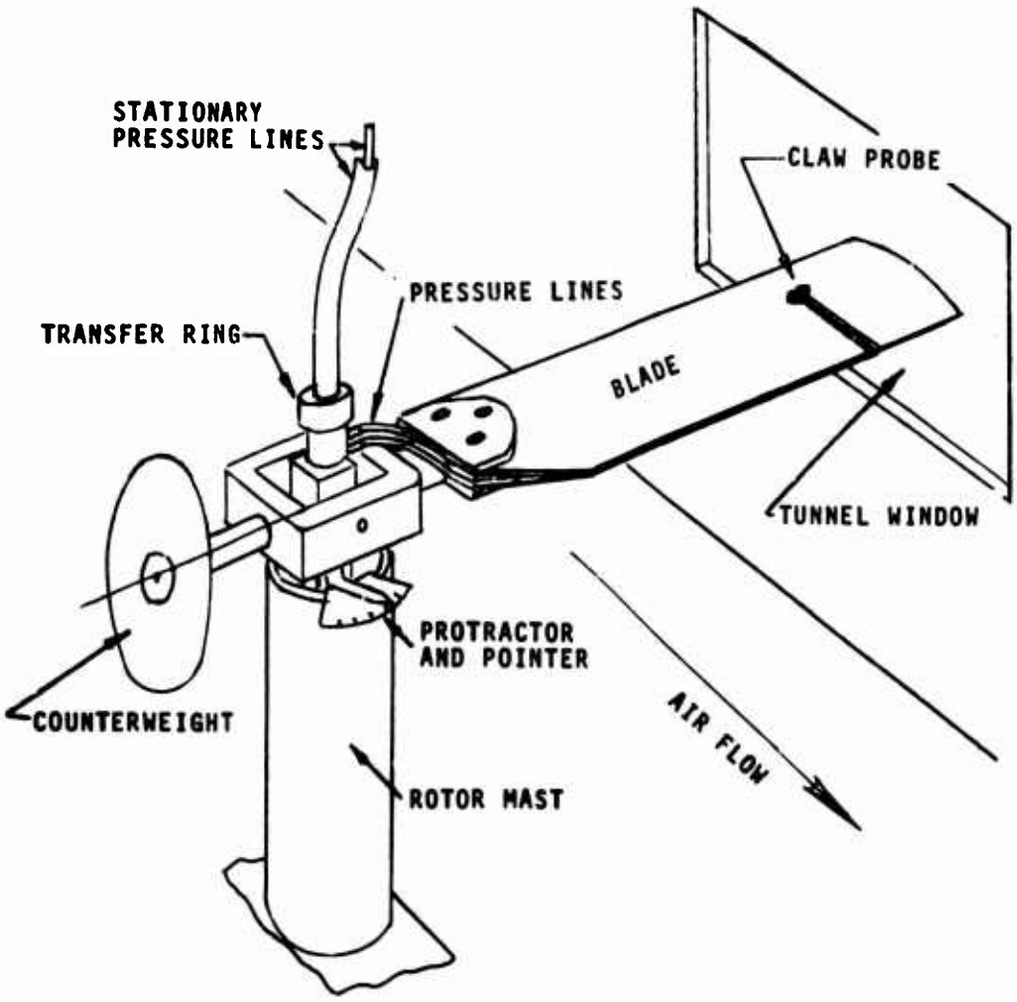

Figure 49. Installation of Model With Yaw Probe in Wind Tunnel.

Figure 50. It can be noted that the central portion of the curve is quite linear. As a consequence of this, the modified calibration curve shown in Figure 51 was prepared for use in reducing the pressure data taken during test to effective angle of flow.

A test was then run with the model rotor in a hovering condition with the blade angle at 0°. A range of rotor speeds up to 500 rpm was covered. The differential pressure readings are shown in Figure 52. The curve gives a strong indication of being parabolic in form. The data points were nondimensionalized and are presented in Figure 53. If there were no effect of rotation, then the points should tend to fall on a horizontal line. The data points in this figure indicate a slightly decreasing differential pressure with increasing speed. It should also be noted that the average pressure is positive, indicating that the fluid pressure is greater in the outer arm of the claw probe. Using the modified calibration curves of Figure 51, the foregoing pressure data were converted to flow angle and are presented in Figure 54. The data points in Figure 54 seem to indicate that a significant outflow exists. The data also indicate that there is a decreasing outflow angle with increasing speed of rotation.

Because of the exploratory nature of the tests conducted and the very limited effort expended using probes as contrasted to the extensive efforts using the ammonia technique, it is not considered possible to draw any significant conclusions from the probe data. It does not seem likely that a flow angle of approximately 10° exists as a general rule on the model blade. The reason for the apparent 10° angle would seem to lie in the instrumentation and procedure. If such an outflow angle does indeed exist, it is believed that it must be rather local in its effect. This conclusion is based upon the results of the ammonia trace work reported in the body of this report. However, the data obtained with the probe are reported in this appendix for completeness. It is believed that further work with pressure probes should be conducted, particularly in conjunction with hot wire or hot film probes, in order to determine more precisely boundary layer flow direction.

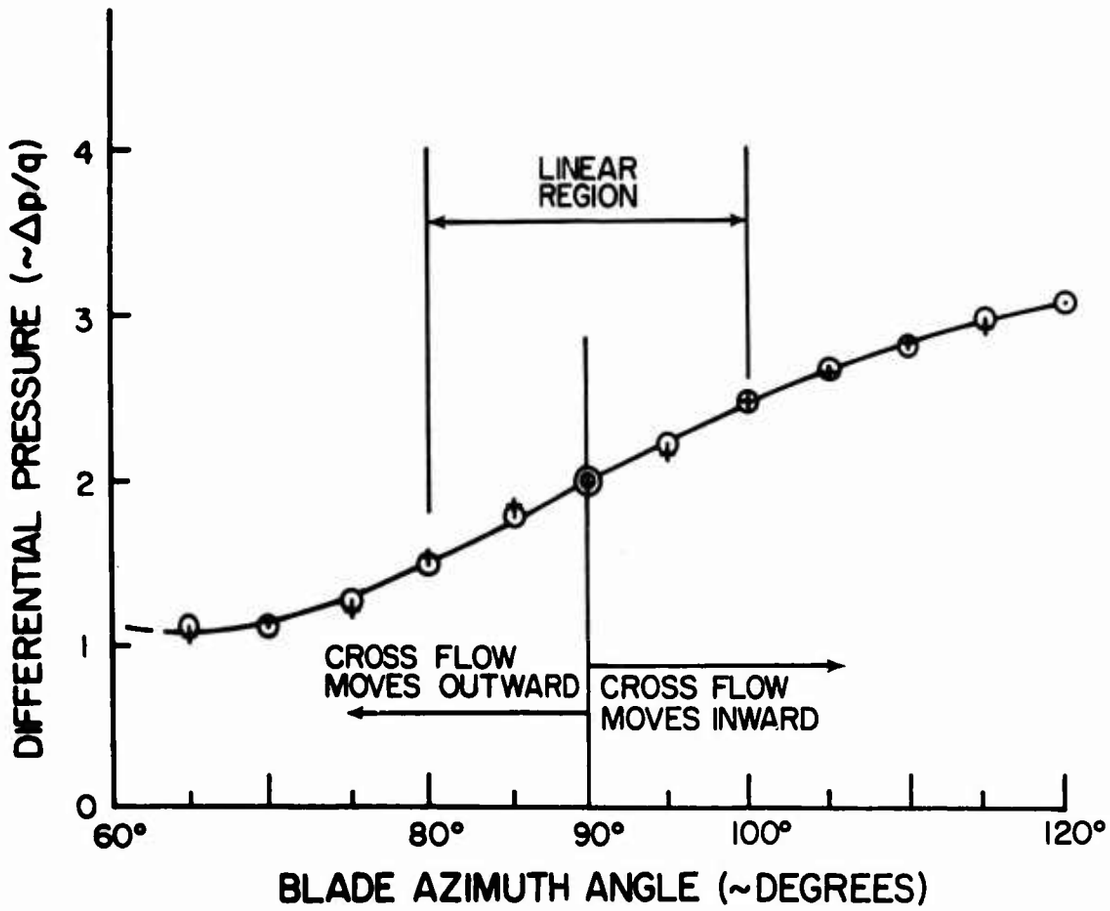

Figure 50. Yaw Probe Calibration, $\theta = 0°$, $q_{tunnel} = 0.2''\ H_2O$.

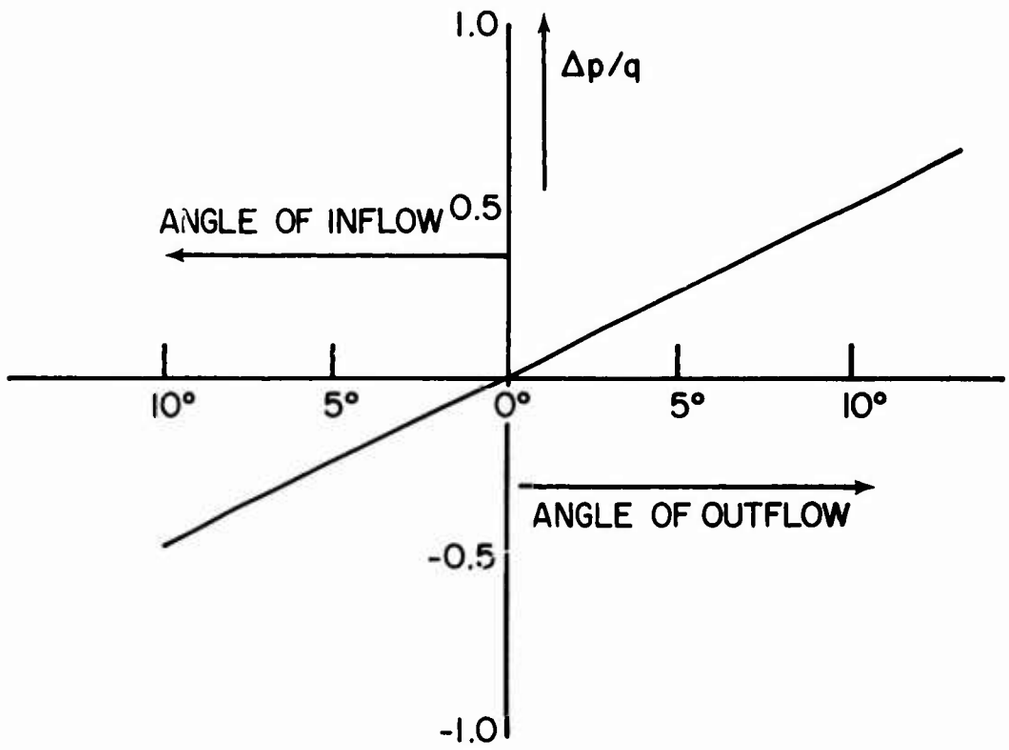

Figure 51. Modified Calibration Curve for Claw Probe, $\theta = 0°$.

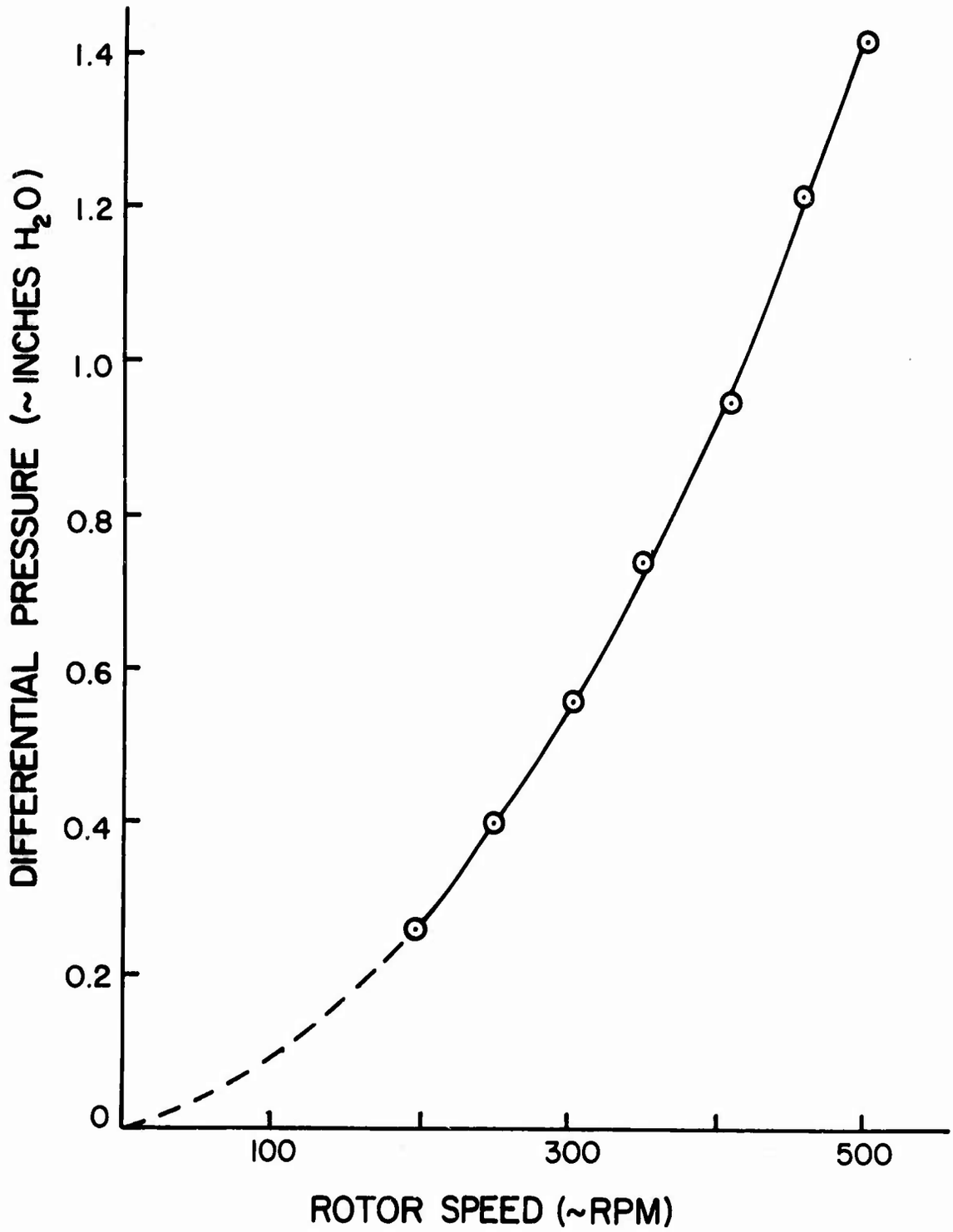

Figure 52. Measured Differential Pressure Using Claw Probe Versus Rotor Speed, $\theta = 0°$, 73.5% R Position.

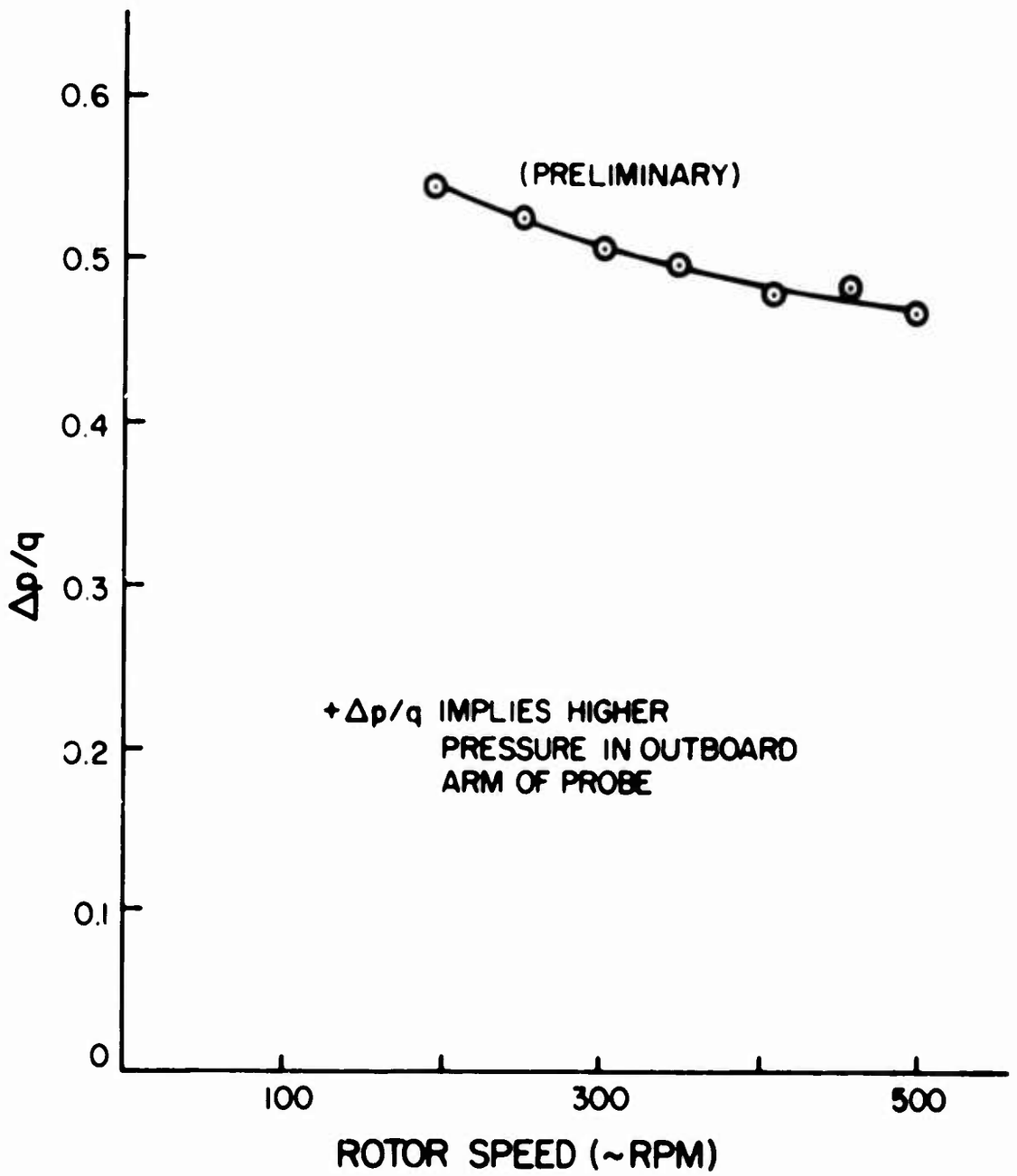

Figure 53. Variation of Differential Pressure With Speed of Rotation $\theta = 0°$, 73.5% R Position.

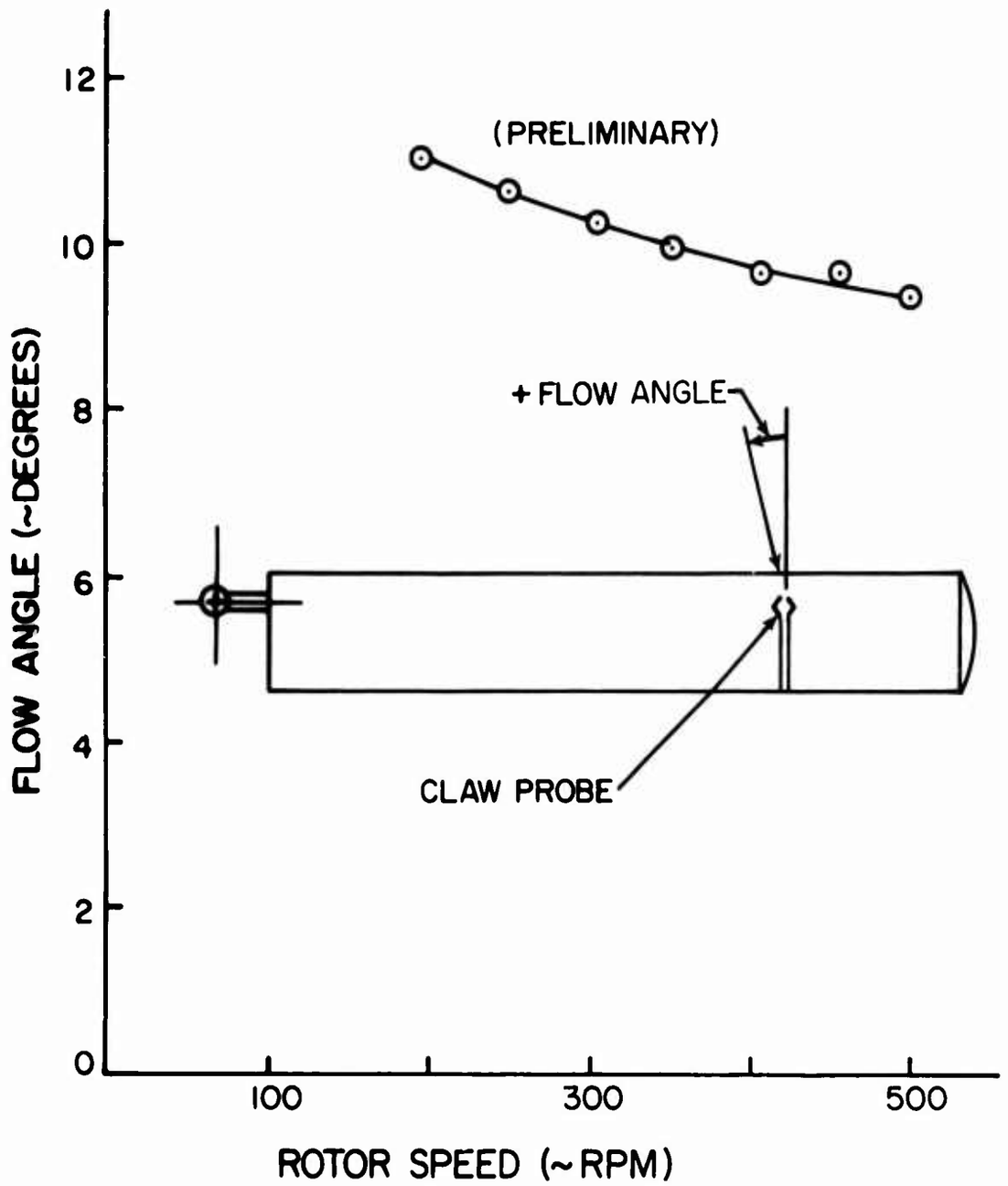

Figure 54. Flow Direction Deviation With Rotational Speed, $\theta = 0°$, 73.5% R

Unclassified

Security Classification

DOCUMENT CONTROL DATA - R & D

(Security classification of title, body, of abstract and indexing annotation must be entered when the overall report is classified)

1. ORIGINATING ACTIVITY *(Corporate author)* The Ohio State University Research Foundation Columbus, Ohio	2a. REPORT SECURITY CLASSIFICATION Unclassified 2b. GROUP

3. REPORT TITLE

EXPLORATORY STUDY OF THE NATURE OF HELICOPTER ROTOR BLADE BOUNDARY LAYERS

4. DESCRIPTIVE NOTES *(Type of report and inclusive dates)*

Final Technical Report

5. AUTHOR(S) *(First name, middle initial, last name)*

H. R. Velkoff G. C. Shumaker
D. A. Blaser K. M. Jones

6. REPORT DATE July 1969	7a. TOTAL NO. OF PAGES 100	7b. NO. OF REFS 21
8a. CONTRACT OR GRANT NO. DAAJ02-67-C-0001 b. PROJECT NO. c. Task No. 1F162204A14234 d.	9a. ORIGINATOR'S REPORT NUMBER(S) USAAVLABS Technical Report 69-50 9b. OTHER REPORT NO(S) *(Any other numbers that may be assigned this report)*	

10. DISTRIBUTION STATEMENT

Ea[redacted]e prior [redacted]stis, Virginia 23604.

11. SUPPLEMENTARY NOTES	12. SPONSORING MILITARY ACTIVITY US Army Aviation Materiel Laboratories Fort Eustis, Virginia

13. ABSTRACT

An experimental study was conducted using flow visualization techniques to investigate the nature of the boundary layer on a helicopter rotor. Hovering and forward flight data were obtained; however, efforts were concentrated on hovering when unanticipated boundary layer behavior was revealed. The primary flow visualization technique involved the use of ammonia injected into the boundary layer at the leading edge. The blade surface was chemically coated, and as the ammonia moved with the local airflow, it formed a trace on the surface indicative of the boundary layer flow. The hovering traces initially moved chordwise along the surface and then abruptly turned outward. A short distance later, the traces moved inward and then continued aft along the blade in a somewhat diffuse pattern. Similar traces were found over wide ranges of pitch angles and rotor speeds. It is hypothesized that a standing laminar separation bubble exists on the blade surface aft of the peak pressure position. No indication of any separation bubbles could be found on the forward flight traces.

An exploratory study of the possible uses of ordinary claw-type pressure probes was undertaken to determine whether such probes could provide an indication of the flow in the boundary layer of a model rotor.

DD FORM 1 NOV 65 1473 REPLACES DD FORM 1473, 1 JAN 64, WHICH IS OBSOLETE FOR ARMY USE.

Unclassified

Security Classification

Unclassified
Security Classification

14. KEY WORDS	LINK A ROLE	LINK A WT	LINK B ROLE	LINK B WT	LINK C ROLE	LINK C WT
Helicopter Rotor Boundary Layers						
Separated Flows						
Flow Visualization						
Separation Bubbles on Rotor Blades						

Unclassified
Security Classification

6960-69